Functional characterization of the potential immune evasion proteins pUL49.5 and p012 of Marek's disease virus (MDV)

Dissertation zur Erlangung des akademischen Grades des

Doktors der Naturwissenschaften (Dr. rer. nat.)

eingereicht im Fachbereich Biologie, Chemie, Pharmazie

der Freien Universität Berlin

vorgelegt von

Timo Schippers

aus Hilden, Deutschland

Berlin 2014

Diese Promotionsarbeit wurde im Zeitraum vom September 2009 bis zum Dezember 2014 am Institut für Virologie der Freien Universität Berlin unter der Leitung von Professor Dr. Nikolaus Osterrieder angefertigt.

1. Gutachter: Prof. Dr. Nikolaus Osterrieder

2. Gutachter: Prof. Dr. Rupert Mutzel

Disputation am 10.03.2015

Thankfully, persistence is a great substitute for talent.

Steve Martin

To Sina

the strongest person I know.

1. Table of contents

2. List of figures and tables

3. Abbreviations

Amp	Ampicillin
ATP	Adenosin triphosphat
APC	Antigen presenting cell
BAC	Bacterial artificial chromosome
BHV	Bovine herpesvirus
bp	Base pairs
BSA	Bovine serum albumin
ca.	circa
Cam	Chloramphenicol
CEC	Chicken embryo cells
CTL	Cytotoxic T lymphocyte
coint.	Cointegrate
ddH2O	Double distilled water
DEV	Duck enteritis virus
DMEM	Dulbecco's modified Eagle medium
DMSO	Dimethyl sulfoxide
DNA	Deoxyribonucleic acid
dpi	Days post infection
dpt	Days post transfection
DRIPS	Defective ribosomal particles
dsDNA	Double strand deoxyribonucleic acid
E	Early genes
E. coli	*Escherichia coli*
EBV	Epstein-Barr virus
EDTA	Ethylendiamine tetraacetic acid
EHV	Equine herpes virus
ER	Endoplasmic reticulum
ERAP	ER associated protease
FBS	Fetal bovine serum
FFE	Feather follicle epithelium
For	Forward
GAG	Glycosaminoglycans
gB	Glycoprotein B
gC	Glycoprotein C
gD	Glycoprotein D
gH/gL	Glycoprotein H and L complex
GaHV-2	Gallid herpesvirus 2
GaHV-3	Gallid herpesvirus 3
GFP	Green fluorescent protein
h	Hour
HCMV	Human cytomegalovirus
HLA	Human leucocyte antigen
HSV-1	Herpes simplex virus 1

hpt	Hours post transfection
hpi	Hours post infection
HVT	Herpesvirus of turkeys
HVEM	Herpes virus entry mediator
ICP0	Infect cell protein 0
ICP47	Infect cell protein 47
IE	Immediate early
IFN	Interferon
ILTV	Infectious laryngotracheitis virus
INM	Internal nuclear membrane
IR	Internal repeat
IRL	Internal repeat long
IRS	Internal repeat short
Kana	Kanamycin
Kb	Kilobases
Kbp	Kilo bae pairs
L	Late
LB	Luria-Bertrani medium or lysogeny broth
LMB	Leptomycin B
LPP	Lambda protein phosphatase
LPS	Lipopolysaccharide
M	Marker
Mb	Mega bases
MD	Marek’s disease
MDV	Marek’s disease virus
MEM	Minimum essential Medium Eagle
MHC	Major histocompatibility complex
min	Minutes
mut	Mutant
NBD	Nucleotide binding domain
NLS	Nuclear localization signal
NES	Nuclear export signal
O/N	Overnight
OD600	Optical density, 600 nm wavelength
PAMPS	Pathogen associated molecular patterns
PBS	Phosphate saline buffer
PCR	Polymerase chain reaction
PFU	Plaque forming unit
pi	Post-infection
PLC	Peptide loading complex
PRV	Pseudorabies virus
P/S	Penicillin/streptomycin
rev	Reverse
R	Revertant
RFLP	Restriction fragment length polymorphism
RNA	Ribonucleic acid
rpm	Rotations per minute
RT	Reverse transcriptase

rt	Room temperature
SD	Standard deviation
SDS	Sodium dodecyl sulfate
sec	Seconds
SEM	Standard error of the mean
SPF	Specific-pathogen-free
TAE	Tris-acetate-EDTA buffer
TAP	Transporter associated with antigen processing
Temp.	Temperature
TRL	Terminal repeat long
TRS	Terminal repeat short
UL	Unique long
US	Unique short
v	Reconstituted virus
vMDV	Virulent Marek's disease virus
vIL-8	Viral interleukin 8
vvMDV	Very virulent Marek's disease virus
vv+MDV	Very virulent plus Marek's disease virus
VZV	Varicella zoster virus
WT	Wildtype

4. Introduction

"A virus is bad news wrapped in a protein"
Sir Peter Medawar (Nobel Laureate)

Viruses are fascinating biological entities. Stripped down to the basics, reduced to the minimum and yet elegant and complex in their makeup. The ongoing debate as to whether those entities should be considered "living" and, hence, even included into the Tree of Life is interesting but at the same time a more philosophical exercise[1,2]. In fact, viruses are omnipresent in our environment and have been with us since our first ancestors entered the scene thousands of years ago. Surely, they will still be around by the time our own species has gone extinct. Nine out of ten cells in our body are of bacterial origin[3], however, this body swims in an endless ocean of viruses. Rough calculations estimate that 10^{31} viral particles exist on our planet, a number that exceeds the amount of stars in our universe by 6 to 7 orders of magnitude[4]. Not only are viruses unbelievably numerous, they also constitute a perfect blueprint for biomolecular Darwinian machines. In essence, viruses might be the most basic realization of the evolutionary driving forces: mutation, variation, selection and inheritance. The only impetus for their existence is procreation and it is this simple principle that can lead to anything from an entirely benign and asymptomatic disease to a horrible death in a matter of hours or days. Viruses are also highly versatile. Even today new viruses emerge and manage to enter our world from the most remote places by means of cross-species transmission. Sometimes those jumps will lead to dead-ends and the virus might vanish as quickly as it surfaced (as in the case of SARS). In other cases the virus will manage to gain a foothold in the human population and spark a global pandemic with millions of deaths (as in the case of HIV). Despite all our efforts, neither of these outcomes is easy to forecast, if being predictable at all. As long as they find a host cell to replicate in, viruses won't go away. Their large population sizes and fast-paced mutation rates allow most viruses to evolve with incredible speed. Whatever tool our remarkable immune system has invented to combat the intruders, one viral species on this planet will already have obtained the perfect counter-strategy. It is an everlasting arms race between them and us. A highly complex multicellular system versus a piece of genetic information and handful of proteins. Viruses are indeed truly fascinating.

4.1 Herpesviruses

Herpesviruses are large, double-stranded DNA viruses that infect a large variety of different hosts. In evolutionary terms, herpesviruses are extremely successful as they are capable of infecting all vertebrates and also invertebrate species like mollusks[5]. Nevertheless, our knowledge regarding the true number of herpesviruses that exist in nature is still limited and all described herpesviral species so far probably only represent a fraction of the ones that remain unidentified.

The actual herpesviral particle, the so called virion, usually reaches diameters of about 200 to 250 nm in size and invariably consists of four layered components[6,7]. The inner core contains the DNA genome and associated proteins. The genomes vary in size between 108 and more than 300 kilo basepairs (kbp). The core itself is embedded in a capsid, a protective shell structure, which is built of 162 identical protein subunits called capsomers. The icosahedral shape of the capsid is one of the hallmarks of the order *Herpesvirales* and its key function lies in protection of genetic information[6]. Apart from the main capsid protein VP5, 6 other capsid proteins are sufficient to build the sophisticated and highly efficient structure[7]. The next layer constitutes the tegument, a layered and sometimes asymmetrical protein coat that mostly fulfills functions immediately upon entry of the virus into the host cells and in virus egress[6,8]. In particular, proteins that exert early functions in modulation of the cellular environment and transcriptional activators are part of the tegument. A prominent example is the viral host shut-off protein vhs, which is capable of degrading cellular mRNAs thereby paving the way for complete takeover of the cellular machinery by the virus[9].

Finally, the whole particle is enveloped by a host cell-derived lipid membrane, which contains up to 20 integrated glycoproteins forming spike structures on the surface[6]. As in other enveloped viruses, those surface glycoproteins control virion attachment and penetration into the host cell through specific interactions with cellular receptors.

One of the reasons for the unusual large size of herpesviral genomes could be due to the fact that it encodes an almost complete DNA replication machinery including a DNA polymerase, a helicase, DNA precursor-generating enzymes and even DNA repair proteins[6,10]. This coding strategy should be beneficial for the virus since it allows cell cycle- independent replication and might even allow modulation of the latter[11,12]. The genes that ensure proper replication, sometimes called core genes, are typically found in the central region of the genome whereas accessory genes usually map to terminal areas and mainly encode extra functions[6].

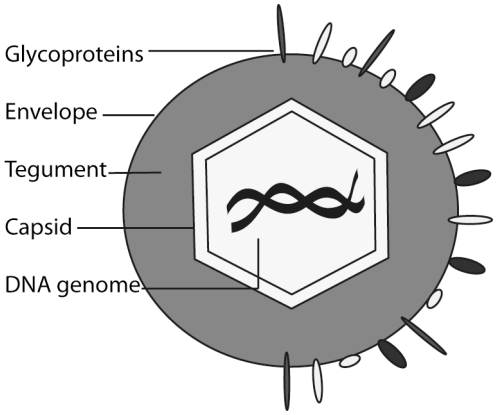

Figure 1: Schematic representation of the herpes virion structure. The double-stranded DNA genome is contained in the nucleocapsid. The capsid is surrounded by a layer of proteins, the tegument. The envelope is derived from the host cell and contains different glycoproteins necessary for attachment and penetration.

4.1.1 Classification of herpesviruses

The Baltimore scheme simplifies the classification of viruses based on the nature of their genome (RNA or DNA, single-stranded or double-stranded, negative or positive polarity)[13]. Within this scheme, herpesviruses are placed in class I which contains all viral families with a double-stranded DNA genome. Traditional classification follows a phylogenetic system with hierarchical categorization into order, family, subfamily, genus and species. The order *Herpesvirales* was introduced only recently by the International Committee for the Taxonomy of Viruses (ICTV) to reflect the fact that herpesviruses found in fish, frogs and bivalve mollusks are significantly different to mammalian, reptilian and avian members of the formerly single family *Herpesviridae*[5]. In order to appreciate this finding, two additional families, the *Alloherpesviridae* (herpesviruses of fish and frogs) and *Malacoherpesviridae* (herpesviruses of bivalve mollusks) were included in the newly founded order. However, the *Herpesviridae* are currently subdivided into three subfamilies named after the first three letters of the Greek alphabet: *Alphaherpesvirinae*, *Betaherpesvirinae* and *Gammaherpesvirinae*, respectively. All three subfamilies are united by the structural composition of their virions (see Fig. 1), the Baltimore class I DNA genome and capability of causing latent infections (see below). However, they share little genetic overlap, are severely different regarding their replication cycle, host range, host cell tropism and the severity of associated disease[6]. Generally, alphaherpesviruses have a variable host range, fast replication cycles and cause latency in sensory ganglia. Betaherpesviruses, on the contrary, are slowly replicating viruses that have a highly restricted host range. Finally, gammaherpesviruses have a tropism for cells of the immune

system and a narrow host range. Currently, the identification of a large number of distinct herpesvirues infecting elephants has prompted ICTV to consider a new subfamily called deltaherpesviruses[14].

4.1.2 The replication cycle of alphaherpesviruses

Many aspects of the replication cycle of alphaherpesviruses have been studied in the prototypic member Herpes simplex virus type 1 (HSV-1). If not indicated otherwise, the following descriptions are based on those findings.

4.1.2.1 Attachment and penetration

One of the most crucial phases of the viral replication cycle is the actual targeting of the host cell. The process called attachment is subdivided into a more passive phase where viruses approach the cell via Brownian motion and loosely associate/disassociate with the cellular membrane due to unspecific physical interactions[15]. In a second phase, the interaction becomes more specific with cellular receptors on the target cell that interact with integrated glycoproteins of the virion membrane allowing strong binding. The actual entry process of alphaherpesviruses like HSV-1 is mediated by glycoprotein (g)C and glycoprotein B which bind to glycosaminoglycans (GAGs). Secondly, gD interacts with one of at least three currently known cellular receptor molecules, which are nectins, the herpes virus entry mediator (HVEM) or heperan sulfate[6,16]. In a not yet fully understood process gD then forms a complex with gB, gH and gL supposedly inducing a conformational change in the fusogenic gB[16]. gB enables merging of the cellular with the viral membrane. At which site the membrane fusion event takes place might vary since direct membrane fusion at the cellular surface as well as receptor-mediated endocytosis (with subsequent fusion of the vesicle with the viral envelope) have been proposed for HSV-1[17,18]. Following successful release of the viral particle into the cytoplasm the capsid is transported to the nucleus via the microtubule network[19]. Once it reaches the nucleus, the DNA is “injected” into its inside where it circularizes and gene expression as well as DNA replication can proceed[6].

4.1.2.2 Lytic replication

The capability to switch from lytic to latent infection is a defining feature of herpesviruses. During the lytic stage, the virus initially multiplies in specific cell types and produces new particles. Therefore lytic replication serves to massively increase viral progeny. Lytic

replication goes along with the expression of a full set of genes in a hierarchically structured, cascade-like fashion, another hallmark of herpesvirus replication[6]. However, the earliest viral proteins that turn up in the infected cell are those brought in by the tegument[8]. Apart from vhs described earlier, those viral factors include transcriptional activators, which can induce the expression of immediate-early genes (IE or α-genes), the first kinetic class of the cascade, without the need for any *de novo* translation. IE genes mostly encode additional sets of transcriptional regulators that are indispensable for triggering the expression of early genes (E or β-genes), whose products in turn kick off DNA replication. The replication process is primed with short RNA molecules and seems to follow the θ replication model early on during infection[6]. However, to be packed into capsids, the DNA replication must switch to a rolling circle mechanism at one point in order to generate the necessary concatemers which can be cleaved into full-length genomes[10,20,21]. With the onset of DNA replication, the third class, late genes (L or γ-genes), can be transcribed and translated. Proteins of the late class mainly encode the structural components that are necessary to form the capsid, the tegument as well as the glycoproteins[20]. Once the entire process is completed, the virus has transformed the cell into a virus producing factory and cytotoxic effects become visible. However, herpesviruses can also enter a different way of replication that does not lead to progeny and hardly any signs of infection.

.

4.1.2.3 Latency

Latency is defined as a state of persistence of viral genomes in a host cell without production of new virions[6]. The concept of latency was originally described for bacteriophages. For viruses of vertebrates, latency offers the advantage of passive replication along with the genome of the infected host cell. At the same time, the virus can efficiently evade the immune system by minimizing the number of expressed proteins, and thus, presented epitopes. During latency the viral genome can exist in form of a circular episome connected to host chromosomes. Tethering to host chromosomes allows the transfer of episomal DNA to daughter cells during cell division[22]. In addition, some herpesviruses are capable of integrating their genome into host chromosomes, thereby ensuring their replication essentially as a provirus[23]. Latency equals a well-balanced state in which herpesviruses can persist over extremely long periods of time (years to decades) without any obvious activation of the immune system. However, in order to leave the host and infect the next target, herpesviruses have to reactivate and switch back to the lytic cycle again. The exact mechanisms leading to entry into the latent state and the seamless

switch between both stages is one of the most intensively studied areas in herpesvirus research[24].

4.1.2.4 Virion maturation and egress

Virion assembly starts when replicated genomes and components of the capsid (mainly encoded by γ-genes) are available in sufficient amounts. The capsid is filled with a single-unit genome with the help of a specific set of viral enzymes, the terminase complex, as well as signal sequences within the DNA, so called *pac* sequences[25,26]. The loading of capsids is probably mediated by "head full" mechanisms comparable to the processes known for some bacteriophages[6]. How the DNA-filled nucleocapsid finally leaves the nucleus is still hotly debated in the literature. According to the most widely accepted theory, which is backed by an increasing amount of experimental evidence, an envelopment-de-envelopment egress process takes place where capsids bud from the inner nuclear membrane into the perinuclear space, thereby acquiring a primary envelope. In a second step, the capsid buds from the ER into the cytoplasm, thereby losing its primary envelope[27]. Within the cytoplasm, the tegumentation process as well as the secondary envelopment step takes place at the membrane network of the Golgi apparatus[27,28].

.

4.2 Marek's disease virus

4.2.1 History and general facts

Marek's disease (MD) is a progressive cancer disease in chickens, which is caused by an alphaherpesvirus. The first description of MD dates back to the beginning of the last century. A seminal publication by the Hungarian veterinarian Józef Marek described polyneuritis, a general inflammation of the nerves, as a hallmark symptom of a previously unidentified disease in chickens[29]. The symptom that is still seen today in chickens with MD is caused by the infiltration of mononuclear cells of the immune system into nerve tissue thereby leading to inflammation[30]. Only years later, a second syndrome, T cell based lymphomas, was attributed to the same illness[31]. It took until the 1960's to finally identify a herpesvirus as the causative agent of MD, a finding that paved the way for the rapid development of vaccines[32–34]. Today, Marek's disease virus (MDV) is classified as an alphaherpesvirus based on sequence homology with other viruses of the subfamily. MDV is also the type strain for the genus *Mardivirus* (Marek's disease like viruses) and classified as gallid herpesvirus type 2 (GaHV-2) following the current nomenclature. Within the genus, two other viruses are recognized, the apathogenic gallid herpes virus

type 3 (GaHV-3) (formerly MDV-2) and the meleagrid herpesvirus type 1 (herpesvirus of turkey, HVT)[35,36].

MD was the first cancer disease to be prevented by a modified live virus vaccine and MDV vaccines that were developed early after the establishment of the herpesvirus etiology have dramatically decreased morbidity and mortality[29]. However, the costs associated with the disease are still high and represent a massive burden on chicken husbandry worldwide[37]. In addition, the search for yet better vaccines is still ongoing since highly virulent strains of MDV capable of breaking vaccine protection have been isolated during the last decades and are expected to cause problems in the future. In addition, MDV is an excellent model for herpesviral pathogenesis and tumor formation[29].

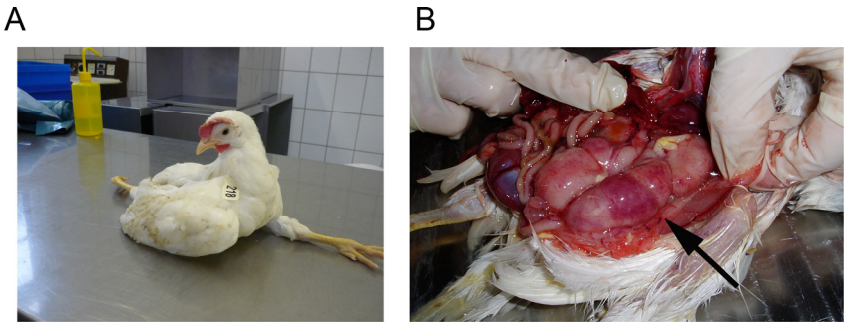

Figure 2: Clinical symptoms of MD. (A) The animal is unable to stand due to virus associated paralysis. Infected lymphocytes infiltrate peripheral nerve tissue and lead to enlargement of the latter. (B) Massive enlargement of the kidneys (arrow) of an infected animal due to progressive tumor development.

4.2.2 MDV genome structure

The genome of MDV represents an E type in which two unique regions, unique long (U_L) and unique short (U_S) are bracketed by inverted repeat elements called internal (I_R) or terminal repeats (T_R) (Fig. 5A).

4.2.3 Replication cycle *in vivo*

In cell culture, MDV is highly cell-associated and shows very slow replication kinetics, with plaques typically appearing only after several days. *In vivo*, comparable to human Epstein-Barr virus (EBV), MDV is highly lymphotropic and infects B and T cells[31]. Apart from its tropism for lymphocytes, our knowledge of the exact sequence of events of MDV infection starting with the uptake of the pathogen from the environment to final shedding of

cell-free virus from feather follicle epithelia still has considerable gaps. The current model (Fig. 3), referred to as the “Cornell model”, proposes that the infectious cycle starts with virus gaining access to the lung of the chicken by inhalation of contaminated dust and dander. Here, antigen-presenting cells (APC) such as macrophages or dendritic cells are supposedly the first to be infected by MDV during the initial phase of replication. While entering secondary lymphoid tissues, the virus then infects B cells, the first target cell for massive lytic replication and production of viral progeny. Subsequently, CD4+ T cells become infected. A subset of these cells act as reservoirs in which the viral latency program is activated about 7 days post infection (dpi). In addition, infected T cells can transport the virus to the feather follicle epithelium in the skin, which in turn becomes infected and sheds viral particles about two weeks post infection. Transformation of individual T cells leads to the formation of solid lymphomas in almost all internal organs, the hallmark of MDV infection, and ultimately death[30].

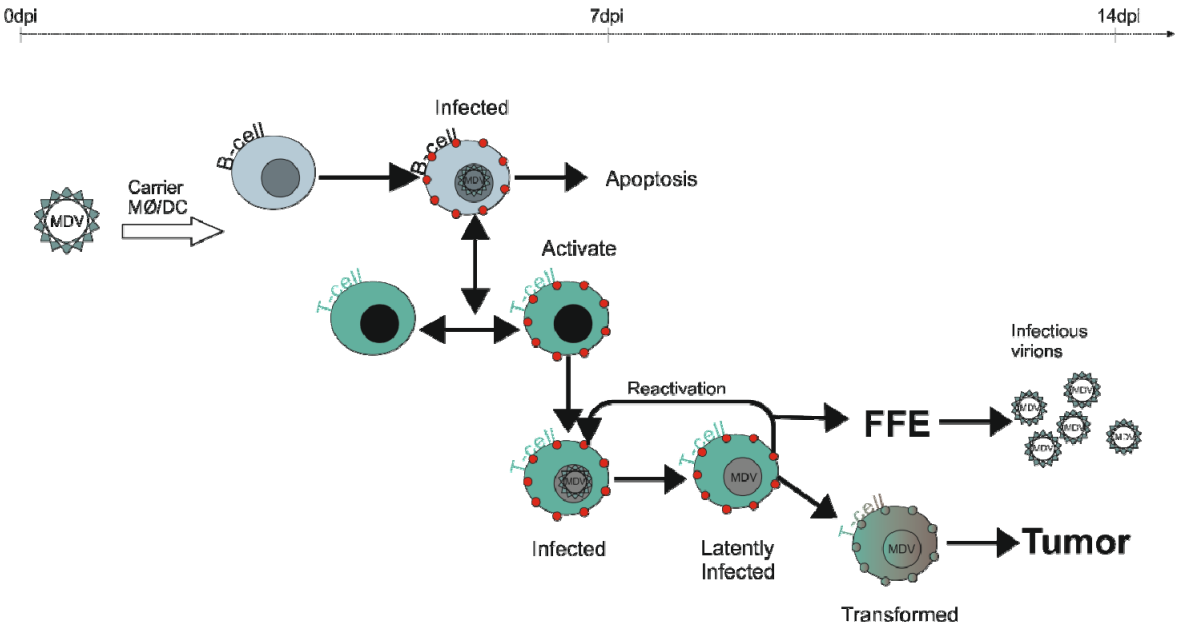

Figure 3: The “Cornell model “of in vivo MDV infection. Virus is taken up with the inhalation of contaminated dust and dander. Supposedly, macrophages and dendritic cells of the lungs are the first cells to be infected. Upon transfer to the lymphoid tissue, B cells become infected and the majority undergoes apoptosis. Virus is transferred from infected B cells to activated T cells, the target cell in which the virus establishes latency 5 to 10 dpi. Around 14 dpi, MDV replication is reactivated in T cells of which some are transported to the feather follicle epithelium of the skin (FFE). Infectious virions are released from infected FFE. Additionally, a minority of T cells become transformed and seed several organs with MD typical lymphomas. MØ: Macrophages; DC: dendritic cells; FFE: Feather follicle epithelium; MDV: Marek’s disease virus. Red dots indicate activated cells. This image was kindly provided by Dr. Annachiara Greco, FU Berlin.

4.3 The vertebrate immune system and viruses

The immune system of vertebrates has been shaped over millions of years while facing the constant bombardment with pathogens of all kinds. It consists of two main lines of defense, the innate and the adaptive immunity. The innate immune system recognizes invariant features of pathogens collectively called pathogen-associated molecular patterns (PAMPs)[38]. Classical examples of PAMPs include the lipopolysaccharide of gram-negative bacteria (LPS) or the double-stranded RNA produced during replication of certain viruses. Detection of those elements by invariant germline encoded receptors, in particular those of the Toll-like and NOD receptor family, allow the early recognition of pathogens based on their biochemical composition and as a consequence the activation of appropriate defense mechanisms[39,40]. Via secretion of cytokines and other soluble mediators that control the proliferation of lymphocytes, the innate system is directly linked to the second arm of the immune system, adaptive immunity. Adaptive immunity is based on receptors that are not invariantly encoded within the genome but underlie extensive mutation and rearrangement in the course of an infection[38]. Compared to the innate system, the adaptive immunity is shaped by clonal expansion of cellular populations, mainly B and T cells, which are capable of responding to small and very specific structures of pathogens with high affinity and accuracy. Taken together, the vertebrate immune system with its several lines of defense is perfectly positioned to ward off viruses.
However, as advanced this system might be in protecting the host, animals and humans still become infected and succumb to disease. This failure can have several reasons. A simple cause might be a poor immune response of the host, which could be too weak, too slow or associated with some kind of deficiency[38]. Active modulation of the immune system by viruses, on the other hand, is a well-known pathogenic principle and an intensively investigated field. In the constant evolutionary arms race with their hosts, herpesviruses have evolved strategies to counteract both arms of the immune system. Innate immune defense can be brought down by virus encoded decoy receptors, virokines (viral proteins that mimic host cytokines) and other factors that either directly interfere with the sensing of PAMPs or downstream signaling events, respectively[41–43].
However, overcoming the innate mechanisms of immune defense is only one side of the coin. For viruses which stay with their hosts over extended time periods, control of the adaptive immunity is essential since this arm holds long term infections at bay and generates immunological memory. As mentioned earlier, adaptive responses are mainly based on the clonal expansion of cells carrying very specific receptor molecules. B cells produce antibodies capable of neutralizing viruses and T helper cells of the CD4 positive type are crucial in directing the humoral response[38]. CD8 positive cytotoxic T lymphocytes

(CTLs) monitor the state of infection by specific interaction with major histocompatibility (MHC) class I molecules presenting viral antigens on the cell surface. Whenever a given T cell receptor is specific for the displayed antigen and at the same time induced by additional co-stimulatory molecules expressed on the presenting cell, it will expand and form a population of armed effector T cells (as well as memory cells) that destroy infected cells by inducing apoptosis[38]. The destruction of infected cells before infectious virions have been produced is obviously detrimental for the virus. Therefore, herpesviruses have evolved strategies to counteract the MHC class I pathway and basically every step of the pathway is tackled by one or another viral protein[44–46].

4.3.1 The MHC class I complex, MHC class I loading and transport, and herpesviral MHC class I evasion

Instead of being randomly distributed in the vertebrate genome, genes that encode immune- related proteins, enzymes and receptors are clustered in the MHC locus. This locus, which in humans is also called human leucocyte antigen (HLA), encodes molecules that together direct immune responses, trigger autoimmune diseases and are responsible for graft rejection after transplantation[38]. In humans, the large MHC encodes for more than 200 genes, contains several pseudogenes and therefore spans several megabases. A peculiarity of the chicken genome is a very small and compact MHC (also called B-F/B-L region), which only encodes around 20 genes and is largely devoid of pseudogenes or large intergenic regions. That is why it has been defined as the “minimal essential MHC”[47,48]. The MHC I region encodes the components that are necessary to build the MHC class I heterodimer. Humans have different MHC class I molecules being co-dominantly expressed from different HLA alleles (A, B and C) on the surface of nucleated cells. The polygenic and polymorphic nature of MHC class I expression enables humans to present a large variety of different epitopes from many different pathogens[38]. In contrast, chickens only express a single predominant haplotype, a factor that is decisive for the susceptibility or resistance to different pathogens[48].

The pathway leading to the display of loaded MHC class I starts with a high-molecular weight machinery located in the cytosol, the proteasome. The cylindrical, multimeric protease assembly is responsible for the degradation of proteins and their turnover. More importantly, it is the central engine of immunosurveillance since it degrades proteins into short peptides of 8-15 amino acids (aa) in length, which can subsequently be loaded onto MHC class I molecules[38]. Interestingly, the activity of the proteasome is stimulated by interferon (IFN)-γ, a cytokine released by cells in response to infection[38]. IFN-γ drives the expression of catalytic proteasome subunits that differ in activity from the standard

subunits contained in the housekeeping proteasome. The immunoproteasome, as it is referred to, generates peptides with higher efficacy and with a sequence context that is more efficiently loaded on MHC class I molecules[49]. Following cleavage, peptides are transported across the membrane of the ER in an energy-dependent fashion. The molecule responsible for this transport, TAP, is described in detail below. Within the ER lumen a partially folded MHC class I precursor molecule consisting of a heavy chain monomer associated with the small subunit, the b2-microglobulin (β2m), awaits loading of the peptide cleft. Correct folding of the MHC molecule and positioning of the peptide is directed by a multimeric protein complex, the peptide-loading complex (PLC). The PLC incorporates chaperones, trimming proteins which modify the length of peptides, and quality control enzymes[50]. The peptides are fixed in a groove that consists of two α-helical domains that are displayed on top of eight β-strands together forming a cleft. The peptide is bound via its N-terminal region and C-terminus in addition to 2 to 3 internal anchor residues that have complementary pockets within this cleft. Peptide loading stabilizes the MHC molecule which is subsequently transported to the cellular membrane via the secretory pathway. After arrival at the plasma membrane, the molecule awaits the interaction with CTLs[50–52] (Fig. 4).

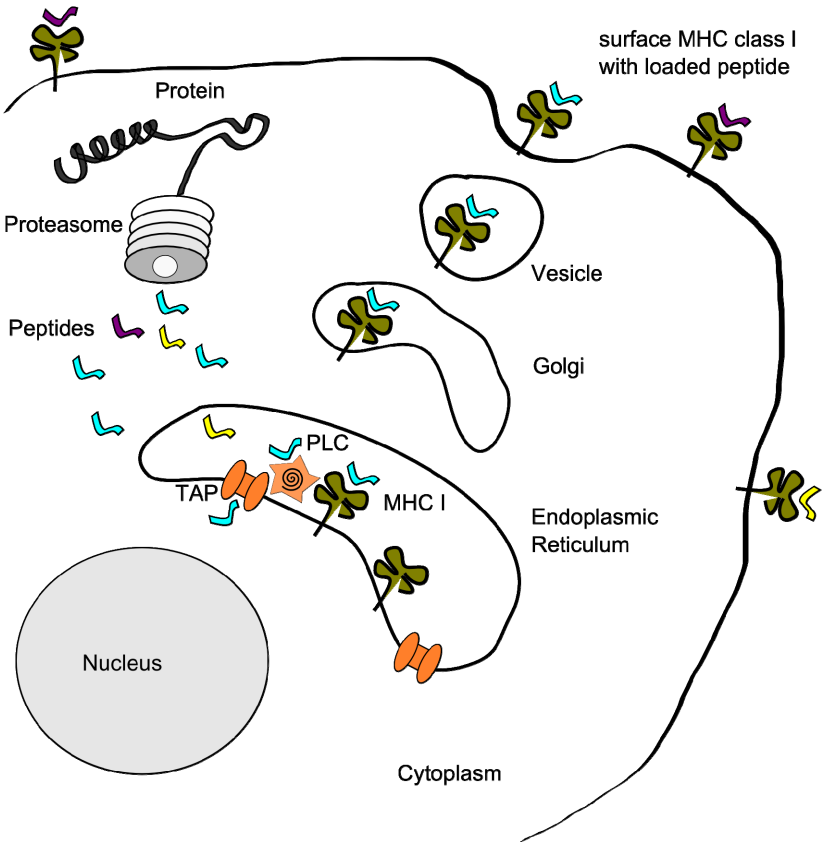

Figure 4: The MHC class I pathway. See text for details.

In theory all proteins can be degraded by the proteasome; however, the origin of peptides that are threaded into the MHC class I pathway is still hotly debated. Two main school of thoughts exist and favor different theories of protein degradation. Firstly, proteins can be degraded by the proteasome in the cause of their normal turnover, such substrates are referred to as “retirees”[53]. However, it was argued that many proteins, in particular those of viral origin, are actually highly stable with half lives of many hours or even days within the cell. This is in stark contrast with the finding that viral epitopes can be detected on the surface of infected cells within minutes following infection[54]. Thus, an alternative model argues that a large variety of epitopes is immediately generated during translation from so called defective ribosomal particles (DRIPS). DRIPs basically represent translation products that were misfolded and/or prematurely terminated at the ribosome. At present, estimations credit about 70% of all presented peptides to DRIPS[38,55,56]. The origin of peptides is further complicated by the fact that ER-resident proteases could also be responsible for degradation of proteins immediately within the lumen and without the necessity for prior peptide import[57]. Increasing evidence also exists for translation of proteins inside the nucleus of cells. Since the nuclear membranes are contiguous with ER membranes, those peptides could also reach the ER lumen and be presented in a TAP-independent manner[58,59].

The more proteins are produced during the replication cycle of a herpesvirus, the more different peptides will be generated and sampled for presentation on the cellular surface. That is why large DNA viruses have to invest a considerable part of their coding capacity into the maintenance and expression of immune modulating proteins, so-called immune evasins. As outlined earlier, herpesviruses stay with their host for long periods of time and have to make sure they shield themselves from immunosurveillance. The importance of this evasion concept is underlined by the fact that every step of the MHC I loading pathway is tackled by at least one herpesviral protein[41,42]. The points of attack can be roughly divided into pre- and post-TAP translocation steps. Classical mechanisms that act prior to TAP-mediated peptide translocation include interference with proteasome-mediated degradation. The EBV nuclear antigen 1 (EBNA1) has been described to interfere with its own degradation as well as translation thereby decreasing the amount of peptides available for presentation[60]. The MHC class I molecule itself is directly tackled by the human cytomegalovirus (HCMV) US2 and US11 proteins which lead to the proteasome-dependent degradation of the molecule[61,62]. In this way, the total amount of available MHC molecules is greatly reduced. Additionally, MHC class I can be retained in the ER or Golgi by the action of HCMV US3 or varicella zoster virus (VZV) ORF66 and, thus, never reaches its destination on the cell surface[63,64]. Once the MHC molecule has

reached the cellular surface, the Kaposi's sarcoma-associated herpesvirus (KSHV) proteins Kk3 and kk5 can mediate internalization by ubiquitination or re-routing to the lysosomal compartment[65]. Recently, the ORF1 gene of equine herpesvirus type 1 (EHV-1), a homologue of the alphaherpesviral UL56, has been shown to encode an early phosphoprotein capable of re-routing MHC class I to lysosomes[66,67]. Apart from these strategies, direct interference with TAP is an efficient way of limiting peptide transport and loading of MHC class I molecules.

4.3.2 TAP transport and its evasion by alphaherpesviruses

TAP is a central unit within the MHC class I pathway since it mediates the communication of the two compartments necessary for peptide generation and loading, the cytoplasm and the ER lumen. TAP is a heterodimer of the proteins TAP1 and TAP2 which do not share extensive sequence homology but a similar structure. Both proteins belong to the family of ATP-binding cassette transporters[68]. A conserved feature of those membrane integral proteins is a hydrophobic transmembrane domain (HTD) consisting of several membrane loops and a nucleotide-binding domain (NBD). In the case of TAP, this molecular architecture is realized by 10 membrane spanning loops (or 9 in the case of TAP2, respectively) and a C-terminally located NBD facing the cytoplasm[69,70]. The heterodimer has a so called `2×6` symmetrical core where 6 transmembrane helices and the NBDs of each protein come together to form a central structure. This core is sufficient and necessary for peptide transport. The remaining 4 transmembrane loops (or 3 in the case of TAP2, respectively) link the TAP to the PLC on the ER luminal side[71,72]. The mechanistic steps necessary for TAP transport are not defined in detail yet, but the widely accepted model proposes a three step sequence. In a first step, the peptide binds the core unit in an ATP-independent fashion. This binding is supposed to induce a conformational change which allows subsequent binding and hydrolysis of ATP at the NBD providing the energy for translocation of the peptide[73]. Within the ER membrane, the heavy chain of the premature MHC class I molecule is properly folded by the action of the chaperones calnexin and, at later stages, calreticulin. In addition, the protein ERp57 creates intermolecular disulfide bridges that stabilize the molecule[38]. The heavy chain then associates with β2m, thereby forming a peptide-receptive structure. Finally, the protein tapasin links the MHC-PLC complex to TAP via its membrane domains[72]. Tapasin is also involved in the quality control of peptides loaded on MHC[74]. TAP can transport peptides from 8 to 40 aa in length. However, the average size of translocated peptides is 8-11 aa, the length that can be most efficiently accommodated in the MHC cleft[75]. In addition, peptides can be trimmed in the ER by the specific action of the ER

aminopeptidase (ERAP)[76]. The central role of TAP in the MHC class I pathway makes it an attractive target for viral interference.

So far, several herpesviral genes have been shown to modulate TAP activity. One of the best studied is the HSV ICP47, a cytosolic protein that interacts with TAP and competes with peptide binding[77,78]. Furthermore, HCMV US6, encoding a class I membrane protein, binds TAP and interferes with ATP binding[79]. Accordingly, peptides can bind to the transporter but not be transported due to the lack of energy conversion. As would be expected, it has been shown experimentally that deletion of the described genes often leads to increased presentation of virus derived peptides on cellular surface. Interestingly, many of the classical alphaherpesviral MHC class I immune evasins are not encoded in the MDV genome[80]. The exception is a protein called pUL49.5 which interferes with TAP.

The UL49.5 gene encodes for a small, non-essential type I membrane protein which is conserved in all herpesviruses[81]. Whereas pUL49.5-TAP interaction seems to be a common theme in all alphaherpesviruses, only some members of the *Varicellovirus* genus were shown to utilize pUL49.5 in order to downregulate MHC class I expression by TAP interference[82–84]. Interestingly, this TAP interference is achieved by entirely different ways for different viruses. Firstly, the EHV-1 and the pseudorabies virus (PRV) pUL49.5's are capable of locking TAP in a translocation-incompetent state, probably by inducing conformational changes[83]. The EHV-1, but not PRV, protein additionally blocks ATP binding thereby preventing energy conversion necessary for the translocation. pUL49.5 of the bovine herpesvirus type 1 (BHV-1) also locks TAP in a translocation-incompetent state and has further evolved a second way of interference, ubiquitin-mediated degradation of TAP[82,83]. As a consequence, the actual amount of TAP in the ER membrane is reduced and the MHC class I pathway is cut off its peptide supply. It is quite amazing that this conserved protein has evolved several different ways of TAP interference. It is not clear what controls these different functions on a molecular level but they might be due to slightly different structural alterations induced by pUL49.5[85]. In addition, different functions can be assigned to different parts of the small protein. pUL49.5 consists of a short N- and C-terminal domain, respectively, which are connected by a single transmembrane region (Fig. 5B). Extensive studies in the *Varicelloviruses* indicated that the C-terminal domain mediates TAP degradation but is not involved in translocation arrest. Accordingly, C-tail deletion proteins did not reduce TAP levels but were still capable of transport inhibition[85]. Subsequently, a conserved arginine rich motif in the C-tail was identified as being crucial for degradation. In contrast, the N-terminus seems to mediate the translocation arrest of TAP[85]. Currently, the role of pUL49.5 in MDV MHC class I downregulation is not clear.

4.4 Project Introductions

4.4.1 Project 1: Functional investigation of MHC class I downregulation by MDV pUL49.5

Immunomodulation is an intensively studied field in herpesvirology, but the literature available on MHC class I downregulation as a consequence of MDV infection is not very extensive.

First investigations by Hunt *et al.* from 2001 showed that MDV induced a drastic reduction of MHC class I expression on the surface of infected cells during lytic replication *in vitro*[86]. Initial flow cytometry experiments where based on *in vitro* infection assays using the permanent chicken cell line OU2, which expresses high levels of MHC class I. MHC I downregulation could also be confirmed following reactivation of MDV from latently infected tumor cell lines[86]. With the clear indication that surface levels of MHC class I were reduced, it was subsequently demonstrated that the entire intracellular pool of MHC molecules remained unaffected during infection. Thus, a specific downregulation of MHC I at the posttranscriptional and posttranslational stage was suggested[86]. However, the responsible proteins still remained enigmatic, in particular since MDV lacks many of the classical MHC class I inhibitors encoded by other herpesviruses. Nevertheless, the conserved UL49.5 gene is also present in MDV and it was speculated that MHC class I downregulation could be due to its specific interference with TAP[87]. Interestingly, MDV pUL49.5 shares the structural features of other homologues, but a publication by Tischer et al. provided evidence that a UL49.5 deletion virus was not viable, a unique characteristic that separated MDV from all other herpesviruses for which UL49.5 was dispensable[88]. The lethal phenotype of the UL49.5 deletion virus largely abrogated the possibility to investigate the protein during infection. Therefore, Jarosinski *et al.* generated a mutant virus in which only the C-terminal domain of pUL49.5 encompassing 12 aa, was deleted. Surprisingly, this virus grew to titers comparable to the wildtype virus. In accordance with infection experiments performed with BHV-1, the C-terminal deletion of MDV pUL49.5 increased the amount of MHC class I on the surface of infected OU2 cells in comparison to the parental wildtype[87]. These results indicated that TAP degradation mediated by the C-terminus of pUL49.5 could indeed play a role in MDV MHC class I downregulation.

The authors also demonstrated surface MHC class I downregulation in the chicken B cell line RP9 which was transiently transfected with an expression plasmid encoding MDV UL49.5[87]. Nevertheless, mechanistic studies were not performed at this stage and a mode

of action for MDV pUL49.5 remained elusive. Currently, little is known about the impact of MHC class I evasion on dissemination of MDV in the chicken, progression of the disease and formation of tumors. The project described here presents a follow-up study based on the two UL49.5 studies. The three main goals were:

1. Generation of an MDV pUL49.5-specific antibody as a tool for future research

2. Characterization of MDV pUL49.5's mode of action in MHC class I downregulation with particular focus on TAP interference

3. Investigation of the relevance of this process with regard to dissemination of virus *in vivo*, tumor formation as well as production of free virus in the feather follicle epithelium of chickens

4.4.2 Project 2: Identification and functional characterization of the predicted MDV ORF012 gene

The genes and gene products that execute the complicated viral replication cycle of MDV are encoded in a 180 kbp double-stranded DNA genome. MDV contains more than 100 genes or open reading frames (ORFs) of which the vast majority have orthologues encoded within the U_L and U_S regions of HSV-1 accordingly annotated as such for MDV nomenclature (e.g, MDV UL49.5). Notwithstanding the extensive homology to other alphaherpesviruses, some regions of the MDV genome are truly unique and contain genes that are not found in any other herpesvirus described so far. Among these unique genes are the multifunctional Meq gene[89] and a virokine called viral interleukin 8 (vIL-8)[90,91], which are encoded in the TR_L and IR_L, respectively. Both Meq and vIL-8 have been the subject of extensive functional studies in the past and were shown to play critical roles in tumor formation (Meq) and replication (vIL-8)[92–94].

Despite the wealth of information on the role of some MDV genes, other genome regions contain distinctive genes whose functions remain to be elucidated. In particular, the 5' end of the MDV U_L region, positioned upstream of the U_L1 gene (a homologue of the HSV-1 gene encoding envelope protein gL), is poorly characterized in this regard. Remarkably, this region contains several potential ORFs that seem to be present only in avian alphaherpesviruses suggesting they may govern host-specificity of the bird viruses[95,96]. Within this relatively unexplored region, only ORF010 was characterized in some detail.

ORF010 encodes a lipase-like enzyme (referred to as vLip), which lacks catalytic activity, but nevertheless is required for efficient replication of the virus[97].

Downstream of ORF010, two predicted ORFs were originally annotated as ORF011 and ORF012 and predicted to express two distinct proteins[80] (Fig. 12). From herein, I will refer to these ORFs as ORF011* and ORF012*. Following the original annotation of the MDV reference sequence for the Md5 strain in 2000, the most recent annotation postulated splicing within the ORF011* and ORF012* region leading to a single ORF called MDV ORF012 (Refseq NC_002229)[98]. ORF011* was consequently excluded from the annotation leaving a gap between ORF010 and the postulated novel ORF012. However, these predictions were solely based on bioinformatic and comparative analyses rather than experimental approaches. Further bioinformatic analysis predicted the presence of a nuclear localization signal (NLS) in the C-terminal domain of the putative protein. Apart from these predictions no further information on ORF012 was available in the past.

Nuclear import and export – mechanisms and signal sequences

Small proteins and molecules can usually traverse freely between the cytoplasm and the nucleus by diffusion[99]. By default, diffusion is a slow process which also cannot work against gradients. However, in order to concentrate functionally important proteins or those that are too large to enter the nucleus by passive means, active and energy driven mechanisms of nuclear transport are necessary. Indeed, nuclear import of proteins is a highly regulated process. A NLS embedded in the sequence of the protein, carrier proteins that specifically bind to the NLS, a Ran-GTP/GDP exchange cycle creating a gradient over the nuclear membrane and finally a nuclear pore are crucial. Classical NLS come in monopartite and bipartite forms, both of which contain basic arginine or lysine residues[100–102]. A simple NLS was first described in the large T antigen of SV40 virus that contains the amino acid sequence PKKKRKV in its C-terminal region[103]. This archetypical NLS now represents the prototype of monopartite NLS with the general motif K-K/R-X-K/R[101]. The bipartite NLS was first identified within the nucleoplasmin protein of *Xenopus* oocytes[104]. It contains an arginine dipeptide motif followed by a spacer of 9 to 10 amino acids and a second stretch of basic residues, KR-9/10(X)-KKKK[101,104]. In recent years, the identification of non-classical NLS, some of them containing unexpected hydrophobic sequence, has added more complexity to the field. In particular, the so called M9 sequence consisting of 38 aa and those NLS containing a characteristic PY motif have been identified lately[105,106]. Despite their variable appearance, NLS represent docking sites for nuclear carrier proteins. Mechanistically, a group of proteins called importins regulate the transport of proteins carrying a classical NLS[99]. In a first step, importin α

binds the classical NLS with an arginine-rich binding domain. Subsequently it interacts with importin β via the importin β- binding (IBB) domain. In contrast, non-classical NLS directly bind importin β, eliminating the need to interact with importin α first[99]. Furthermore, non-classical NLS of certain proteins are bound by an entirely different class of carrier called transportin[107]. Despite this obvious complexity, the common theme in nuclear transport seems to be carrier-mediated contact with the nuclear pore complex (NPC) during translocation[99]. The structural composition of the NPC, a ring-like complex that sits between the inner and outer leaflet of the nuclear envelope, is largely conserved across different species. The macromolecular complex consists of about 30 different proteins that form a pore in the nuclear membrane[108]. Once the carrier-cargo complex has traversed the NPC, it dissociates in the nucleus due to the binding of Ran-GTP, a small monomeric GTPase which is part of the Ras superfamily[99]. Like all GTPases, Ran can exist in a GTP- as well as GDP-bound form. Ran-GTP is mainly found in the nucleus whereas Ran-GDP predominates within the cytoplasm. This gradient is absolutely critical to drive nuclear import as well as export. Within the nucleus, Ran becomes loaded with GTP by the action of GDP/GTP exchange factors[99]. Ran-GTP binds to importin β thereby releasing the import complex. Subsequently, the Ran-GTP-importin complex leaves the nucleus. In the cytoplasm Ran-GTP is converted to Ran-GDP, importin is released, and both factors are ready to shuttle back into the nucleus[99]. The export of proteins runs in the opposite direction and so-called exportins participate in this process[109]. However, the signals that mediate export differ considerably from those that control import. Usually nuclear export signals (NES) are rich in leucines and mostly contain a motif with the sequence LxxxLxxLxL, where x is any amino acid[109]. The combination of a NES and NLS within a single protein allows its shuttling between both compartments.

The three main goals of this project were:

1) Verification of the predicted novel ORF012 and splicing of its mRNA

2) Detailed characterization of the ORF012-encoded protein (p012)

3) Investigations into the function of the protein during MDV infection

Parts of this project have been published in:
The ORF012 gene of Marek's disease virus (MDV) produces a spliced transcript and encodes a novel nuclear phosphoprotein essential for virus growth. Schippers T, Jarosinski K, Osterrieder N. J Virol. 2014 Nov 12. pii: JVI.02687-14. [Epub ahead of print]

.

5. Materials and Methods

5.1 Materials

All chemicals indicated below were used according to the instructions of the manufacturer.

5.1.1 Chemicals, consumables and equipment

5.1.1.1 Chemicals

Name	Type/Cat.No.	Company
Acetone ($(CH_3)2CO$)	[Cat. No. A160, 2500]	Applichem, Darmstadt
Agar (agar bacteriological)	[Cat. No. 2266.2]	Carl-Roth, Karlsruhe
Agarose- Standard Roti® grade	[Cat. No.3810.4]	Carl-Roth, Karlsruhe
Ampicillin Na-salt	[Cat. No.K029.2]	Carl-Roth, Karlsruhe
Ammonium chloride (NH4Cl)	[Cat. No. A9493]	Sigma-Aldrich, St Louis
Ammoniumpersulfate	[Cat. No. K38297601]	Merck, Darmstadt
Arabinose L (+)	[Cat. No. A11921]	Alfa Aesar, Karlsruhe
Bafilomycin A	[Cat. No. B1793]	Sigma-Aldrich, St Louis
BSA (albumin bovine fraction V)	[Cat. No. A6588.0100]	Applichem, Darmstadt
CaCl2 (calcium chloride) dihydrate	[Cat. No. T885,2]	Carl-Roth, Karlsruhe
CH3COOH (acetic acid)	[Cat. No. A3686, 2500]	Applichem, Darmstadt
Chloramphenicol	[Cat. No. 3886.1]	Roth, Karlsruhe
Chloroform	[Cat. No. 411 K3944831]	Merck, Darmstadt
Chloroquine	[Cat. No. PHR1258]	Sigma-Aldrich, St Louis
Digitonin	[Cat. No. 300410]	Calbiochem, Carlsbad
Dimethyl sulfoxide (DMSO)	[Cat. No. 1.02952.2500]	Merck, Darmstadt
dNTP Mix (10mM total)	[Cat. No. BIO-39053]	Bioline, Luckenwalde
EDTA (ethylendiamine tetraacetic acid)	[Cat. No. A2937, 1000]	Applichem, Darmstadt
Emulsigen adjuvant	-	MVP Tech., Omaha
Ethidium bromide 1%	[Cat. No. 2218.2]	Carl-Roth, Karlsruhe
EtOH den. absolute	[Cat. No. A1613]	Applichem, Darmstadt
FACS Rinse	[Cat. No. 340346]	BD, San Jose
FACS Clean	[Cat. No. 340345]	BD, San Jose
Fast media hygroagar	[Cat. No. FAS-HG-S]	Invivogen, San Jose

Fugene HD	[Cat. No. E2311]	Promega, Mannheim
Glycerol	[Cat. No. A2926,2500]	Applichem, Darmstadt
HCl 37% (hydrochloric acid)	[Cat. No. 4625.2]	Roth, Karlsruhe
Hoechst 33342, Trihydrochloride, Trihydrate	[Cat. No. H3570]	Invitrogen Life Technologies, Eugene
Isopropyl alcohol (2-propanol)	[Cat. No. A0892]	Applichem, Darmstadt
Kanamycin sulphate	[Cat. No. T832.2]	Carl-Roth, Karlsruhe
KCH3CO2 (potassium acetate)	[Cat. No. A4279,0100]	Applichem, Darmstadt
Lactacystin	[Cat. No. L6785]	Sigma-Aldrich, St Louis
Leptomycin B	[Cat. No. L2913]	Sigma-Aldrich, St Louis
Lipofectamine 2000	[Cat. No. 11668027]	Life Tech., Carlsbad
β-mercaptoethanol (2-mercaptoethanol)	[Cat. No.28625]	Serva, Heidelberg
MG132	[Cat. No. M7449]	Sigma-Aldrich, St Louis
Mounting Medium Vectashield with DAPI	[Cat. Nr: H-1200]	Vector Laboratories Inc, Burlingame
NaCl (sodium chloride)	[Cat. No. A3597,5000	Applichem, Darmstadt
NaOH (sodium hydroxide)	[Cat. No. 1.06462]	Merck, Darmstadt
Optimem	[Cat. No. 31985062]	Life Tech., Carlsbad
Paraformaldehyde	[Cat. No. P6148]	Sigma-Aldrich, St Louis
Permfluor Mounting Medium	[Cat. No. TA-030_FM]	Thermo Scientific, Darmstadt
Phenol/Chloroform	[Cat. No. A0889,0500]	Applichem, Darmstadt
Phos-tag	[Cat. No. AAL-107]	Wako Chemicals, Neuss
Roti-Phorese Gel 30	[Cat. No. 3029.1]	Roth, Karlsruhe
Roti™-Phenol	[Cat. No. 0038.3]	Roth, Karlsruhe
Saponin	[Cat. No. S7900]	Sigma-Aldrich, St Louis
SDS (sodium dodecyl sulfate)	[Cat. No. 75746]	Sigma-Aldrich, St Louis
Sodium Phosphate, monobasic, monohydrate	[Cat. No. S9638]	Sigma-Aldrich, St Louis
di-Sodium Hydrogenophsohate dodecahydrate	[Cat. No. A3906]	Applichem, Darmstadt
Temed	[Cat. No. 2367.3]	Roth, Karlsruhe
Tris	[Cat. No. A1086,5000]	Applichem, Darmstadt
Triton X-100 detergent	[Cat. No. 8603]	Merck, Darmstadt
Tween-20	[Cat. No. 9127.2]	Roth, Karlsruhe
Water Molecular biology grade	[Cat. No. A7398]	Applichem, Darmstadt

5.1.1.2 Consumables

Name	Feature/Cat.No.	Company
Cell culture dishes	6-well, 24-well	Sartsedt, Nümbrecht
Cell culture flasks	25 ml, 75 ml	Sartsedt, Nümbrecht
Conical test tubes 17x120 (15 ml)	-	Sartsedt, Nümbrecht
Conical test tubes 30x115 (50 ml)	with and without feet	Sartsedt, Nümbrecht
Cryotubes 1.8 ml	-	Nunc, Kamstrupvej
BD Falcon Cell Strainers	[Cat. No. 352340]	BD Falcon, San Jose
Eppendorf tubes	1.5 and 2 ml	Sarstedt, Nümbrecht
Expendable cuvettes	-	Biodeal, Markkleeberg
Kimtech Science, Precision Wipes	[Cat. No 05511]	Kimberly-Clark, Roswell
Microscope cover glasses	[Cat. No. ECN631-1569]	VWR, Sacramento
Nitrile gloves	-	Hansa-Medical 24, Hamburg
Parafilm® M	-	Bems, Neenah
Pipettes	5, 10, 25 ml	Sarstedt, Nümbrecht
Pipette tips	P1000, 200, 100 and 10	VWR International, West Chester
dishes for cell culture	60 mm, 100 mm, 150 mm	Starstedt, Nümbrecht
Petri dishes for bacteria	-	Sarstedt, Nümbrecht
PVDF 0.45	[Cat. No. T830.1]	Roth, Karlsruhe
SuperFrost® Plus	[Cat. No. J1800AMNZ]	Menzel Glaser, Braunschweig
Transfection polypropylene tubes	-	TPP, Trasadingen
Whatmann blotting paper	(WM Whatmann 3MM)	GE Healthcare, Freiburg
Sterile syringe filters PVDF	0,45 µm	VWR International, West Chester

5.1.1.3 Equipment

General Equipment

Name	Feature/Cat.No.	Company
Bacterial incubator	07-26860	Binder, Turtlingen
Bacterial incubator	shaker Innova 44	New Brunswick Scientific, New Jersey
Bunsen burner	Type 1020	Usbeck, Radevormwald
Cell incubators	Excella ECO-1	New Brunswick Scientific, New

		Jersey
Centrifuge 5424,	Rotor FA-45-24-11	Eppendorf, Hamburg
Centrifuge 5804R,	Rotors A-4-44 and F45-30-11	Eppendorf, Hamburg
Chemismart imaging system	5100	Peqlab, Erlangen
Electroporator	Genepulser Xcell	Bio-Rad, Munich
Electrophoresis power supply Power Source 250 V		VWR International, West Chester
FACScalibur flow cytometer	FACScalibur	BD Bioscience, San Jose
Freezer -20°C	-	Liebherr, Bulle
Freezer -80°C	-	GFL, Burgwedel
Galaxy mini centrifuge	-	VWR International, West Chester
Gel electrophoresis chamber Mini Electrophorese System	-	VWR International, West Chester
Gel electrophoresis chamber	SUB-Cell GT	Bio-Rad, München
Ice machine	AF100	Scotsman, Vernon Hills
INTEGRA Pipetboy	-	IBS Integrated Biosciences, Fernwald
Magnetic stirrer RH basic KT/C	-	IKA, Staufen
Mini Protean 2D gel chambers	Protean	Biorad, München
Protean Tetra Cell chambers	Protean	Biorad, München
Photospectrometer	Nanodrop 1000	Peqlab, Erlangen
Newbauer counting chamber	-	Assistant, Sondheim/Rhön
Nitrogen tank	ARPEGE70	Air liquide, Düsseldorf
Orbital shaker	0S-10	PeqLab, Erlangen
Pipetman	P1000, P100, P10	VWR International, West Chester
Perfect Blue™ Horizontal Maxi-Gel System	Perfect Blue	PeqLab, Erlangen
pH-meter	RHBKT/C WTW pH level 1	Inolab, Weilheim
Sterile laminar flow chambers	-	Bleymehl, Inden
Thermocycler Flexcycler	ThermoFlex	Analytik Jena, Jena
Thermocycler	GeneAmp PCR System 2400	PerkinElmer, Waltham
Thermocycler	T-Gradient	Biometra, Göttingen
UV Transiluminator	Bio-Vision-3026	PeqLab, Erlangen
Transiluminator printer	P93D	Mitsubishi, Rüsselsheim
Transiluminator	VL-4C, 1x4W-254 nm	Vilber-Lourmat, Eberhardzell
Vortex	Genie 2™	Bender&Hobein AG, Zurich
Water baths	TW2 and TW12	Julabo, Seelbach
Water bath shaker	C76	New Brunswick Scientific, New Jersey

Microscopes

fluorescence microscope	Axiovert S 100	Carl Zeiss MicroImaging GmbH, Jena
fluorescence microscope	Axio-Observer.Z1	Carl Zeiss MicroImaging GmbH, Jena
Microscope AE20	AE20	Motic, Wetzlar

5.1.1.4 Software

software for Zeiss microscopes	Axiovision 4.8	Carl Zeiss MicroImaging GmbH, Jena
Chemi-Capt	-	Vilber-Lourmat, Eberhardzell
Graphpad Prism 5	Version 5	Graphpad Software Inc, La Jolla
Image J 1.41	Version 1.41	NIH, Bethesda
ND-1000	V.3.0.7	PeqLab, Erlangen
Vector NTI 9	Version 9	Invitrogen Life Technologies, Grand Island
Vision-Capt	-	Vilber-Lourmat, Eberhardzel

5.1.2 Enzymes and markers

Name	**Cat.No.**	**Company**
ApaLI	[Cat. No. R0507L]	New England Biolabs, Ipswich
AvrII	[Cat. No. R0174S]	New England Biolabs, Ipswich
BamHI	[Cat. No. R0136]	New England Biolabs, Ipswich
BamHI HF	[Cat. No. R3136]	New England Biolabs, Ipswich
DpnI	[Cat. No. ER1701]	New England Biolabs, Ipswich
EcoRI	[Cat. No. R0101	New England Biolabs, Ipswich
EcoRI HF	[Cat. No. R3101]	New England Biolabs, Ipswich
EcoRV	[Cat. No. R0195]	New England Biolabs, Ipswich
HindIII	[Cat. No. R0104]	New England Biolabs, Ipswich
KpnI	[Cat. No. R0142L]	New England Biolabs, Ipswich
Lamba protein phosphatase	Cat. No. P07535]	New England Biolabs, Ipswich
NotI	[Cat. No. R0189]	New England Biolabs, Ipswich
Phusion Hot Start High-Fidelity DNA Polymerase	[Cat. No. M0530S]	New England Biolabs, Ipswich
Proteinase K	[Cat. No. 7528.2]	Finnzymes, Thermo Scientific, Rochester

RNase A	[Cat. No. 7528.2]	Carl-Roth, Karlsruhe
RNase free DNAse	[Cat. No. 19253]	Qiagen, Hilden
SacI	[Cat. No. R0156L]	New England Biolabs, Ipswich
Taq DNA-Polymerase	[Cat. No.01-1020]	PeqLab, Erlangen
T4 ligase	[Cat. No. M02025]	New England Biolabs, Ipswich
XbaI	[Cat. No.R0145S]	New England Biolabs, Ipswich
XmaI	[Cat. No R0180S]	New England Biolabs, Ipswich
Protein Prestained plus marker	[Cat. No. 26619]	Thermo Scientific,
Generuler TM 1kb Plus DNA	[Cat. No. SM0311]	Darmstadt
Ladder		Fermentas, Mannheim

5.1.3 Plasmids

Name	**Cat.No.**	**Company**
pcDNA3.1 (-)	[Cat. No. V795-20]	Invitrogen, Carlsbad
pEGFP-C1	[Cat. No. 632470]	Clontech, Mount View
pVitro-2-Hygro-MCS	[Cat. No. pvitro-mcs]	Invivogen, San Diego

5.1.4 Antibodies

Name	**Dilution**	**Company**
Chicken anti MDV US2, polyclonal	1:1,000	[110]
Alexa goat anti-chicken IgG (H+L) 488	1:1,000	Invitrogen Life Technologies, Grand Island
Alexa goat anti-chicken IgG (H+L) 546	1:1,000	Invitrogen Life Technologies, Grand Island
Alexa goat anti-rabbit IgG (H+L) 568	1:1,000	Invitrogen Life Technologies, Grand Island
Alexa goat anti-mouse IgG (H+L) 647	1:1,000	Invitrogen Life Technologies, Grand Island
Goat anti-mouse HRP	1:5,000	Sigma-Aldrich, St Louis
Goat anti-rabbit HRP	1:5,000	Cell Signaling, Boston
Rabbit anti- 6xHis epitope	1:5,000	Rockland, Limerik
Rabbit anti-NA/K-ATPase	1:5,000	Cell Signaling, Boston
Mouse anti-human Transferrin receptor	1:1,000	Life Tech., Carlsbad
Rabbit-anti Flag epitope	1:1,000	Sigma-Aldrich, St Louis
Mouse anti Flag-FITC labelled	1:1,000	Sigma-Aldrich, St Louis

Mouse anti-chicken MHC class I (C6B12)	1:1,000	DHSB, Iowa
Mouse anti-chicken TAP2	1:1,000	Kindly provided by J.Kaufman, Cambridge, UK
Mouse anti-MDV pUL49.5	1:200	Generated in this thesis

5.1.5 Bacteria, cells, viruses and animals

5.1.5.1 Bacteria

Name	**Features**	**Reference**
DH10B	F- endA1 recA1 galE15 galK16 nupG rpsL ΔlacX74 Φ80lacZΔM15 araD139 Δ(ara,leu)7697 mcrA Δ(mrr-hsdRMS-mcrBC) λ	Invitrogen
GS1783	DH10B λcI857 ∆(cro-bioA)<>araC-PBAD, I-SceI	[111]

5.1.5.2 Cells

Name	**Features**	**Reference**
CEC	Chicken embryo fibroblasts/cells, primary cells, VALO SPF strain	Primary cells
DF-1	Spontaneously transformed chicken embryo fibroblasts	ATCC CRL-12203
RK13	Rabbit epithelial kidney cell line	ATCC CCL-37
293T	Human epithelial kidney cell line, SV-40 T-antigen	ATCC CRL-11268

5.1.5.3 Viruses

Name	Features	Reference
rRB-1B	Bacterial artificial chromosome (BAC) of vvMDV strain RB-1	[112]
rBAC20	BAC of a avirulent, cell-adapted vv+ strain	[113]

5.1.5.4 Animals

Name	Features	Reference
BALBC and C57BL/6N mice	6 weeks old, female	Charles River

5.1.6 Kits for molecular biology

5.1.6.1 Kits

Name	Cat.No.	Company
EasyXpress II In Vitro Translation Kit	[Cat. No. 32561]	Qiagen, Hilden
GF-1 AmbiClean PCR/Gel Purification Kit	[Cat. No. GF-GC-200]	Vivantis, USA
Hi Yield Gel/PCR DNA Fragments Extraction Kit	[Cat No. 30 HYDF100-1]	SLG, Gauting
Imject KLH Carrier Protein Coupling Kit	[Cat. No. 77600]	Thermo Scientific, Darmstadt
Omniscript RT Kit	[Cat. No. 205110]	Qiagen, Hilden
PeqGold Plasmid Mini Kit	[Cat. No. 12-6942-02]	Peqlab, Erlangen
RTP® DNA/RNA Virus Mini Kit	[Cat. No. 1040100300]	STRATEC Molecular GmbH, Berlin
QuikChange Site-directed Mutagenesis Kit	[Cat. No. 200523]	Agilent, Santa Clara
Qiagen Plasmid Midi Kit	[Cat. No. 12145]	Qiagen, Hilden

5.1.7 Buffers, media and antibiotics

1x Phosphate saline buffer	1x Tris-acetate-EDTA buffer	0.8% Agarose Gel
(1xPBS)	(TAE)	80 mM Agarose
2 mM KH_2PO4	40 mM Tris	1x TAE buffer

10 mM Na_2HPO_4
137 mM NaCl
2.7 mM KCl, pH 7.3

1 mM $Na_2EDTAx2H_2O$
20 mM Acetic acid 99 %,
pH 8.0

4 µl Ethidium bromide
10 mg/ml

10x SDS-Page running buffer
250 mM Tris
1.9 M Glycine
1% SDS

2x Western blot stripping buffer
50 mM glycine
2% SDS
pH 2

LB medium (1l)
10 g BactoTM Tryptone
5 g BactoTM Yeast Extract
10 g NaCl
15 g BactoTM Agar

SOB medium (1l)
20 g BactoTM Tryptone
5 g BactoTM Yeast Extract
0.584 g NaCl
0.186 g KCl
pH 7.0

SOC medium
SOB medium
20 mM Glucose

Buffer (P1)
50 mM Tris HCL pH 8.0
10 mM EDTA
100 µg/ml RNAse

Lysis Buffer (P2)
200 mM NaOH
1% SDS

Neutralization Buffer (P3)
3 M K-Acetate pH 5.5

Buffer TE
10 mM Tris HCl pH 7.4
1 mM Na_2EDTA

Genomic DNA Lysis buffer
10 mM Tris-Cl (pH 8.0)
0.1 M EDTA (pH 8.0)
0.5% (w/v) SDS
20 µg/ml RNase A

5.1.7.1 Antibiotics

Name	Working concentration	Company
Ampicillin (Amp) [Cat.No. K0292]	100 µg/m diluted in ddH2O	Roth, Karlsruhe
Kanamycin sulphate (Kana) [Cat. No.T832.3]	50 µg/ml diluted in ddH2O	Roth, Karlsruhe
Chloramphenicol (Cam) [Cat. No. 3886.3]	30 µg/ml diluted in 96% EtOH	Roth, Karlsruhe

Penicillin (P) [Cat. N. A1837]	100 U/ml diluted in MEM	Applichem, Darmstadt
Streptomycin (S) [Cat. N. A1852]	100 U/ml diluted in MEM	Applichem, Darmstadt

5.1.7.2 Cell culture supplements

Name	**Cat.No.**	**Company**
Chicken Serum	[Cat.No. C5405]	Sigma-Aldrich, St Louis
Dulbecco's MEM (DMEM)	[Cat. No. F 0435]	Biochrom AG, Berlin
Fetal bovine serum (FBS)	[Cat. No. S 0415]	Biochrom AG, Berlin
L-alanyl-L-Glutamine	[Cat.No. K 0302]	Biochrom AG, Berlin
Minimum essential Medium Eagle (MEM)	[Cat.No. F 0315]	Biochrom AG, Berlin
Non-Essential Amminoacids (NAE) (100X)	[Cat.No. K 0293]	Biochrom AG, Berlin
RPMI 1640 (w/o Glutamine)	[Cat.No. F 1215	Biochrom AG, Berlin
Sodium Pyruvate	[Cat.No. L 0473]	Biochrom AG, Berlin
Trypsin	[Cat.No. L 2103-20G]	Biochrom AG, Berlin

5.1.7.3 Cell culture media and buffers

CEC Medium	**DF-1 Medium**	**RK13 and 293T Medium**
MEM	DMEM	RPMI
10% FBS	10% FBS	10% FBS
1x Penicillin/Streptomycin	2 mM Na-Pyruvate	1x Penicillin/Streptomycin
	1% L-Glutamine	
	1x Penicillin/Streptomycin	

2xHBS buffer	**Trypsin**
140 mM NaCl	1.5 M NaCl
1.5 mM Na2HPO4 x 2H2O	0.054 M KCl
50 mM HEPES	0.055 M C6H12O6
pH 7.05	0.042 M NaHCO3
	106 U Penicillin (P)
	1457.4 Streptomycin (S)
	0.0084 M Versene (EDTA)
	Ethhylene diaminetetracetate
	Trypsin 1:250

Table 1. Primers used in the MDV UL49.5 project.

Primers	Sequence (5' → 3') [a]
MDV UL49.5 for	ACTCGAGCGGCCGCGCCACCATGGGACTCATGGACATTCATAATG
MDV UL49.5 rev	GAGCTCGGATCCTTACCACTCCTCTTTAAACATATCTGC
MDV UL49.5Flag rev	CGAGCTCGGATCCTTACTTGTCGTCATCGTCTTTGTAGTCCCACTCCTCTTTAAACATATCTGCG
MDV UL49.5His rev	GAGCTCGGATCCTTAGTGATGGTGGTGATGGTGCCACTCCTCTTTAAACATATCTGCG
MDV UL49.5 sequencing for	TCTATTGTACCGTGTGGCGTC
MDV UL49.5 sequencing rev	ACACGGAATTGCAGACGC
MDV UL49.5 RT-PCR for	ATGGGACTCATGGACATTCATAATG
MDV UL49.5 RT-PCR rev	TTACCACTCCTCTTTAAACATATCTGC
V20_UL49.5Δ1Met for	ATAACTAAACTACAGACTGCATTATGAATGTCCATGAGTCGCGACCTCGTCGAGATCGTGATAGGGATAACAGGGTAATCGATTT
V20_UL49.5Δ1Met rev	TTCCAACGTTATATTCTCCAAATCACGATCTCGACGAGGTCGCGACTCATGGACATTCATAGCCAGTGTTACAACCAATTAACC
V20_UL49.5Δ1+2Met for	AACGCCGATAACTAAACTACAGACTGCATTATGAATGTCCGCGAGTCGCGACCTCGTCGATAGGGATAACAGGGTAATCGATTT
V20_UL49.5Δ1+2Met rev	TTATATTCTCCAAATCACGATCTCGACGAGGTCGCGACTCGCGGACATTCATAATGCAGTCTGCCAGTGTTACAACCAATTAACC
MDV UL49.5mutKtoA for	CCTTACCACTCCTCTGCAAACATATCTGCGGTGAATAGTCGAAAGC
MDV UL49.5mutKtoA rev	GCTTTCGACTATTCACCGCAGATATGTTTGCAGAGGAGTGGTAAGG
MDV UL49.5mutTtoA for	CGCAGCCTTTCGACTATTCGCCGCAGATATGTTTG
MDV UL49.5mutTtoA rev	CAAACATATCTGCGGCGAATAGTCGAAAGGCTGCG
MDV UL49.5mutCtoA for	CGGGTTCGTATCACGCAGCCTTTCGACTATTCACCG
MDV UL49.5mutCtoA rev	CGGTGAATAGTCGAAAGGCTGCGTGATACGAACCCG
MDV gMHis for	ACTCGAGCGGCCGCGCCACCATGGCCAGTCGAGCACGA
MDV gMHis rev	GAGCTCGGATCCTTAGTGATGGTGGTGATGGTGATCATCCCATTCGCTCTCAGAT
chGAPDH RT-PCR for	ATGGTGAAAGTCGGAGTCAACG
chGAPDH RT-PCR rev	TCACTCCTTGGATGCCATGTG
BHV1 UL49.5Flag for	TCTAGACTCGAGGCCACCATGCCGCGGTCGCCGCTCA
BHV1 UL49.5Flag rev	GAGCTCGGATCCTTACTTGTCGTCATCGTCTTTGTAGTCGCCCCGCCCCCGCGACT

[a] Regions of interest are underlined: restriction sites, mutated sequences or epitope tags.

Table 2. Primers used in the MDV ORF012 project.

Primers	Sequence (5' → 3') [a]
TS1	ATGACTAGCGAGAGAGCTCTTACTCT
TS2	TGTACGCCAAATTTTACAACGATTAT
TS3	CTATTCATCATCTGAACTCGACATCC
chGAPDH for	ATGGTGAAAGTCGGAGTCAACG
chGAPDH rev	TCACTCCTTGGATGCCATGTG

vRΔ012 for	AACGAGAGGTTGGTAACAAACAGCTTTTGAAAATAAACTAGCGAGAGAGCTAGGGATAACAGGGTAATCGATTT
vRΔ012 rev	TACCAGGCGCGAGAGTAAGAGCTCTCTCGCTAGTTTATTTTCAAAAGCTGGCCAGTGTTACAACCAATTAACC
vRΔ012R for	AACGAGAGGTTGGTAACAAACAGCTTTTGAAAAATGACTAGCGAGAGAGCTAGGGATAACAGGGTAATCGATTT
vRΔ012R rev	TACCAGGCGCGAGAGTAAGAGCTCTCTCGCTAGTCATTTTTCAAAAGCTGGCCAGTGTTACAACCAATTAACC
v20_012Flag for	AGATCTTGTGGTTCTTGGGATGTCGAGTTCAGATGATGAAGACTACAAAGACGATGACGACAAGTAGCATTTGCCAGTGTTACAACCAATTA ACC
v20_012Flag rev	ACAGTGGATTTGCAATCACACAACATATACACAAATGCTACTTGTCGTCATCGTCTTTGTAGTCTTCATCATTAGGGATAACAGGGTAATCGA TTT
v20_012ΔNLSFlag for	CTTGGATACCGTTGTCGTTCGAGATCACCCAGTAACACATGACTACAAAGACGATGACGAGCCAGTGTTACAACCAATTAACC
v20_012ΔNLSFlag rev	ATATACACAAATGCTACTTGTCGTCATCGTCTTTGTAGTCATGTGTTACTGGGTGATCTCTAGGGATAACAGGGTAATCGATTT
v20_012mutshortNLSFlag for	ATAACAGTGAAGATCCAAACCGTAGTCGGAGCCGGAGTCGATCTAGGGAGGCAGCGGCAGCAGCCGCAGCAGTTAGGCCTGCCAGTGTT ACAACCAATTAACC
V20_012mutshortNLSFlag rev	CCACAAGATCTCGTATAGTTGTAGCCGTACTCCTACGCCCAGGCCTAACTGCTGCGGCTGCTGCCGCTGCCTCCCTAGATTAGGGATAACA GGGTAATCGATTT
012*Flag for	ACTCGAGCGGCCGCGCCACCATGTTTACCGGAGGAGGAACTATTG
012*Flag rev	GAGCTCGGATCCTTACTTGTCGTCATCGTCTTTGTAGTCTTCATCATCTGAACTCGACATCCC
012ΔintFlag for	CTCGAGCGGCCGCGCCACCACCATGACTAGCGAGAGAGCTCTTACTCTCGCGCCTGGTAAAGTTTCGACGGCAGATATTTATGAAGCCGA TTTCAGTTTCCGTCGTGAATTTGTACGCCAAATTTTACAACGATTATTCCCAAGGACCTT
012ΔintFlag rev	AACTTAAGCTTCTACTTGTCGTCATCGTCTTTGTAGTCTTCATCATCTGAACTCGACATCCCA
GFPcterm for	CAGATCTCGAGTAGTTCGAGATCACCCAGTAACACATCG
GFPcterm rev	AATTCGAAGCTTTTATTCATCATCTGAACTCGACATCCC
GFP_GSlinker for	CAGATCTCGAGCTCAAGGAGGCAGTGGTGGAGG
GFPlongNLS template	AAGGAGGCAGTGGTGGAGGCAGTGGTCGTAGTCGGAGCCGGAGTCGATCTAGGGAGCGTAGGCGAAGACGGCCACGAGTTAGGCCTGG GCGTAGGTAA
GFPlongNLS rev	TCGACTGCAGAATTCTTACCTACGCCCAGGCCTAAC
GFPshortNLS template	AAGGAGGCAGTGGTGGAGGCAGTGGTCGTAGGCGAAGACGGCCACGATAA
GFPshortNLS rev	GTCGACTGCAGAATTCTTATCGTGGCCGTCTTCGC
GFP_RSrepeat template	GAGCTCAAGGAGGCAGTGGTGGAGGCAGTGGTCGTAGTCGGAGCCGGAGTCGATCTAGGGAGTAAGAATTC
GFP_RSrepeat rev	TCGACTGCAGAATTCTTACTCCCTAGATCGACTCCGG
012mutshortNLS for	TCGGAGCCGGAGTCGATCTAGGGAGGCTGCGGCAGCAGCGGCAGCAGTTAGGCCTGGGCGTAGGAGTACG
012mutshortNLS rev	CGTACTCCTACGCCCAGGCCTAACTGCTGCCGCTGCTGCCGCAGCCTCCCTAGATCGACTCCGGCTCCGA
012mutRSrepeat for	ACAGTGAAGATCCAAACGCCGCAGCGGCTGCAGCAGCTGCCAGGGAGCGTAGGCGAAGACGG
012mutRSrepeat rev	CCGTCTTCGCCTACGCTCCCTGGCAGCTGCTGCAGCCGCTGCGGCGTTTGGATCTTCACTGT
012mutStoA for	GTGAAGATCCAAACCGTGCTCGGGCCCGGGCTCGAGCTAGGGAGCGTAGGCGA
012mutStoA rev	TCGCCTACGCTCCCTAGCTCGAGCCCGGGCCCGAGCACGGTTTGGATCTTCAC
pVitro-GFP-012 for	GATATCGGATCCGCCACCACCATGACTAGCGAGAGAGCTCTTACTCTC
pVitro-GFP-012 rev	CCTGCTCCTAGGTTATTCATCATCTGAACTCGACATCC

[a] Regions of interest are underlined: restriction sites, mutated sequences,epitope tags or sequences representing the exon/exon border of ORF012 (primer TS2).

5.2 Methods

5.2.1 Bioinformatics

5.2.1.1 Bioinformatic predictions

For comparison of p012 related proteins in different avian herpesviruses, amino acid sequences were aligned with the Clustal Omega Software (http://www.ebi.ac.uk/Tools/msa/clustalo). Splicing of the ORF012 mRNA message was predicted with the help of NetGene2 Server (http://www.cbs.dtu.dk/services/NetGene2/). In order to predict the NLS, the amino acid sequence of p012 was analyzed with the prediction tool NLStradamus (http://www.moseslab.csb.utoronto.ca/NLStradamus/) as well as the tool NucPred (http://www.sbc.su.se/~maccallr/nucpred/). Phosphorylation was predicted with the NetPhos 2.0 Server (http://www.cbs.dtu.dk/services/NetPhos). The structure of MDV UL49.5 was predicted using the I-Tasser server (http://zhanglab.ccmb.med.umich.edu/I-TASSER/). To predict potential sites of ubiquitination in MDV pUL49.5, the UBPred server was used (http://www.ubpred.org/).

5.2.2 Animal experiments

5.2.2.1 Generation of a pUL49.5 specific antiserum

Two peptides, one corresponding to the N-terminal region (CTFVDWGSSITSMGDFWESTCSAVGVSIAFSSGFS) and the other corresponding to the C-terminus of pUL49.5 (CFRLFTADMFKEEW) were synthesized by Genscript Inc, USA. Reconstituted peptides were coupled to keyhole limpet hemocyanin (KHL) via free cysteines using the Thermo Scientific Imject KHL coupling kit as described by the manufacturer. 10 BALB/C and 10 C57BL/6N mice at the age of 4 weeks where housed in cages in groups of 5 animals. 80 µl of pre-immunisation serum was obtained from 2 mice of each group. Mice were immunized subcutaneously with 75 µg of KHL-coupled peptide (N- or C-terminal peptide for individual groups) diluted in sterile phosphate buffer saline (PBS) supplemented with 15% (v/v) Emulsigen adjuvant. 22 days later mice were boosted with 75 µg of KHL-coupled peptides diluted as described above. Total blood was collected by cardiac puncture 2 weeks after this boost. Purified serum was aliquoted and stored at -80˚C.

5.2.3 Cell culture methods

5.2.3.1 Cells and viruses

Primary chicken embryo cells (CEC) were maintained in minimal essential medium (MEM) supplemented with 1 to 10% fetal bovine serum (FBS) and 1% penicillin/streptomycin. CEC were grown at 37˚C under a 5% CO_2 atmosphere. The spontaneously immortalized chicken embryonic fibroblast cell line DF-1 (ATCC CRL-12203, kindly provided by L. Martin, MPI Berlin), was maintained in Dulbecco's modified essential medium (DMEM) supplemented with 10% FBS, 1% penicillin/streptomycin, 5% glutamine and 2 mM sodium pyruvate. DF-1 cells were grown at 39˚C under a 5% CO_2 atmosphere and passaged twice a week. Rabbit RK13 cells were maintained RPMI medium supplemented with 10% FBS and 1% penicillin/streptomycin. Human 293T cells were maintained in 10% FBS DMEM medium with 1% penicillin/streptomycin. The pathogenic MDV strain RB-1B (vRb, GenBank EF523390.1) represents a very virulent (vv) and clinically relevant virus that is available as an infectious bacterial artificial chromosome (BAC) clone[112]. Strain 584Ap80C (cloned as BAC20, v20) represents a cell culture-adapted, avirulent strain that was obtained by serial passage of the very virulent plus (vv+) strain 584[114] and can be grown to high titers *in vitro*.

5.2.3.2 Preparation of chicken embryo cells

CEC were prepared from 11 day old, embryonated Valo-SPF eggs as described previously[115]. The eggshells were carefully cracked, embryos extracted and transferred to sterile PBS. Extremities as well as internal organs were removed. The remaining torso was disintegrated into small pieces with forceps and washed in sterile PBS for 10 minutes (min) on a magnetic stirrer. Subsequently, the tissue was digested in 100 ml of a 0.05% trypsin solution. The resulting cell suspension was filtered through a sterile gauze into 10% FBS MEM. This digestion was repeated 2 more times. Subsequently, the cell suspension was aliquoted into 50 ml Falcon tubes and pelleted by centrifugation for 10 min at 1200 rpm. Resulting pellets were pooled, washed again, and resuspended in 10% FBS MEM. Finally, cells were seeded at the desired confluency. In order to passage confluent CEC, medium was aspirated, cells were washed with PBS and finally detached with 0.05% trypsin at 37˚C. For inactivation of trypsin activity, cells were resuspended in 10% FBS MEM and seeded at desired ratios.

5.2.3.3 Transfection of DF-1 cells and CEC

DF-1 cells in 6 well plates (1×10^6 cells per well) were transfected with Fugene HD reagent. 1 µg of plasmid DNA was diluted in 100 µl Optimem and briefly mixed. 5 µl of transfection reagent were added to the DNA solution, briefly mixed and incubated for 15 min at room

temperature (rt). Finally, the DNA mixture was added to cells in a dropwise manner. For transfection of CEC in 6 well plates, the Lipofectamine reagent was used. Briefly, 2 µg of DNA were mixed with 250 µl of Optimem. 10 µl of Lipofectamine were mixed with 250 µl of Optimem in a separate reaction tube. After 5 min of incubation, both solutions were combined, mixed and further incubated for 30 min. Subsequently, the mixture was added to cells in a dropwise manner.

5.2.3.4 Reconstitution of viruses from BAC DNA

For the reconstitution of viruses from BAC DNA, a calcium phosphat transfection method was used[116]. 2 µg of DNA were dissolved in 50 µl of 10 mM Tris-HCl buffer in polypropylene transfection tubes. 388 µl of ddH_2O were added. The resulting solution was incubated for 30 min at rt after which 62 µl of 2 M $CaCl_2$ were added dropwise. Subsequently, samples were incubated for 4 hours (h) at 4˚C. 500 µl of 2xHBS buffer were added dropwise to the DNA solution while mixing and incubated for 15 min at rt. CEC at 80% confluency in 6 well plates, were supplied with 500 µl of fresh 10% FBS MEM. 500 µl of DNA mixture was added in a dropwise manner to individual wells. Following an incubation step of 4 h at 37˚C, the medium was removed from cells and washed with PBS. A glycerol shock with 15% glycerol in 1xHBS buffer was performed for 2 min and 30 sec after which the cells were washed with PBS. Finally, cells were supplemented with fresh media and incubated at 37˚C. Upon confluency of the monolayer, the serum concentration was reduced to 0.5%. With the development of viral plaques around 5 to 6 days post transfection (dpt), viruses were further propagated on CEC. Infected and uninfected cells were co-seeded into 10 cm cell culture dishes at desired ratios and incubated until plaques appeared in the cell monolayer.

5.2.3.5 Plaque size assays

One microgram of recombinant (r)RB-1B BAC DNA (rRb), rRbΔMet012 mutant or rRbΔMet012R revertant was transfected into 1×10^6 CEC by the $CaPO_4$ method as described previously[116]. Six days after transfection, cells were fixed with 90% ice-cold acetone, air-dried, blocked with 10% FBS in PBS, and stained with polyclonal anti-MDV chicken serum[110] diluted 1:5,000 in 1% bovine serum albumin (BSA) in PBS. Following three washing steps with PBS, cells were stained with secondary rabbit anti-chicken Alexa 488 antibody diluted 1:1,000. Using an Axio-Observer Z1 fluorescence microscope images of at least 50 plaques from each respective virus group were recorded at a 100× magnification in three independent experiments. Corresponding plaque areas were measured using the NIH Image J 1.410 software and mathematically transformed into plaque diameter values. Graphs were produced with GraphPad Prism 5 and diameters expressed relative to those of parental vRb.

For statistical analysis, values were first tested for normality and subsequently analyzed for significance by one-way Anova.

5.2.3.6 Inhibitor treatment of UL49.5 transfected cells

CEC were transfected with an expression plasmid encoding MDV UL49.5. 12 h post transfection (hpt), the cells were incubated with fresh medium containing the autophagy/lysosomal inhibitors bafilomycin A (1 µM), chloroquine (5 µM) or NH_4Cl (50 mM), respectively. In a second experiment, cells were treated with inhibitors of proteasomal degradation, lactacystin (10 µM) or MG132 (10 µM) for 8 h. Subsequently, cells were subjected to western blot analysis.

5.2.3.7 Leptomycin B (LMB) treatment of MDV ORF012 transfected cells

In order to test the effects of the nuclear export inhibitor LMB on p012 localization, DF-1 cells (1×10^4) plated on glass coverslips in a 24-well plate were transfected with 1 µg of plasmid DNA using the Fugene HD transfection reagent. At 6 hpt, cells in individual wells were incubated with fresh medium containing 2 µM LMB or cells were mock-treated with diluent only. Cells were further incubated for 9 h, fixed with 3% paraformaldehyde and analyzed for subcellular localization. In a different experiment, cells were incubated with 20 µM LMB at 10 hpt, and then fixed after 5 h of treatment. Differences between absolute cell numbers were tested for significance by $\chi 2$ test.

5.2.3.8 Cryoconservation of cells

Infected or uninfected cells were washed with PBS, trypsinized, resuspended in 10% FBS MEM supplemented with 8% dimethylsulfoxide (DMSO). Aliquots were slowly frozen in isopropanol filled cryocontainers at -80˚C overnight (O/N) and subsequently stored in liquid nitrogen.

5.2.4 Molecular biology methods

5.2.4.1 Generation of electrocompetent bacteria

The *Escherichia coli* strain GS 1783 containing the BAC to be modified was grown at 32˚C O/N in 5 ml of LB medium containing chloramphenicol (Cam). 5 ml of fresh LB Cam were inoculated with 100 µl of the O/N culture and further incubated at 32˚C until it reached an OD_{600} of 0.5 to 0.6. At this point, cultures were transferred to a 42˚C waterbath shaking at 220 rpm in order to induce the Red recombination system. After this 15 min heat shock, the cultures were transferred to a water-ice bath and incubated for 20 min at 220 rpm on a

shaker. Bacteria were pelleted by centrifugation for 2 min at 12000 rpm and 4˚C. Pellets were washed three times with ice-cold 10% glycerol in ddH_2O and resuspended in 60 µl of 10% glycerol. Electroporation was performed with 100 to 200 ng of purified, desalted PCR product which was added to the electrocompetent bacteria. Subsequently, electroporation was carried out at 1.25 kV, 25 µF and 200 Ω. Samples were resuspended in 1000 µl of prewarmed SOC medium and incubated 2 to 3 h shaking at 32˚C before plating on selective LB agar plates.

5.2.4.2 Generation of recombinant viruses via *en passant* mutagenesis

All recombinant viruses were generated with a two-step Red-mediated mutagenesis technique which is referred to as *en passant* mutagenesis[111]. The Red-recombination system has its origin in the λ phage were three proteins called Exo, Bet and Gam mediate homologous recombination of double-stranded DNA. The *E. coli* strain GS1783 is a derivative of the DH10B strain and was engineered to expresses the Red system under a temperature inducible promoter which is activated at 42˚C. Gam takes a central role in the recombination event since it protects free double-stranded DNA ends from degradation by the *E. coli* RecB/C/D system. The 5'-3' exonuclease Exo generates free 3' single strand overhangs in the DNA template and Bet serves to protect and stabilizes those free strands. During amplification of the BAC DNA, bet also mediates the strand invasion which is necessary to achieve homologues recombination with the target sequence. Apart from the temperature inducible recombination system, GS1783 express the I-SecI gene, *a Saccharomyces cerevisiae* homing endonuclease, under an arabinose inducible promoter. The enzyme cleaves a very large and therefore seldom found restriction site of 18 base pairs (bp) and makes specific cleavage of the mutated region possible. The cleavage allows for the final recombination event in which the kanamycin cassette is removed from the mutated sequence.

Briefly, the aphAI–I-SceI cassette containing a kanamycin resistance marker and a unique I-SceI restriction site was amplified from the vector pEPkanS1 using PCR with primers (Table 1 and 2) containing the specific mutation to be generated, as well as homologous sequences that allowed the desired recombination events. PCR products were purified and introduced by electroporation into the *E. coli* strain GS1783 harboring the specific BAC to be mutated. Kanamycin-resistant clones were analyzed by restriction fragment length polymorphism (RFLP) analysis with multiple restriction enzymes. Following the second recombination step, kanamycin-sensitive clones were analyzed by RFLP to ensure integrity of the genome, and by PCR and DNA sequencing to confirm the presence of the desired mutation. A virus with a mutation of the first UL49.5 start codon (v20_UL49.5Δ1Met, met: methionine) as well as a virus with mutations of the first and the second in-frame start codon (v20_UL49.5Δ1+2Met),

respectively, were based on the cell culture adapted MDV v20. An ORF012 start codon mutant virus (vRbΔMet012), as well as the respective revertant virus (vRbΔMet012R) was based on vRb. Viruses encoding p012 with C- or N-terminal Flag epitope tags (v20_012Flag or v20_Flag012), respectively, a mutant with a deletion in the 3' end of p012, containing the NLS (bp 1036 – 1467, v20_012ΔNLSFlag) and a mutant containing an alanine substitution of the short NLS (v20_012mutshortNLSFlag) were based on v20.

5.2.4.3 DNA preparation from bacteria

BAC DNA was isolated from bacteria using alkaline lysis as described previously[116]. 5 ml of LB O/N cultures grown at 32˚C were pelleted at 5000 rpm for 5 min. The supernatant was discarded and the bacteria were resuspended in 300 µl of P1 buffer. Subsequently, 300 µl of P2 lysis buffer were added, samples were carefully inverted 4 to 5 times and incubated for 5 min at rt. In order to neutralize the mixture and precipitate proteins, 300 µl of P3 buffer was added to the samples. In a subsequent step cellular debris was removed by centrifugation for 10 min at 10000 rpm. Supernatants were transferred to 1.5 ml reaction tubes and mixed with 400 µl of chloroform. Samples were briefly vortexed and centrifuged for 10 min at 10000 rpm. The upper, aqueous phase was aspirated and mixed with 0.7 volumes of isopropanol. DNA was precipitated by centrifugation for 10 min at 10000 rpm and 4˚C. Subsequently, pellets were washed with 70% ethanol and briefly dried at 37˚C. DNA was dissolved in ddH_2O and stored at -20˚C until further use. Midi preparations of BAC or plasmid DNA were carried out with the Qiagen Midi Kit according to the protocols provided by the manufacturer. Mini preparations of plasmid DNA were performed with the PeqGold Plasmid Mini Kit, Peqlab. Quality of obtained DNA was evaluated with a Nanodrop spectrophotometer.

5.2.4.4 Extraction of viral DNA from infected cells

Viral DNA was extracted from infected CEC using a phenol-chloroform extraction. Trypsinized cells were pelleted in 15 ml Falcon tubes for 10 min at 1200 rpm. After two washing steps with ice-cold PBS, cells were resuspended in TE buffer. Subsequently, cells were lysed in lysis buffer (1m l per 5×10^6 cells) supplemented with 100 µg/µl RNAse and incubated at 37˚C for 1 h. After a protease K treatment (final concentration 100 µg/ml) for 3 h at 50˚C, samples were cooled to rt. Subsequently, an equal volume of phenol was added, mixed and centrifuged for 10 min at 5000 rpm. The aqueous upper phase was collected and mixed with an equal volume of phenol:chloroform solution. The extraction was repeated once more. Finally, DNA was precipitated with 2.5 volumes of ice-cold ethanol and incubated at -20˚C for 15 min. Subsequently, DNA was pelleted by centrifugation for 30 min at 4˚C and 12000 rpm. Obtained pellets were washed once with 70% ethanol, air-dried and dissolved in TE buffer.

5.2.4.5 Cloning of expression plasmids and site-directed mutagenesis

MDV UL49.5, tagged derivatives of UL49.5 or tagged MDV UL10 (gM) were cloned via NotI and BamHI restriction sites into the pcDNA3.1(-) vector. Tagged BHV-1 UL49.5 was cloned via BamHI and XhoI restriction sites. Expression plasmids pc011*Flag, pc012*Flag, pc012Flag and pc012$^{\Delta int}$Flag (all based on pcDNA3.1 and containing a C-terminal Flag tag) were also generated by PCR cloning. pc012$^{\Delta int}$Flag was generated by fusion PCR and is devoid of the intron in the 5' region of the gene. Respective inserts were amplified by standard PCR from rRB DNA with Phusion polymerase and primers containing restriction sites for directional cloning and the epitope tags (Table 1 and 2). Both vector and inserts were cut with restriction enzymes, gel-purified, ligated with T4 DNA ligase and transformed into Top10 competent cells. pc012$^{\Delta int}$Flag was cloned via NotI/HindIII sites. Positive colonies were selected on ampicillin agar plates and analyzed by restriction digests and Sanger sequencing (LGC Genomics). For site-directed mutagenesis, the QuickChange II mutagenesis kit was used according to the protocol provided by the manufacturer. Primers were designed with the corresponding software available at the Agilent homepage (Table 1 and 2). GFP fusion constructs pGFP-012cterm, pGFP-longNLS, pGFP-shortNLS and pGFP-RSrepeat were based on the pEGFP-C1 expression vector (Clontech). Briefly, fragments to be fused to the C-terminus of GFP were amplified as described above with primers and templates given in Table 2 and cloned via SacI/EcoRI restriction sites. pGFP-012cterm was cloned via AvaI/HindIII sites. All forward primers, except for cloning of pGFP-012cterm, also contained a double glycine-serine (GS) linker that served as a spacer and to add flexibility of the fused sequences[117]. Positive colonies were selected on kanamycin LB agar plates, analyzed by restriction digestion and agarose gel electrophoresis as well as Sanger sequencing (LGC Genomics). Dual-expression vectors expressing MDV ORF012 (or ORF012Flag) and the green fluorescent protein (GFP) were based on pVITRO2-GFP. ORF012 and ORF012Flag were cloned downstream of the hFerH promotor via EcoRI and AvrII restriction sites.

5.2.4.6 RNA extraction and reverse transcriptase–PCR (RT-PCR) analysis

In order to investigate the level of UL49.5 transcripts in different cells, total RNA was extracted using the Qiagen RNeasy kit following the manufacturer's protocol. Genomic DNA was removed with gEliminator columns as well as an additional on-column DNAse digest. Eluted RNA was quantified using a Nanodrop spectrophotometer. RT-PCR was performed with indicated primers (Table 1) in a two-step reaction. First, cDNA was synthesized from 500 ng of total RNA using the Omniscript RT kit in a 20 µl reaction. Half a microliter of the reactions was used in Taq polymerase PCR (95˚C for 5 min, 30× (95˚C for 30 sec, 62˚C for 30 sec, 72˚C for 2.5 min), 72˚C for 10 min) and amplicons were separated on 1% agarose

gels. Amplification of cDNA obtained from chicken glyceraldehyde-3-phospate dehydrogenase (GAPDH) mRNA served as an internal control. To investigate putative mRNA splicing of ORF012, 1×10^6 CEC were infected with MDV vRb or mock-infected. Additionally, DF-1 cells were transfected with pc012$^{\Delta int}$ as a positive control. Five dpi or 24 hpt, RNA was extracted as described above. In addition, amplicons were subjected so Sanger sequencing (LGC Genomics). Reactions to which no RT was added served as a control for genomic DNA contamination.

5.2.4.7 Western blot analysis

CEC (1×10^6) were infected with the same plaque forming unit (pfu) of MDV v20, a mutant virus encoding a C- (v20_012Flag) or N-terminally Flag-tagged p012 (v20_Flag012), respectively. Infected cells were harvested 5 dpi and lysed in radioimmunoprecipitation assay buffer (RIPA, 20 mM Tris-HCl, 150 mM NaCl, 1% (v/v) Nonidet P-40, 0.5% (w/v) sodium deoxycholate, 0.1% (w/v) SDS) supplemented with Complete® mini protease inhibitor and phosphatase inhibitor cocktail. Lysates were separated by sodium dodecyl sulfate (SDS) polyacrylamide gel electrophoresis (PAGE) and proteins transferred onto polyvinylidene difluoride (PVDF) membranes using the Biorad wet blot system. Subsequently, membranes were blocked with 3% BSA in PBS and incubated O/N at 4˚C with polyclonal rabbit anti-Flag antibody or rabbit polyclonal anti-actin antibody, both diluted 1:1,000 in blocking buffer. Following washing with PBS containing 0.1% Tween 20, membranes were incubated for 1 h at rt with horseradish peroxidase-conjugated goat anti-rabbit antibody, diluted 1:10,000. Finally membranes were incubated with enhanced chemiluminescence (ECL) Plus western blot detection reagent and the signal was recorded using a Chemi-Smart 5100 detection system. To remove bound antibodies, membranes were incubated twice with stripping buffer (25 mM glycine, 1% (v/v) SDS, pH 2) at rt on an orbital shaker, washed twice with PBS, blocked with blocking buffer and reprobed with antibodies. For dephosphorylation experiments, DF-1 cells transfected with pc012Flag were lysed in RIPA buffer 24 hpt. Prior to western blotting, some lysates were treated with lambda protein phosphatase or mock-treated for 30 min according to the manufacturer's protocol to analyze the phosphorylated state of proteins.

For western blot detection of UL49.5 in MDV infected CEC, UL49.5 transfected CEC or UL49.5 transfected DF-1 cells, respectively, cells were separated on 7.5%-20% SDS-Page and subsequently blotted as described above. For the detection, the primary antibodies rabbit-anti Flag (1:2,000), rabbit anti-His (1:2,000) or a specific mouse anti-pUL49.5 antiserum (1:1,000) were used.

For western blot detection of TAP2, a membrane protein enrichment protocol was used. Cells were harvested, washed with PBS and the resulting pellet was resuspended in 500 µl

PBS containing 1 mM $MgCl_2$. Samples were freeze-thawed (-80˚C and 37˚C) three times in order to disrupt the cellular membrane. Subsequently, samples were pelleted for 30 min at 12000 rpm and 4˚C. The supernatant was discarded and pellets were prepared for western blotting as described above with the exception that a digitonin containing lysis buffer was used. Supernatant of a mouse hybridoma cell line producing chicken TAP2 antibody (kindly provided by J. Kaufman, Cambridge, UK) was used as a primary antibody without dilution.

5.2.4.8 Phos-tag western blotting to determine phosphorylation of p012

In order to validate the phosphorylation of p012, the Phos-tag™ reagent (Wako Chemicals) was used as described in the manual provided by the supplier. Phos-tag binds specifically to phosphorylated proteins in the presence of manganese ions ($MnCl_2$) and decreases migration of phosphoproteins in SDS-Page[118]. Briefly, 25 µM of Phos-tag solution and 1 mM of $MnCl_2$ solution were added to the gel mixture prior to casting. Subsequent western blotting was performed as described above.

5.2.4.9 *In vitro* translation of pUL49.5

For *in vitro* translation of MDV pUL49.5, the Qiagen EasyXpress II kit was used as described by the manufacturer. Translation reactions were performed in ER membrane containing insect cell lysates, thus allowing a rather native expression and localization of membrane proteins. Briefly, 1 µg of target DNA was mixed with the *in vitro* transcription reagents, vortexed and incubate for 2 h at 37˚C. Subsequently, the transcription was added to a DryEx column and centrifuged to isolate mRNA. The obtained mRNA was then mixed with the *in vitro* translation reagents, briefly vortexed and incubate for 90 min at 27˚C and 500 rpm on a thermomixer. Finally, samples were subjected to western blotting as described above.

5.2.5 Flow cytometry and immunofluorescence microscopy

5.2.5.1 MHC class I downregulation assays

To investigate MHC downregulation following *in vitro* infection, CEC (1×10^5) were infected with 1×10^2 pfu of MDV v20, a mutant virus harboring a deletion of the UL49.5 C-terminal domain (v20_ UL49.5ΔCt) or a mutant virus with a deletion of the first two start codons of UL49.5 (v20_ UL49.5Δ1+2). Five dpi, cells were trypsinized, washed with PBS and fixed with 2% paraformaldehyde (PFA) in PBS for 10 min at rt. Cells were stained with mouse anti-chicken MHC class I antibody (C6B12) diluted 1:1,000 in staining buffer (1% BSA in PBS) for 1 h at rt on an orbital shaker. Following three washing steps with PBS, cells were stained with goat anti-mouse IgG Alexa 647 diluted 1:5,000 and incubated for 1 h in the dark while

shaking. All following steps were performed in the dark. To stain for MDV infection, cells were first permeabilized with 0.2% saponin in staining buffer for 10 min. Subsequently, unspecific binding was blocked with 5% FBS diluted in PBS for 30 min. Following a washing step with PBS, cells were incubated with polyclonal anti-MDV chicken serum diluted 1:5,000 in staining buffer for 1 h. Following three washing steps with PBS, cells were further incubated with goat anti- chicken IgG Alexa 488 antibody diluted 1:2,000 for 1 h. Samples were resuspended in PBS and analyzed by dual-color flow cytometry with a FACScalibur flow cytometer. Transferrin staining of infected samples served as a control for specific MHC class I downregulation. For MHC class I downregulation assays with transiently transfected cells, DF-1 cells (1×10^6) were seeded in 6 well plates 24 h prior to transfection. At a confluency of about 80%, cells were transfected with the UL49.5 expression plasmids, control plasmids or mock transfected. 24 hpt cells were stained as described above with the following antibodies: primary mouse anti-chicken MHC class I antibody, secondary goat anti-mouse IgG2a Alexa 647, primary FITC-labeled mouse-anti Flag antibody.

5.2.5.2 Transfection of expression plasmids, indirect immunofluorescence microscopy and quantification of cellular localization

DF-1 cells (1×10^4) on glass coverslips in a 24 well plate were transfected with 1 µg of plasmid DNA using 3 µl Fugene HD transfection reagent. Cells were washed with PBS at 24 hpt, fixed with 3% PFA in PBS for 10 min at rt, and permeabilized with 0.1% Triton-X 100 in PBS for 10 min at rt. Following a blocking step with 5% FBS in PBS, cells were stained with polyclonal rabbit anti-Flag antibody diluted 1:1,000 in 1% BSA-PBS for 1 h at rt, washed and incubated with goat anti-rabbit Alexa 568 antibody (diluted 1:2,000) for 1 h. Finally, cells were stained with Hoechst 33342 to visualize the nucleus and coverslips were mounted with PermFluor mounting medium. For pEGFP-C1 fusion constructs, cells were fixed 24 hpt and stained with Hoechst 33342. To quantify the intracellular distribution of p012, NLS deletion proteins and the GFP fusion constructs, a blinded, semi-quantitative transfection assay based on expression plasmids was used as described previously by Brock *et al.*[119]. Pictures of at least 200 fluorescence-positive cells for each transfected construct were taken with an Axiovision microscope (400× magnification) in a randomized fashion. In replicated experiments, cellular distribution of the fluorescence signal within each cell was classified by an individual blinded to the experimental groups into one of three categories: 1) predominant nuclear localization, 2) mixed nuclear/cytoplasmic localization or 3) predominant cytoplasmic localization.

5.2.6 Microarray analysis

DF-1 cells (2×10^7) were transfected with pVITRO-GFP-012, which expresses GFP and MDV ORF012 under control of two independent promotors, or mock transfected with pVITRO-GFP. 24 hpt cells were trypsinized, washed and GFP positive cells were cell-sorted using a BD FACSAria III cell sorter (kindly provided by the flow cytometry core facility of the MPI, Berlin). Sorted cells were pelleted and total RNA was extracted as described previously. The microarray experiment and its analysis were kindly performed by Dr. Bertrand Pain, INSERM Lyon. The experiment was carried out with 4x44k GE chicken V2 slides (Agilent) as described previously[120]. Using a cutoff of p-values ≤0.05 and a threshold of Log2 of the fold change (Log_2FC)>2, a list of differentially expressed genes was compiled.

5.2.7 Statistics

5.2.7.1 Statistical analysis

Statistical analysis was performed using the GraphPad Prism 5 Software. Plaque size data of MDV recombinant viruses were tested for normality of distribution and analyzed for significance using one-way ANOVA. Quantification of p012 localization following LMB treatment was analysed by $\chi 2$ test.

Table 3. Two-step PCR protocol for the generation of recombinant viruses.

Temperature (°C)	Time	PCR steps	Cycles
95°C	5 min	Polymerase activation	
95°C	30 sec	Denaturation	
51°C	30 sec	Annealing	10
72°C	2 min	Elongation	
95°C	30 sec	Denaturation	
62°C	30 sec	Annealing	20
72°C	2 min	Elongation	
72°C	10 min	Extension	

Table 4. One-step PCR protocol for cloning and sequencing.

Temperature (°C)	Time	PCR steps	Cycles
95°C	5 min	Polymerase activation	
95°C	30 sec	Denaturation	
51°C	30 sec	Annealing	10
72°C	2 min	Elongation	
72°C	10 min	Extension	

6. Results

6.1 Functional investigation of MHC class I downregulation by MDV pUL49.5

6.1.1 Position of UL49.5 in the MDV genome and structural features

The MDV homologue of HSV-1 UL49.5 is located in the unique long region between the UL49 (encoding the tegument protein VP22) and UL50 genes (encoding the viral dUTPase)[98]. Contrary to UL49 and UL50, the gene is transcribed in a leftward orientation and overlaps the UL50 gene with a small part of its 5' region (Fig. 5A).

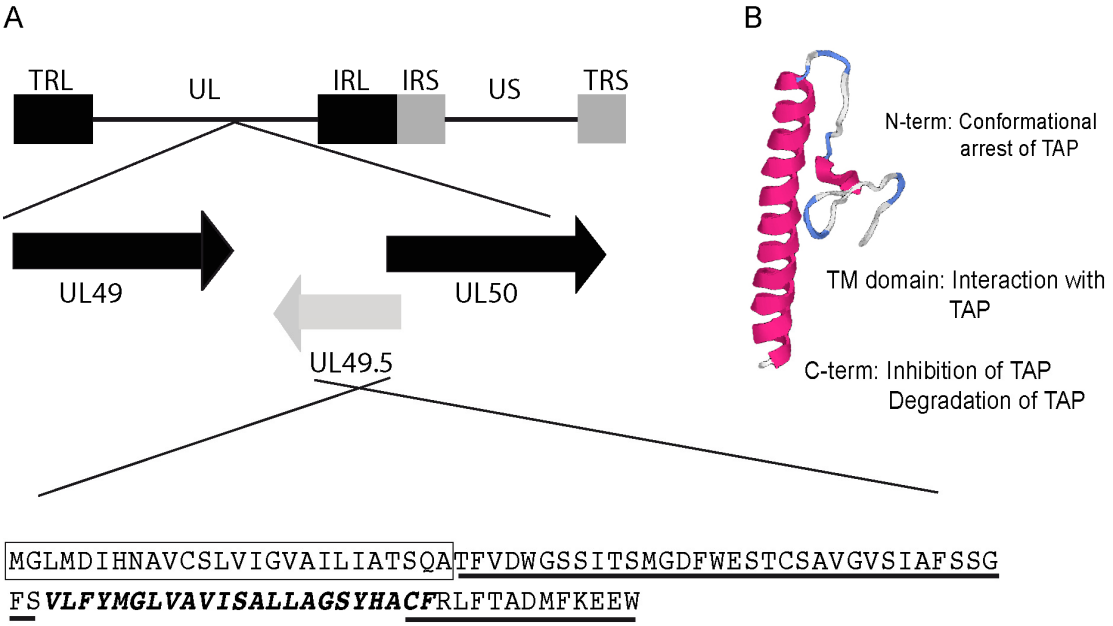

Figure 5: Location of UL49.5 in the MDV genome, sequence of pUL49.5 and predicted structure of the protein. (A) A schematic representation of the MDV genome is shown. The unique (UL and US) and the internal and terminal repeat regions (IRL, IRS and TRL, TRS, respectively) are indicated. UL49.5 is positioned between UL49 and UL50 with a leftward orientation. The amino acid sequence of the encoded protein is depicted. A cleaved signal peptide is boxed and the transmembrane domain (TM) is indicated with bold/italic letters. The sequence of two peptides used for the generation of specific mouse pUL49.5 antisera is underlined. (B) The tertiary structure of MDV pUL49.5 was predicted with the I-Tasser server. Published functions of individual protein domains in members of the genus *Varicellovirus*, but not MDV, are indicated on the right. Figures A and B summarize results obtained in references 84 and 87.

The protein encoded by MDV UL49.5 is a class I transmembrane protein of 95 amino acids, hence it contains a potentially cleavable signal peptide and an N-terminus on the inside of the ER lumen. A structural prediction of pUL49.5 using I-Tasser was performed and the structure is depicted in Fig. 5B. The single transmembrane domain and a very short C-terminal tail of 12 aa, which protrudes into the cytoplasm, are indicated. In addition, functions that have been assigned to individual domains of the homologous protein in some *Varicelloviruses*, but not to the MDV protein, are indicated[85]. Finally, the position of two peptides that were used for the generation of a pUL49.5-specific mouse antiserum (see next paragraph), is shown (Fig. 5A).

6.1.2 Generation of a MDV pUL49.5 specific mouse antiserum

In order to elucidate the MHC class I regulatory function that had been established for MDV pUL49.5[87], reagents that allow detection of the protein in various experimental setups are instrumental. Although generation of epitope-tagged pUL49.5 constructs was already achieved earlier in the project, the small size of the target protein and its dense clustering of potentially functional domains, in particular at the N- and C-terminus, could make structural modifications by introduction of an epitope tag detrimental. However, a pUL49.5-specific antibody had not been available in the past. For this reason, two monospecific antisera against peptides of the protein were raised in mice. Briefly, mice where immunized with KLH-coupled peptides derived either from the N-or C-terminal domain of pUL49.5 (Fig. 5A) and boosted once 3 weeks after the first immunization. Serum was collected by cardiac puncture 2 weeks after the booster immunization. The reactivity of the obtained serum was tested by western blotting and indirect immunofluorescence (Fig. 6). The antiserum specifically reacted with a protein of approximately 10 kilo Dalton (kDa) in western blots performed with lysates of MDV v20 infected CEC. Unexpectedly, the antiserum failed to detect the presence of pUL49.5 in CEC transfected with an expression vector encoding the target gene under the control of the HCMV IE promoter (pcUL49.5; Fig. 6B). To further characterize the antibody, the pUL49.5 antiserum was pre-incubated with the immunization peptide prior to western blotting. A peptide of random sequence served as a control. As seen in Fig. 6C, the 10 kDa band was absent on western blots only after pre-treatment with the specific but not the random peptide, indicating specificity of the serum. As shown by indirect immunofluorescence, the antiserum also recognized pUL49.5 in infected CEC that were fixed and permeabilized by aceton/methanol treatment (Fig. 6D). In line with the western blot results, I was unable to detect the protein by immunofluorescence microscopy in transfected CEC (data not shown).

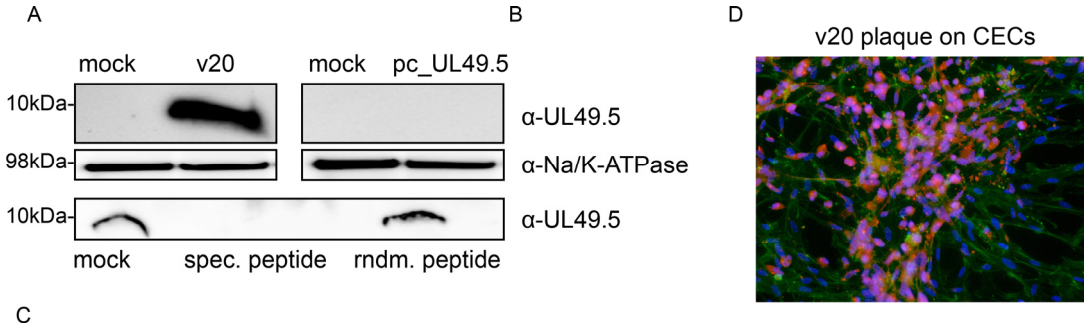

Figure 6: Characterization of a MDV pUL49.5 specific mouse antiserum. (A): Western blot analysis of CEC infected with MDV. Cells were infected with 200 pfu of MDV v20 or mock infected and collected 5 dpi. Lysates were separated by 20% - 7.5% gradient SDS-PAGE followed by immunoblotting. Membranes were incubated with polyclonal mouse anti-pUL49.5 antiserum, washed and incubated with secondary goat anti-mouse HRP antibody. For the detection of Na/K-ATPase as a loading control (middle panel), blots were stripped, blocked and reprobed with rabbit anti-Na/K-ATPase antibody. (B): Western blot analysis of CEC transfected with pcUL49.5. Cells were transfected with pcUL49.5 or mock transfected and collect 24 hpt. Lysates were treated as described in (A). Positions of marker bands are indicated on the left. Predicted molecular weight of UL49.5 approx. 8kDa. (C): Specificity of the antiserum assayed by blocking. Respective antiserum was pre-incubated with immunization peptide or random peptide, respectively, for 24 h prior to western blotting. (D): Indirect immunofluorescence of CEC infected with MDV. Cells were infected with 200 pfu of MDV v20 and fixed/permeabilized 5 dpi. Subsequently, cells were stained with rabbit anti-actin antibody, mouse anti-UL49.5 antiserum and Hoechst to visualize the nuclei. Blue: DNA, green: actin, red: pUL49.5.

6.1.3 Generation of a MDV UL49.5 knock-out virus

Contrary to other UL49.5 homologues of the varicelloviruses, a previous publication defined UL49.5 of MDV as being essential for viral replication[88]. The authors were not able to reconstitute an UL49.5 knock-out virus following transfection of the infectious viral DNA into CEC. However, these earlier results were obtained with a mutant virus in which the entire UL49.5 ORF was disrupted by insertion of a kanamycin resistance marker cassette. Given the relatively large size of the selection marker within the considerably smaller ORF, replication deficiency could have been the result of interference of the integrated sequence with unidentified regulatory elements (e.g., promoters, enhancers of other genes) within UL49.5. Such bystander effects would always superimpose on the intended modification and could not be excluded with absolute certainty. Therefore, to keep the overall change within the viral genome as small as possible, seamless *en passant* mutagenesis was applied to

generate a novel UL49.5 knock-out virus based on the cell culture adapted MDV v20 strain. The start codon of the ORF was deleted by two point mutations. However, the UL49.5 ORF contains a second in-frame start codon downstream of the first start position that could potentially drive expression. In order to obtain a clean knock-out virus it was mandatory to mutate both putative start codons. Indeed, a single start codon deletion virus (v20_UL49.5Δ1Met) showed residual traces of the protein on western blots (data not shown). Unexpectedly and in stark contrast with the earlier publication, deletion of the first and second start codon yielded a replication-competent virus (v20_UL49.5Δ1+2Met) that was completely devoid of pUL49.5 but grew with kinetics that were virtually indistinguishable from parental virus (personal observation). As seen in Fig. 7B, pUL49.5 was absent in lysates of cells infected with v20_UL49.5Δ1+2Met. The desired mutation was confirmed by Sanger sequencing and integrity of the mutated BAC was also confirmed by RFLP analysis which showed identical bands in restriction enzyme digests of v20 and the final mutant (Fig. 7A). The results clearly indicated that MDV UL49.5 is not essential for viral replication in primary CEC. Albeit unexpected and contradicting the earlier report published in 2002, this interesting finding is very important and will impact future research on MDV UL49.5.

6.1.4 Flow cytometry-based MHC class I downregulation assays with v20_UL49.5Δ1+2Met

An earlier study showed that deletion of the C-terminal domain of MDV pUL49.5 yielded a virus that was less efficient in MHC class I downregulation compared to parental virus[87]. The results were in line with results obtained in members of the genus *Varicellovirus*. Jarosinski *et al.* used the continuous chicken cell line OU2 for infection assays with either wildtype virus (v20) or a pUL49.5 C-tail deletion mutant (v20_UL49.5ΔCt). Nevertheless, the remaining N-terminal portion and transmembrane region of pUL49.5 could potentially still be expressed by v20_UL49.5ΔCt and influence MHC class I levels to a certain extent. Therefore, I was eager to test the novel v20_UL49.5Δ1+2Met, which proved to be completely devoid of pUL49.5 (Fig. 7B), next to v20 and v20_UL49.5ΔCt in MHC class I downregulation assays. Despite multiple attempts, the previously used OU2 cell line could not be infected with an efficiency that would have allowed the assays to be performed. The experimental setup in this regard is not trivial due to the slow growth kinetics of MDV and its strict cell association, which requires co-seeding of infected CEC with uninfected OU2 cells. Therefore the experiment was repeated with infected CEC, which express lower but clearly detectable amounts of MHC class I on their surface. Cells were infected with equal pfu of wildtype virus or the respective mutants and tested for MHC I cell surface expression by dual-color flow cytometry 4 dpi

(Fig. 8). The dual-color staining for MHC and MDV infection allowed simple comparison of MHC class I levels on infected compared to non-infected cells.

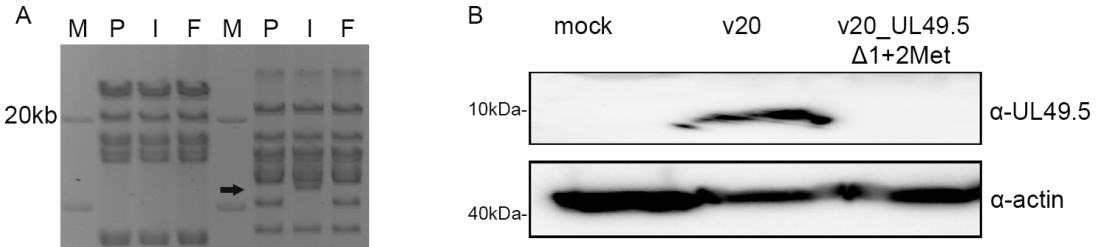

Figure 7: Generation and analysis of a MDV UL49.5 deletion mutant. (A) RFLP analysis of the parental virus v20 (P), the kanamycin cassette containing intermediate (I) and the resolved final clone v20_UL49.5Δ1+2Met (F) with restriction enzymes ApaLI and SacI, respectively. Maker bands are indicated on the left. Arrows indicate the fragment length variation caused by insertion of the kanamycin cassette which is removed in the final mutant. M: 1kb plus DNA ladder. (B) Western blot analysis of CEC infected with a MDV UL49.5 deletion mutant. Cells were infected with 200 pfu of MDV v20, v20_UL49.5Δ1+2Met or mock infected, respectively, and collected 5 dpi. Lysates were separated by 20% - 7.5% gradient SDS-PAGE followed by immunoblotting. Membranes were incubated with polyclonal mouse anti-pUL49.5 antiserum, washed and incubated with secondary goat anti-mouse HRP antibody. For the detection of actin as a loading control (lower panel), blots were stripped, blocked and reprobed with rabbit anti-actin antibody. Note the complete absence of protein in the mutant virus.

When this kind of double staining is plotted, two different populations become apparent. The uninfected cells which are MHC^{high} and MDV^{low} can be found in the lower right quadrant. In contrast, those cells of the total population that are MDV infected have severely reduced levels of surface MHC I and thus can be found in the MDV^{high}/MHC^{low} quadrant (upper left quadrant; Fig. 8). However, if a viral mutant were less capable of MHC I downregulation, cells that have a MHC^{high}/MDV^{high} phenotype would appear in the upper right quadrant. This distribution was shown previously[87]. Surprisingly, no differences could be detected regarding MHC class I levels on cells infected with either of the mutant viruses compared to the parental virus. In multiple attempts, the percentage of cells in the upper right quadrant was below the false positive rate (about 1-2%) as determined by isotype controls (not shown). Thus, I concluded that pUL49.5 does not play a role in MHC class I downregulation of

infected primary CEC, the cell type which is most commonly used for *in vitro* infection studies.

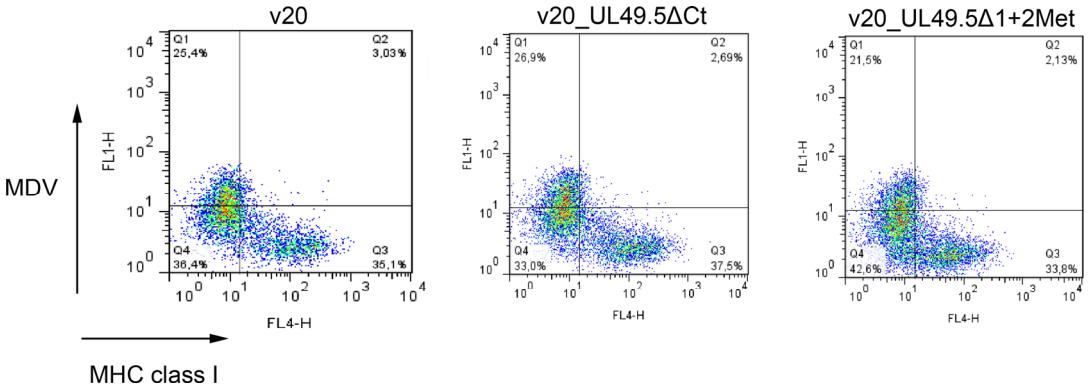

Figure 8: MDV pUL49.5 is not responsible for MHC class I downregulation in infected CEC. *In vitro* flow cytometry-based MHC class I downregulation assays are shown. CEC were infected with v20, v20_UL49.5ΔCt or v20_UL49.5Δ1+2Met, respectively. 5 dpi, cells were stained with mouse anti-chicken MHC class I antibody and polyclonal anti-MDV chicken serum, respectively. Samples were resuspended in PBS and analyzed by dual-color flow cytometry with a FACScalibur flow cytometer. Note the absence of an MDV^{high}/MHC I^{high} cell population in the upper right quadrant in all three viruses.

6.1.5 Post-translational stability of MDV pUL49.5

The inability to detect pUL49.5 in preliminary studies using an expression vector (Fig. 6) had implied instability of the target protein when expressed in CEC outside of the viral background. This confronted me with the problem of being unable to perform any transfection-based assays, a tool which can be instrumental in MDV research since not all experimental setups are compatible with the unique biological properties of the virus.

A reason for the protein's instability could be ubiquitin-mediated degradation of pUL49.5. A potential ubiquitination motif that could potentially control protein stability was identified within the C-terminal domain of pUL49.5 (Fig. 9A). The motif was tested for its involvement in degradation by mutation of the predicted lysine residue (K) at position 92 to an alanine in the pcUL49.5 expression vector. Two amino acids, a cysteine (C) at position 83 and a threonine (T) at position 88, represented additional potential sites for ubiquitination. In a second construct, all three residues were changed to alanine by site-directed mutagenesis. However, none of the modified proteins seemed to have increased expression levels in CEC and detection of the modified proteins by western blot analysis was not possible (data not shown).

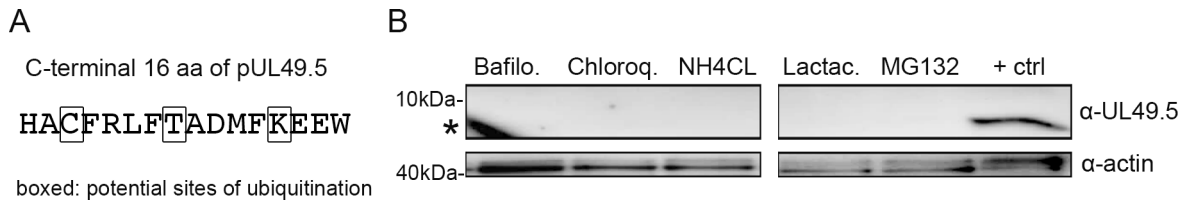

Figure 9: The stability of pUL49.5 is not influenced by cellular degradation pathways. (A) Identification and site-directed mutagenesis of potential ubiquitination sites in the C-terminus of MDV pUL49.5. Alanine substitution of any of the three amino acids lysine, threonine or cysteine did not allow detection of pUL49.5 following transfection of CEC with pcUL49.5 (not shown). (B) Treatment of transfected CEC with inhibitors of proteasomal and lysosomal protein degradation. 12 hpt cells were incubated with fresh medium containing the lysosomal inhibitors bafilomycin A, chloroquine or NH_4Cl (left panel), respectively, and further incubated for 8 h. In a second experiment, cells were treated with inhibitors of proteasomal degradation, lactacystin or MG132, for 8 h (right panel). Subsequently, cells were subjected to western blot analysis. Actin served as a loading control and lysates of infected cells as an antibody control (right panel). The asterisk indicates a background artefact which could not be reproduced.

However, in order to validate the obtained results and the hypothesis that pUL49.5 could be targeted by the cellular protein degradation machinery, transfected CEC were treated with two different inhibitors of proteasomal degradation, lactacystin and MG132. Both reagents block the catalytic subunits of the proteasome[121]. Since lysosomal degradation could provide another pathway to destruction, cells were also treated with the inhibitors bafilomycin A, chloroquine and ammonium chloride (NH_4Cl), which act by inhibiting endosome acidification and, consequently, lysosomal degradation[122–124]. As seen in Fig. 9B, none of the treatments substantially increased pUL49.5 levels in CEC. Furthermore, addition of a cell- permeable protease inhibitor mixture to the media did not have any obvious effect on expression levels making the involvement of proteases rather unlikely (data not shown). Therefore, degradation can be most likely excluded as the reason for the absence of pUL49.5. To further investigate the issues with protein stability, the MDV UL49.5 ORF was cloned in-frame with different N- and C-terminal epitope tags into mammalian expression vectors. Interestingly, N-terminally tagged constructs also failed to express properly whereas their C-terminal counterparts showed an intermediate expression in CEC as detected by western blotting (Fig. 10A, right panel).

6.1.6 Context dependent expression of MDV pUL49.5

Glycoprotein M (gM) is conserved in all herpesviruses and its MDV homologue is encoded by the UL10 gene[98]. The transmembrane protein is necessary for efficient spread of MDV and a

respective knock-out virus was shown to be replication-incompetent[88]. During infection, pUL49.5 interacts with gM and mediates its processing as a glycoprotein in a number of herpesviruses[125,126]. Thus, apart from its function as an immune evasin, pUL49.5 actually serves a dual role. Despite being very likely, the interaction between MDV gM and pUL49.5 has not been experimentally proven yet. In order to investigate if the presence of gM could stabilize ectopically expressed UL49.5, a gM expression construct containing a 6×His epitope tag at its C-terminus was cloned into the pcDNA3.1 vector (pcgMHis). However, when pcgMHis and pcUL49.5 were cotransfected into CEC, the presence of UL49.5 could still not be detected by either western blot or immunofluorescence analysis (not shown). Further studies should evaluate the putative interaction of both proteins by co-immunoprecipitation studies.

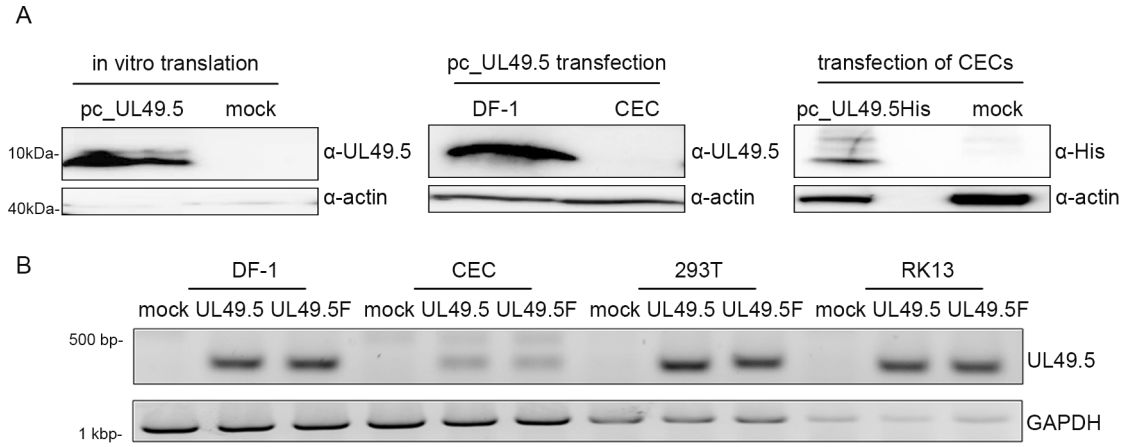

Figure 10: Context dependent detectability of MDV pUL49.5. (A) left panel: *In vitro* translation of pUL49.5. The commercially available EasyXpress Kit (Qiagen, Hilden) was used to translate pUL49.5 in ER-membrane containing lysates of insect cells. Compared to a mock control, pUL49 showed strong expression as detected by western blotting. (A) middle panel: Expression of UL49.5 in DF-1 and CEC. Both cell types were transfected with pcUL49.5 and lysates were subjected to western blot analysis. Note that pUL49.5 can not be detected in lysates of transfected CEC albeit present in infected cells (compare Fig. 6A). (A) right panel: Expression of MDV UL49.5 epitope-tagged constructs in CEC. Western blot analysis of cells transfected with pcUL49.5His or empty vector. (B) RT-PCR analysis of UL49.5 transcripts in different cell lines. Cells were transfected with pcUL49.5, pcUL49.5Flag or mock-transfected and collected 24 hpt. cDNA was produced from total RNA with specific primers and amplified via standard PCR. cDNA generated from chicken GAPDH transcripts served as an internal control.

Since degradation could be ruled out as a main reason for the absence of the protein, I sought to exclude interacting cellular factors masking the detection of pUL49.5. Therefore, *in*

vitro translation assays were performed with ER-membrane containing insect cell lysates (Fig. 10A, left panel)). As seen in Fig. 10A, in *vitro* synthesized pUL49.5 could readily be detected by western blotting. Subsequent experiments also revealed that expression of pUL49.5 seemed to be cell-type specific since it was not detected in lysates of transfected rabbit RK13 and human 293T cells (data not shown). Surprisingly, albeit derived from the same host, the continuous chicken fibroblast cell line DF-1 supported stable expression and detection of pUL49.5 as opposed to primary CEC (Fig. 10A, middle panel). To explore these somewhat variable results with different cell lines, an RT-PCR analysis was performed. DF-1 cells, CEC, rabbit RK13 as well as human 293T cells were transfected with pcUL49.5, pcUl49.5Flag or mock-transfected. At 24 hpt, total RNA was prepared from cells and cDNA was amplified with specific primers (Table 1). A primer set specific for the 5' and 3' end of the UL49.5 ORF was used in the subsequent PCR. cDNA of chicken GAPDH served as an internal control. As seen in Fig. 10B, a specific band of the expected size could be found in all cells transfected with pcUL49.5 (or pcUL49.5Flag) but not mock-transfected cells. The reduced number of transcripts in CEC can most probably be attributed to the much lower transfection efficiency compared to the other cell lines. The solid production of UL49.5 transcripts in all cells is quite remarkable given the fact that only DF-1 cells allowed the reliable detection of the protein. It clearly indicates that the detection problems seem to be caused at the post-transcriptional level. However, DF-1 cells could be used for further experimental investigation of pUL49.5.

6.1.7 Flow cytometry-based MHC class I downregulation assays with transfected DF-1 cells

Previous results with v20_UL49.5Δ1+2Met had shown that UL49.5 does not seem to be responsible for MHC class I downregulation in infected CEC. This was in contrast to a study that demonstrated effects in v20_ UL49.5ΔCt infected OU2 cells[87]. In the same study, the authors tested UL49.5 expression plasmids for their capability to induce MHC class I downregulation outside of the viral context. The investigators transfected the chicken B cell line RP9 and could demonstrate downregulation triggered by pUL49.5[87]. As RP9 cells were not available to me, DF-1 cells were used in order to validate or falsify these results. MHC class I cell surface levels on transfected DF-1 cells were analyzed by dual-color flow cytometry. The MDV US3 protein, which is not involved in MHC I downregulation, served as a negative control and the established TAP inhibitor BHV-1 pUL49.5 as a positive control. Figure 11A shows the relative expression of MHC class I on the surface of transfected compared to non-transfected cells within the same sample. Thus, values below 100% represent a specific reduction of MHC class I. MDV pUL49.5 was capable of reducing MHC

class I surface levels by only 10% compared to the negative control (Fig. 11A). As expected, the positive control, BHV-1 pUL49.5, induced a more pronounced downregulation of 40%. In most of the performed experiments, differences induced by MDV pUL49.5 were not statistically significant (or at the edge of significance) with p >0.05 as determined by Student's t-test. Thus, the mild effects only represent a trend.

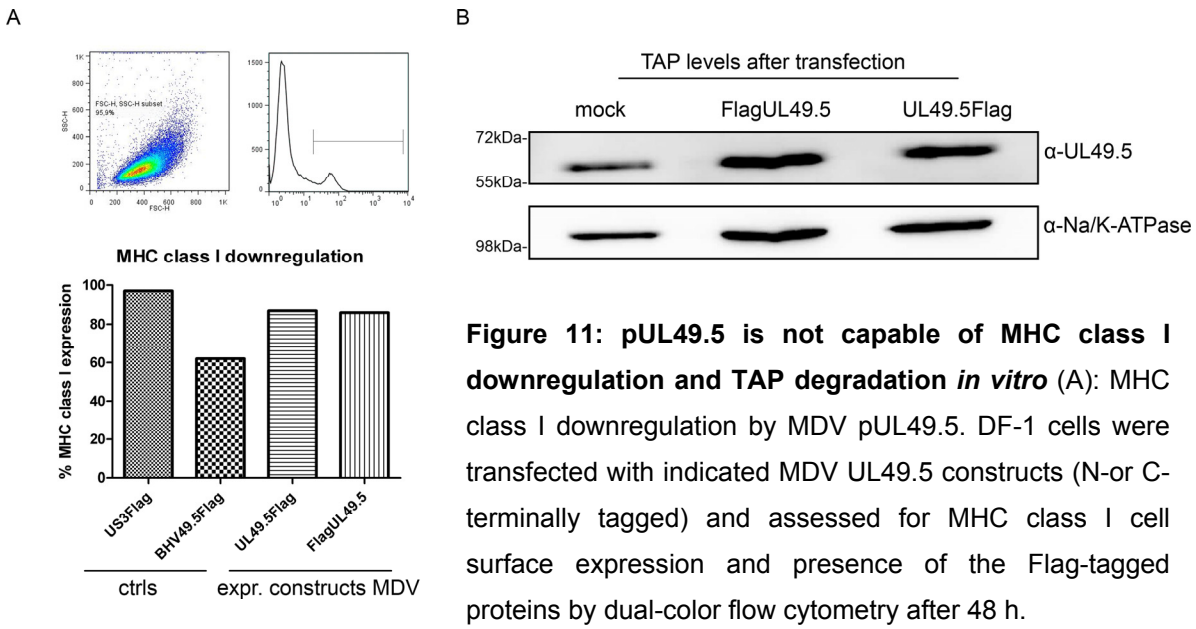

Figure 11: pUL49.5 is not capable of MHC class I downregulation and TAP degradation *in vitro* (A): MHC class I downregulation by MDV pUL49.5. DF-1 cells were transfected with indicated MDV UL49.5 constructs (N-or C-terminally tagged) and assessed for MHC class I cell surface expression and presence of the Flag-tagged proteins by dual-color flow cytometry after 48 h. The ratio of mean fluorescence intensity (MFI) of the Flag-positive to the Flag-negative population is given as a percentage of relative MHC class I downregulation. MDV US3Flag: neg. control, BHV-1 UL49.5Flag: pos. control. Gating of the total cell population as well as Flag-postive cells is shown in the upper left and right pictures. (B) TAP2 expression levels in UL49.5-transfected DF-1 cells. Lysates of cells were subjected to western blotting and incubated with TAP2 antibody.

6.1.8 TAP degradation studies with transfected DF-1 cells

So far, the obtained results argued against an involvement of pUL49.5 in modulation MHC class I expression on the cell surface. Nevertheless, potential effects on TAP levels were tested in transfected DF-1 cells. Using an antibody specific for chicken TAP2 (kindly provided by Dr. J. Kaufman, Cambridge, UK), no obvious difference in TAP2 expression levels could be seen in UL49.5 transfected DF-1 cells (Fig. 11B) arguing against specific degradation of the transporter. In order to assess if the target protein acts via interference with peptide translocation, further studies will focus on peptide transport assays.

6.2 Identification and functional characterization of the predicted MDV ORF012 gene

6.2.1 Location of ORF012 in the MDV genome

Despite its extensive colinearity with VZV and HSV-1, the MDV genome contains a sequence stretch within the U_L region that seems to be exclusively present in avian alphaherpesviruses (Fig. 12). A potential role in host range has therefore been proposed for the genes encoded in this area[127]. Notwithstanding, the region is poorly characterized regarding its coding capacity. The annotation of MDV ORFs that do not have comparable homologues in other herpesviruses is not a trivial task and usually relies heavily on bioinformatic predictions. Early attempts of genome-wide annotations for several MDV strains deposited in GenBank resulted in the provisional prediction of two potential ORFs, named ORF011 and ORF012, in the 5' region of U_L. I will refer to these ORFs as ORF011* and ORF012* in the presented work in order to clearly differentiate them from the newly identified ORF012.

The putative ORF011* has a length of 258 bp (Genbank AAG14191.1) followed by ORF012* with a predicted size of 1,155 bp (Genbank AFG14192.1, Fig. 12). Both predicted ORFs are separated by a short intergenic sequence of 139 bp. However, a more recent annotation predicted splicing within the 011* and 012* region (Refseq, Genbank NC_002229.3). I confirmed these predictions by bioinformatic analysis using the NetGene2 Server[128]. The analysis revealed putative splicing of a small intron of 82 bp within the ORF011*, because the sequence matched the consensus sequence for classical splice acceptor and donor sites with high scores (Fig. 12). The splicing would lead to fusion of the two putative exons of ORF011* and, as a consequence, result in a frame-shift mutation and read through to ORF012*. The predicted spliced transcript, therefore, represents a mRNA in which ORF011* and ORF012*, as well as the former intergenic region are joined together to form a single transcript termed ORF012. The predicted protein encoded by ORF012 is a 489 amino acid protein with a calculated mass of 55 kDa. Interestingly, ORF012 is already annotated as a putatively spliced gene following an update of the Md5 strain reference sequence in 2007 and consequently ORF011* has been excluded from this new annotation (NC_002229.3). However, to my knowledge no experimental evidence has been provided for this splicing event nor has any functional characterization been performed.

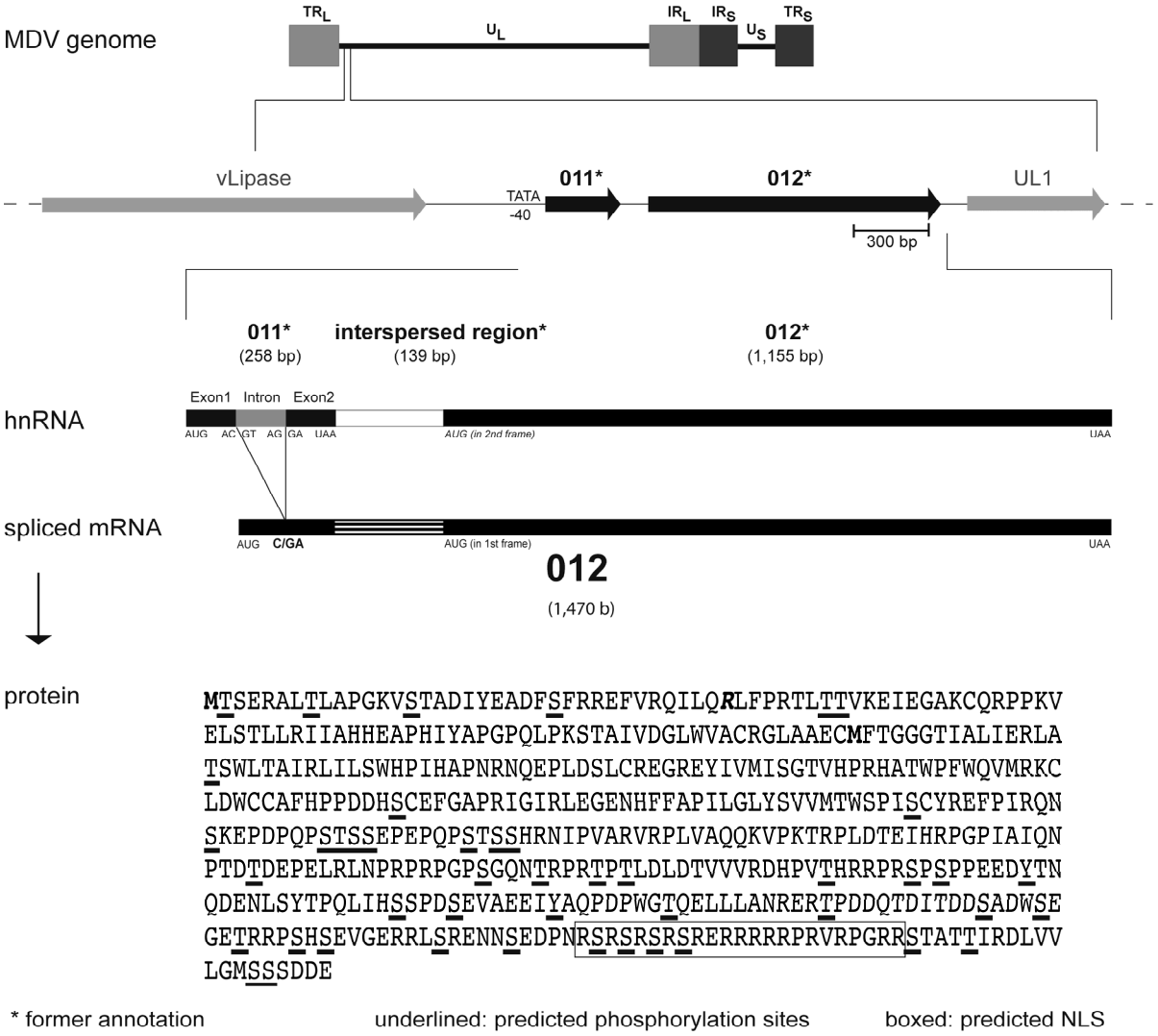

Figure 12: p012 is generated from a spliced transcript. Position of MDV ORF012 and splicing of its mRNA. The structure of the MDV genome is outlined and the position of the hypothetical ORF011* and ORF012* genes (black) in relation to other genes is indicated. Sizes are given in basepairs (bp) for DNA or bases (b) for RNA, respectively. The 82-bp intron in the former ORF011* is indicated in grey. Predicted splicing results in a frame-shift and absence of the predicted ORF011* stop codon. Splicing leads to fusion of the remaining sequence with the formerly predicted short intergenic region and the 5' end of former ORF012* thus creating the novel ORF012 transcript. The splice donor and acceptor sites are indicated. The primary sequence of p012 with predicted phosphorylation sites (underlined) and a predicted NLS (boxed) is shown. Initiator methionines of ORF012 and former ORF012*, respectively, are marked in bold. Amino acid corresponding to exon/exon border (arginine, R) is marked in bold and italic. UL unique long, US unique short, TRL terminal repeat long, TRS terminal repeat short, IRL internal repeat long, IRS internal repeat short.

6.2.2 Splicing of MDV ORF012 during infection of chicken cells

As a tool for determining the predicted splicing of ORF012 by RT-PCR, a synthetic ORF012 construct that was devoid of the predicted intron was generated using fusion PCR and cloned into the pcDNA3.1 expression vector. The construct was termed pc012$^{\Delta int}$ to differentiate it from the original ORF012 sequence (with intron).

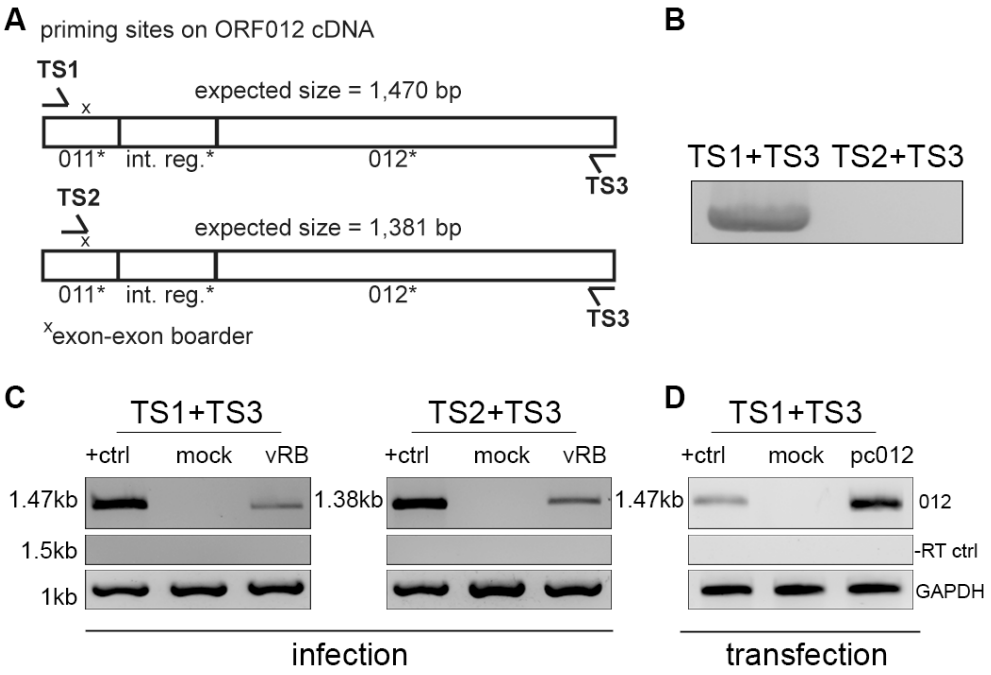

Figure 13: Analysis of ORF012 splicing in MDV infection by RT-PCR. (A) Position of primer binding regions on ORF012 cDNA. Two sets of primers specific for the 5' and 3' coding region of the ORF012 transcript (TS1 and TS3) or the exon/exon border (TS2), respectively, were used. Primer sequences are given in Table 1. (B) Primers were tested using genomic vRb DNA. Note that no product should be obtained with primer combination TS2 and TS3 due to the absence of the exon/exon border in genomic DNA. (C) Total RNA of MDV-infected or mock infected CEC was extracted 5 dpi. RNA was reverse-transcribed into cDNA with indicated primers. Amplification products obtained by subsequent PCR were analyzed by agarose gel electrophoresis. cDNA prepared from DF-1 cells transfected with an expression plasmid encoding an intron-less ORF012 construct (termed pc012Δint) served as a positive control and size marker (first lanes, + ctrl). Amplificons were subjected to Sanger sequencing and showed 100% identity with the predicted mRNA. cDNA of chicken GAPDH mRNA served as an internal control (lower panels) and RT-negative control reactions excluded genomic DNA contamination (middle panels). D) To show that splicing of ORF012 is independent of other viral factors, total RNA of DF-1 cells transfected with pc012Δint, pc012 or pcDNA3.1 vector (negative control) were extracted 24 hpt. Samples were subsequently treated as described in (C). Sequencing revealed 100% sequence identity with the predicted ORF012 mRNA sequence.

Additionally, forward and reverse primers specific for the 5' and 3' coding region of the ORF012 transcript (TS1 and TS3), as well as a forward primer spanning the predicted exon-exon border within its 3' terminal portion (TS2), respectively, were designed (Fig. 13A).
First, both primer sets were controlled in PCR reactions using rRb BAC DNA. The combination of primers TS1 and TS3 yielded an expected DNA fragment of 1,552 kb that contained the intron sequence. Due to the nonexistent exon-exon border in genomic DNA, the combination of primers TS2 and TS3 did not yield any product (Fig. 13B). In order to demonstrate splicing, cDNA was produced from total RNA of vRb or mock-infected CEC at 5 dpi. Using both primer sets, a single fragment from cDNA of infected cells was amplified that corresponded in size to control cDNA generated from chicken cells transfected with the intronless pc012$^{\Delta int}$ (Fig. 13C). In addition, the band was absent in mock-infected cells. The PCR products were gel purified, subjected to Sanger sequencing and revealed perfect sequence identity with the predicted spliced mRNA. PCR reactions performed on RT-negative (-RT) samples served as control for a possible DNA contamination (middle panels). In addition, DNA contamination of RNA was excluded using primer TS2, which is only capable of priming the exon-exon border within the spliced mRNA. Chicken GAPDH cDNA served as an internal control (lower panels). To further validate my results, the RT-PCR analysis was repeated with cDNA generated from chicken DF-1 cells transfected with pc012$^{\Delta int}$ (positive control), pc012 or pcDNA3.1. Again, a single band of the expected size whose sequence was identical to the predicted ORF012 mRNA could be amplified (Fig. 13D). It was therefore concluded that ORF011* and ORF012* do not represent independent elements, but one single unit that is comprised of two exons that are separated by an 82 bp intron close to the 5' region of the novel ORF012. The intron is spliced during both transfection of the expression construct and virus replication, suggesting it is spliced independently of viral factors.

6.2.3 p012, but not p012* by itself, is produced during MDV infection

Despite the clear indication for a splicing event, the possibility that ORF012 only represents a splice variant and that an individually expressed ORF012* may be produced was considered. That is, p012* could be translated from the predicted in-frame start codon of ORF012* encoded within the ORF012 mRNA (compare Fig. 12). In order to investigate the protein coding capacity of the ORF012 mRNA, protein translation from its transcript was analyzed. To do this, ORF012* and ORF012 were cloned individually into the pcDNA3.1 expression vector with C-terminal Flag tags. Furthermore, the cell culture-adapted, apathogenic MDV strain v20 was used to generate FLAG epitope-tagged versions of p012 (v20_012Flag). Due to the significant differences in the predicted molecular mass of p012* and p012 (44 kDa vs.

55 kDa, respectively), the v20_012Flag virus would allow the differentiation of each protein by western blot analysis. CEC were infected with 200 pfu of v20 or v20_012Flag for 5 days, and then protein lysates of infected cells were subjected to western blot analysis. Lysates of cells transfected with pc012*Flag or pc012Flag expression plasmids served as controls and internal size markers. As shown in Fig. 14, the presence of a specific band of ~55 to 60 kDa in lysates of cells transfected with pc012*Flag (lane 1), as well as a band of 75 to 80 kDa in lysates of cells transfected with pc012Flag (lane 2) could be detected indicating that both proteins can be produced from expression plasmids in DF-1 cells. Most importantly, only a single band corresponding to the size of p012Flag, but not p012*Flag was present in lysates of v20_012Flag infected cells (lane 4). As expected, no p012Flag-specific band could be detected in the negative control, v20-infected cells (lane 3), using the Flag antibody. Interestingly, both p012* and p012 appeared to have higher molecular weights than predicted. Although some deviation of apparent molecular masses after SDS-PAGE from those predicted, based on the amino acid sequence is common[129], the differences observed were much greater and thus could also be due to extensive posttranslational modification.

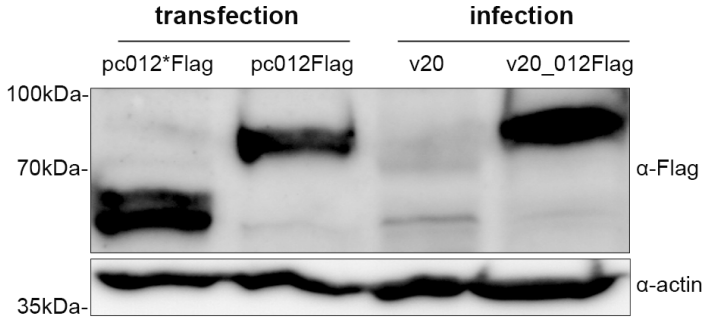

Figure 14: Detection of p012, but not p012*, in MDV infected cells by western blot analysis. CEC infected with 200 pfu of MDV v20 or v20_012Flag were collected 5 dpi. Lysates were separated by 7.5% SDS-PAGE followed by immunoblotting. Lysates of cells transfected with pc012*Flag or pc012Flag, respectively, were used as controls and internal size markers. Membranes were incubated with polyclonal rabbit anti-Flag antibody, washed and incubated with secondary goat anti-rabbit HRP antibody. For the detection of actin as a loading control, blots were stripped, blocked and reprobed with rabbit anti-actin antibody. Note the absence of a band corresponding to p012 in lysates of virus-infected cell lysates. Positions of weight marker bands are indicated on the left.

Contrary to expression of p012* alone, the production of a protein from ORF011* is highly unlikely due to the efficiency of the splicing process. Mechanisms that suppress splicing of ORF011* (e.g., intron skipping) and retain the stop codon would have to be active in order to generate a functional protein. It was not possible to detect any such protein (predicted molecular mass of the theoretical protein: 10 kDa) in pc011*Flag transfected DF-1 cells when

applying indirect immunofluorescence microscopy or western blotting (data not shown). Nevertheless, to corroborate the results a Flag tag was introduced immediately downstream of the initiation codon of the putative ORF011* (v20_Flag011*). Again, the presence of a low molecular weight protein could not be detected by western blotting of infected CEC (data not shown). In summary, it was concluded that only p012 from a spliced mRNA is synthesized in infected cells.

6.2.4 ORF012 is essential for viral replication *in vitro*

Next, I determined whether ORF012 was dispensable for viral replication *in vitro*. Using two-step Red-mediated mutagenesis, the start codon of ORF012 in the pathogenic RB-1B strain was replaced with a stop codon (rRbΔMet012) to prevent translation of the protein. The resulting mutant virus, vRbΔMet012, was severely replication-impaired following reconstitution in CEC. Numbers, as well as sizes, of plaques were significantly smaller compared to parental vRb (Fig. 15).

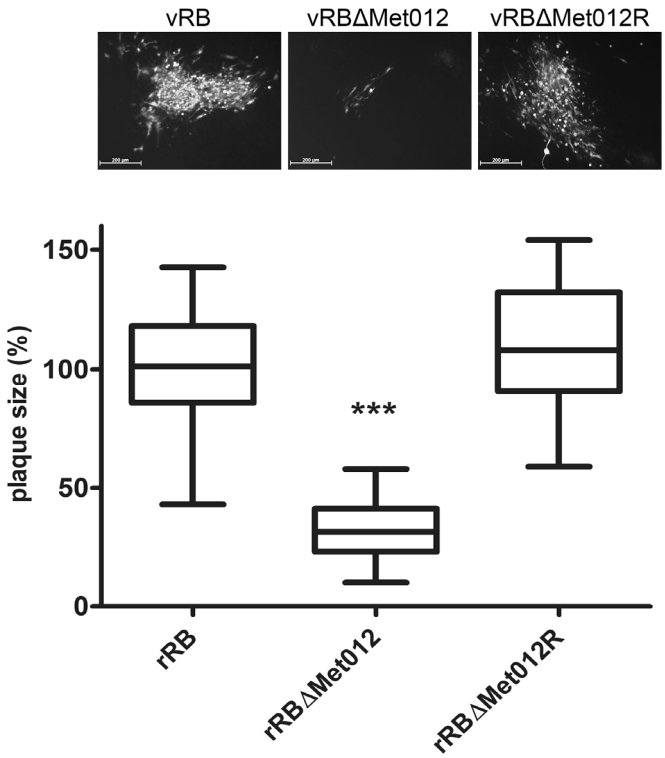

Figure 15: p012 is essential for viral replication *in vitro*. Quantification of viral replication by plaque size assay is shown. Cells were transfected with rRb DNA, a mutant BAC in which the start codon of ORF012 was replaced with a stop codon (rRbΔMet012) and a revertant construct in which the start codon was repaired (rRbΔMet012R). At 5 dpt, plaques were stained by indirect immunofluorescence using an MDV-specific polyclonal antiserum and plaque diameters of at least 50 plaques in three independent experiments were determined. Whisker plots of plaque diameter distributions relative to wild-type virus are shown. Exemplary pictures of plaques are included. Results were tested for normality and subsequently analyzed for significance by 1-way Anova, (*** $p < 0.01$).

vRbΔMet012 plaques also displayed a different phenotype as they appeared less “dense” and reminiscent of a cluster of single infected cells with many interspersed uninfected cells rather than the characteristic dense clusters of infected cells normally seen for parental vRb. More importantly, vRbΔMet012 could not be expanded by serial passaging of infected cells despite multiple attempts (n = 6). Even in very early passages following reconstitution, scant signs of cytopathic effects were observed, indicating a severe impact on viral replication due to the absence of p012. Consequently, classical single- or multi-step growth kinetics could not be performed. To exclude the possibility of secondary site mutations introduced during BAC mutagenesis, a revertant virus (vRbΔMet012R) was generated in which the start codon was restored in vRbΔMet012. In three independent experiments, sizes of at least 50 plaques for each virus were determined and compared based on calculated diameter values. As demonstrated in Fig. 15, vRbΔMet012 induced significantly smaller plaques and reached only approximately 30% of the mean diameters determined for wild-type and revertant virus, which were not significantly different from each other. Computed diameters were tested for normality of distribution and for significance by 1-way Anova ($p<0.01$). Given the dramatically reduced size of the vRbΔMet012 plaques, and, more importantly, the inability to expand the virus by serial passaging, I concluded that ORF012 is important for replication of the RB-1B wild-type virus.

6.2.5 p012 localizes predominantly to the nucleus of transfected and infected cells

Next, I targeted my studies at elucidating the potential role p012 may play during MDV replication. First, the protein’s subcellular localization was determined in DF-1 cells. Surprisingly, p012 exhibited a predominantly nuclear localization in transfected DF-1 cells (Fig. 16A) that were analyzed by indirect immunofluorescence. The remaining fraction of positive cells showed an either mixed nuclear/cytoplasmic or predominant cytoplasmic distribution of p012. The same localization pattern was apparent in cells transfected with the pc012$^{\Delta int}$ control plasmid that expresses the synthetic intron-less version of p012 (Fig. 16A). This was not unexpected since the construct is devoid of the intron but otherwise leads to the production of an identical protein. In order to quantify the subcellular localization, the distribution of p012 was categorized in a blinded approach in more than 200 cells per construct by indirect immunofluorescence microscopy. Although the approach is of a rather semi-quantitative nature, this method has already been used to quantify the nuclear localization of viral factors[119]. Distribution of p012 was categorized into three classes: 1) predominantly nuclear 2) mixed nuclear/cytoplasmic or 3) predominantly cytoplasmic. The number of cells in each category in relation to all analyzed cells is displayed as percent values. Figure 16B shows the combined results of two independent experiments. In

approximately 55-65% of analyzed cells, an entirely nuclear distribution of the target protein was detected 24 hpt (black). In the remaining cells, 30-35% were predominately cytoplasmic (white), while 5-10% contained p012 in both the nucleus and cytoplasm (grey). A similar distribution was apparent in cells transfected with the pc012$^{\Delta int}$ control plasmid (second bar). The distribution of p012 was also comparable at 48 hpt (third bar). Since the synthesis of viral proteins from expression vectors does not necessarily reflect the situation during infection, the results were validated in CEC infected with v20_012Flag. In agreement with the transfection experiments, p012 localized mainly to the nucleus in MDV-infected cells, while a smaller fraction of cells showed predominantly cytoplasmic or mixed (nuclear and cytoplasmic) localization (see 6.2.6).

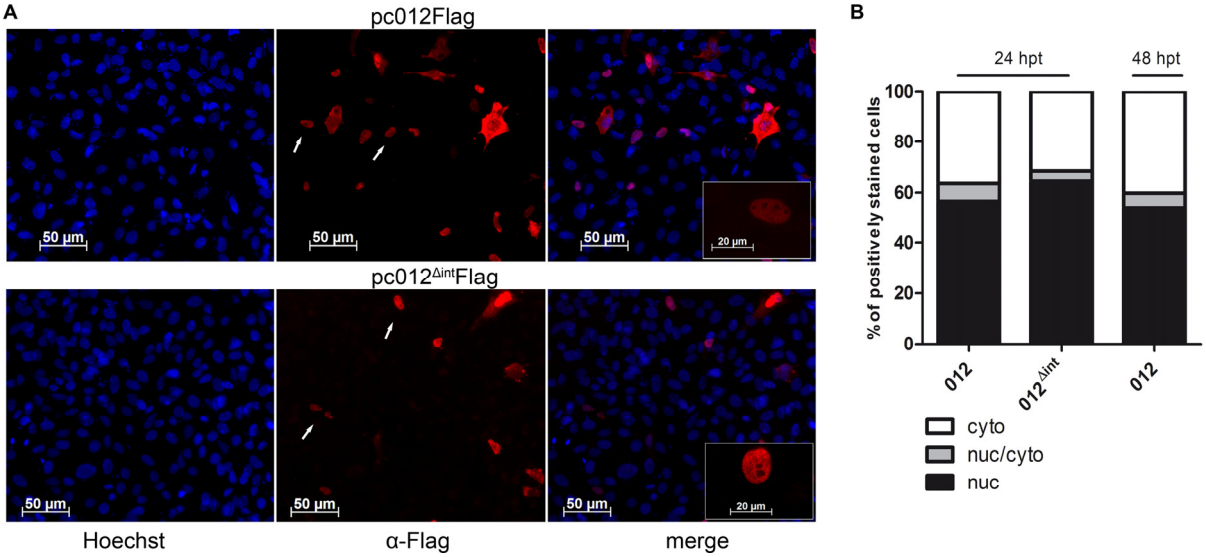

Figure 16: Nuclear/cytoplasmic localization of MDV p012 in transfected cells. (A) DF-1 cells on coverslips were transfected with pc012Flag. Expression plasmid pc012$^{\Delta int}$Flag served as a control. At 24 hpt (and 48 h in the case of p012), cells were fixed, permeabilized and stained with polyclonal rabbit anti-Flag antibody (red). Transfected cells were co-stained with Hoechst 33342 to visualize the nucleus (blue). (B) Localization was quantified by indirect immunofluorescence microscopy as described in the Materials and Methods. Results shown are from two independent experiments.

6.2.6 p012 contains a functional nuclear localization signal in its C-terminal domain

The predominant nuclear localization of p012 prompted a bioinformatic search for potential nuclear localization signals (NLS). Interestingly, two different analysis tools predicted a potential monopartite NLS in the C-terminal portion of p012. NucPred[130] predicted a signal comprised of six basic arginines and one proline ranging from amino acid 457 to 463

(^{457}RRRRRPR^{463}) with high probability. The sequence stretch was provisionally termed “short NLS”. In addition, analysis of the protein sequence with the tool NLStradamus[131] identified an NLS with the sequence ^{447}RSRSRSRSRERRRRRPRVRPGRR^{469}, which overlapped with the short NLS, but was considerably longer and was thus termed “long NLS” (Fig. 17A). In order to determine the importance of the NLS sequence in p012, the 3’ region of the ORF012 gene was deleted within the viral genome of vRb. The deletion removed about 1/3 of the protein encompassing both potential NLS. In another vRb mutant, the basic amino acids were substituted with alanine residues within the short NLS. Interestingly, both modifications resulted in a replication incompetent virus; however, when these mutations were replaced with wild type sequences, the revertant virus could fully restore viral growth (data not shown). These results were reminiscent of the growth defect induced by ORF012 null virus vRbΔMet012 and already pointed towards the functional importance of the NLS sequence in viral replication. At the same time, it presented me with the problem of being unable to further investigate the localization of p012 in the context of viral infection.

I therefore turned to the avirulent and cell culture-adapted v20 strain to further investigate the expression of p012 during MDV replication. As with vRb, the region containing the predicted NLS was deleted in the v20 virus carrying a C-terminal Flag tag, a virus that had been previously used to detect p012 by western blotting (Fig. 14). Again, the deletion massively impaired viral replication of the mutant compared to the parental virus, but still allowed visualization of plaques. As seen in Fig. 17B, p012 nuclear localization was virtually absent in cells infected with the deletion mutant v20_012ΔNLSFlag. In contrast, nuclear localization was again observed with the parental virus v20_012Flag. To validate the observations, localization of p012 was investigated in a viral mutant containing an alanine substitution of the short NLS. The virus, termed v20_012mutshortNLS, exhibited the same phenotype as the deletion mutant (Fig. 17B, lower panels). I therefore hypothesized that a) the predicted NLS sequence has an essential function in nuclear import of p012 and b) that not only the presence of p012, but also its nuclear localization during infection is important for viral growth. It is not known why the effects of the NLS mutations are more severe in the vRb background compared to the v20 virus, but it most likely is the result of the cell-culture adaptation of v20 that has led to numerous deletions, insertions and point mutations affording it a greater capacity to replicate *in vitro*[114].

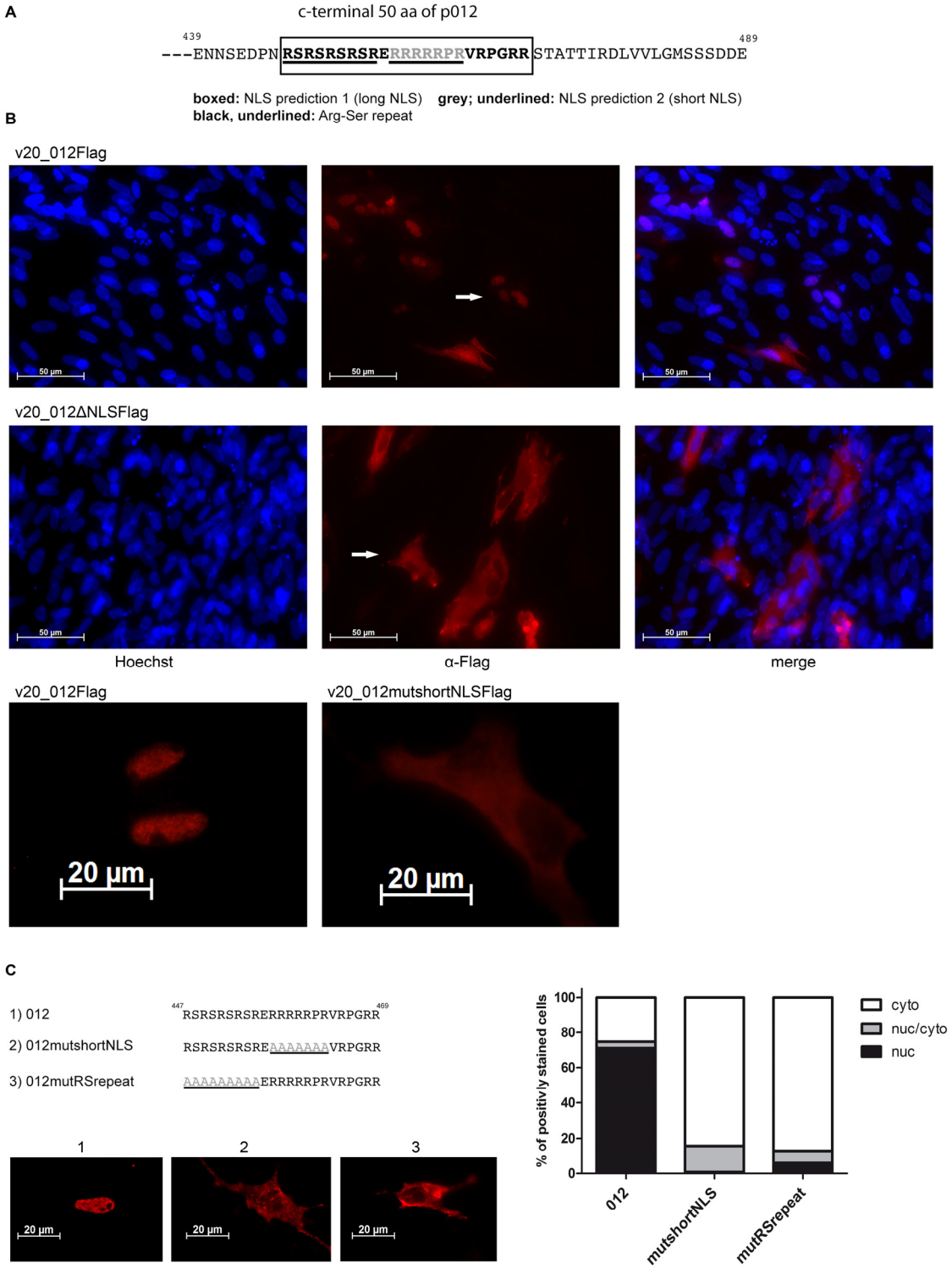

Figure 17: Prediction and mapping of a nuclear localization signal in p012. (A) Schematic representation of the C-terminal 50 amino acids of p012. The position of two putative, overlapping NLS is indicated. (B) Mutational disruption of the p012 NLS in MDV v20 inhibits nuclear accumulation. CEC were infected with v20_012Flag, a C-terminal deletion mutant (v20_012ΔNLSFlag) or an alanine substitution mutant corresponding to the predicted short NLS (v20_012mutshortNLS, lower panel), respectively.

At 5 dpi, cells were fixed, permeabilized and stained with polyclonal rabbit anti-Flag antibody. Arrows indicate cells with representative localization of p012 (C) Mutational mapping of essential NLS regions in p012. Alanine substitutions in the NLS are indicated in grey. DF-1 cells were transfected with pc012Flag, pc012FlagmutRS, or pc012FlagmutshortNLS, respectively. Pictures of representative result as well as the quantification of three independent experiments are shown.

6.2.7 Mutational mapping of the p012 NLS

Previous results with a mutant virus indicated the importance of the predicted NLS sequence for nuclear import of p012. Given the fact that two different, but overlapping NLS were predicted, I wished to determine the bona fide NLS sequence by substitution mutagenesis and reporter-based mapping approaches. To do this, DF-1 based transfection assays were employed as described previously. Firstly, the short NLS with the sequence ^{457}RRRRRPR^{463} was substituted with alanine residues by site-directed mutagenesis in the pc012Flag expression vector, resulting in plasmid pc012mutshortNLS (Fig. 17C). Accordingly, a region encoding an arginine-serine rich dipeptide repeat motif (^{447}RSRSRSRSR^{455}) was deleted, which represents approximately the first half of the predicted long NLS sequence, but is separated from the short NLS by one glutamic acid residue (Fig. 17C). The plasmid was termed pc012mutRSrepeat. Mutation of the short NLS sequence almost completely abolished nuclear localization as was observed with immunofluorescence microscopy in transfected cells. Surprisingly, the mutation of the RS repeat sequence had a comparable effect on nuclear localization, reducing the percentage of cells in this category to 7% (Fig. 17C). Nevertheless, a small percentage of cells with mixed cytoplasmic/nuclear localization could be identified in both cases. I concluded that not only the short NLS region, but also the preceding RS-rich motif is necessary for efficient nuclear import of p012.

6.2.8 The p012 NLS is transferable and can shuttle GFP to the nucleus

The previously described NLS mutation experiments suggested the involvement of the “long NLS” in nuclear localization of p012. Nevertheless, deletion experiments alone are not adequate to determine whether a specific sequence within a nuclear protein is sufficient for localization. Therefore, different p012 NLS-GFP fusion constructs based on the pEGFP-C1 expression vector were cloned (Fig. 18A). Again, GFP localization was quantified in transfection assays. Figure 18C shows the combined results of two independent experiments. Interestingly, a baseline level of nuclear/cytoplasmic localization in a small percentage of cells transfected with the GFP control vector was apparent and reached about 8%. This effect can probably be attributed to a non-specific accumulation of GFP and has been documented before[132]. Complementing my previous results of the NLS mutagenesis experiments, GFP proteins fused with either the C-terminal 150 amino acids of p012 or the “long NLS”, respectively, were equally efficient at shuttling GFP to the nucleus (Fig. 18B and

C). Nuclear localization was found in about 70% of transfected cells in both cases. Importantly, neither a GFP protein fused to the RS repeat nor to the sequence encompassing the short NLS was able to enter the nucleus above control levels. I concluded from these experiments that the long NLS (^{447}RSRSRSRSRERRRRRPRVRPGRR^{469}) is necessary and sufficient for NLS function and nuclear import of p012. Most likely, the sequence ^{457}RRRRRPR^{463} only constitutes part of the functional signal.

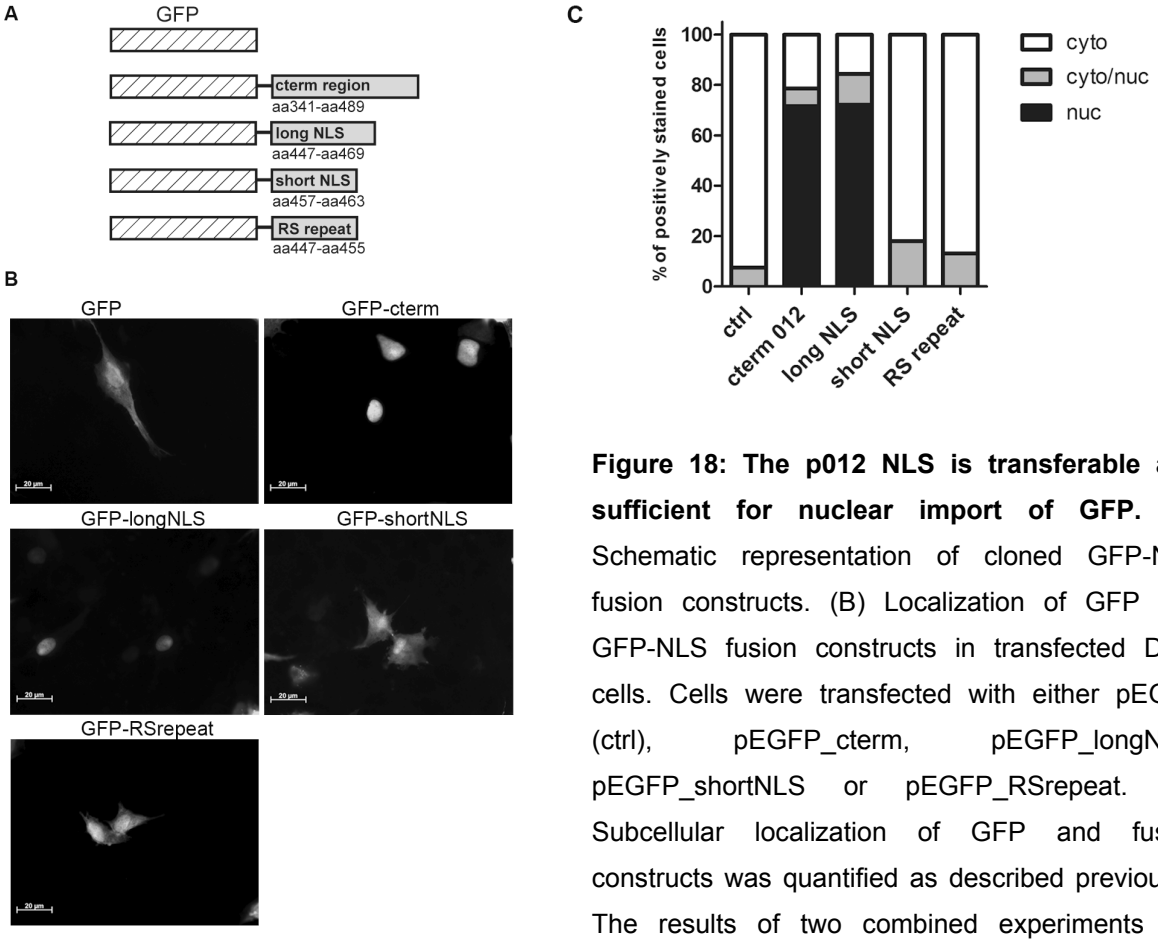

Figure 18: The p012 NLS is transferable and sufficient for nuclear import of GFP. (A) Schematic representation of cloned GFP-NLS fusion constructs. (B) Localization of GFP and GFP-NLS fusion constructs in transfected DF-1 cells. Cells were transfected with either pEGFP (ctrl), pEGFP_cterm, pEGFP_longNLS, pEGFP_shortNLS or pEGFP_RSrepeat. (C) Subcellular localization of GFP and fusion constructs was quantified as described previously. The results of two combined experiments are shown.

6.2.9 Nuclear export of p012 can be inhibited with LMB

As is evident from Fig. 16 and 17, p012 exhibited a clear nuclear localization in transfected, as well as infected chicken cells. When the distribution of the viral protein was quantified in transfected cells, about 70% of cells displayed an exclusively nuclear localization, whereas the remaining 30% of cells were categorized as “predominantly cytoplasmic”. This distribution raised the question of whether p012, apart from its NLS-driven nuclear import, could also be actively exported from the nucleus. This hypothesis was tested by quantifying

the subcellular distribution of p012 at different time points post transfection over a period of 48 h. Figure 19A shows the results of two combined experiments.

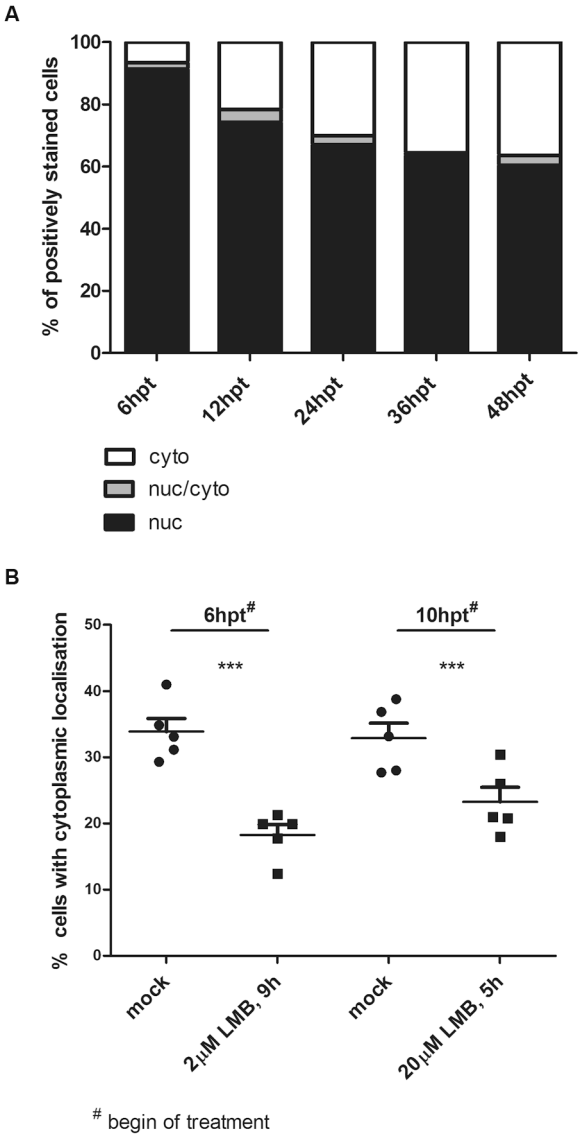

Figure 19: p012 is actively exported from the nucleus. (A) p012 leaves the nucleus over time. DF-1 cells were transfected with pc012Flag. At indicated time points, cells were fixed and stained. The results of two independent experiments are shown. (B) LMB inhibits nuclear export of p012. DF-1 cells were transfected with pc012Flag. At 6 h (or 10 h, respectively) after transfection, cells were incubated with 2 µM (or 20 µM, respectively) of LMB and treated for 9 h (or 5 h, respectively) before fixation and staining. The combined results of 5 independent experiments are shown as percentages of cells with predominant cytoplasmic localization. Note that the axis is scaled to 50%. Differences were tested for significance by χ^2 test (*** $p<0.01$).

Within the first 6 hpt, almost all transfected cells displayed nuclear localization of p012 (Fig. 19A, first bar). However, from this time point onwards, the protein was found to localize more to the cytoplasm reaching an equilibrium around 36 hpt with little change at later time points. These results suggested active export of p012 from the nucleus to the cytoplasm, at least in the context of transfected cells.

In a second experiment, LMB, a potent inhibitor of nuclear export, was applied to transfected cells. LMB acts by binding to the karyopherin export protein CRM-1 and prevents its interaction with proteins harboring leucine-rich nuclear export signals[133,134]. If p012 were actively exported from the nucleus by CRM-1, LMB treatment would lead to increased nuclear accumulation of the protein. Figure 19B shows the summarized results quantifying the cytoplasmic localization of p012 in three independent experiments under LMB treatment. In one experiment, cells were incubated at 6 hpt with 2 µM LMB for 9 h, an inhibitor concentration and time period that did not induce any visible cytotoxicity (data not shown). A mean reduction of cells with cytoplasmic localization of around 18% compared to mock treated cells was noticed (Fig. 19B). In a second experiment, 20 µM of LMB, the highest concentration recommended by the supplier, was used for a shorter period of time. Again, difference of about 10% was detected between treated and non-treated cells. The effect of LMB on cells appeared rather mild, but differences in combined absolute numbers of 5 independent experiments were highly significant as determined with a χ^2 test ($p<0.001$). This result indicates that p012 is indeed actively exported from the nucleus. Initial bioinformatic predictions yielded no clear candidates for a classical NES and the potential link between LMB treatment and potential export signals remains to be established. However, p012 contains 36 leucine residues, amounting to approximately 8% of its 489 total amino acids. Together with arginine, which is a major component of the NLS, leucine is among the most prevalent amino acids in the p012 sequence. Thus, there may potentially be an unknown NES within p012 that bioinformatic analysis cannot predict at this time.

6.2.10 Phosphorylation of p012

Closer examination of the C-terminal portion of p012 near the NLS revealed a number of serine and tyrosine residues. Both amino acids can serve as targets for phosphorylation. This is of particular interest since phosphorylation of amino acids proximal to an NLS can modulate its activity and influence subcellular protein localization[135]. When western blot analysis of transfected and infected cells was performed (compare Fig. 14), I noted that p012 migrated as multiple bands that often appeared as a smear, suggesting posttranslational modification of p012. In order to assess whether p012 is a potential target for phosphorylation, lysates of DF-1 cells transfected with pc012Flag were treated with lambda protein phosphatase (LPP) prior to western blotting. As shown in Fig. 20A, treatment with LPP clearly changed the migration properties of p012 compared to mock-treated lysates. In

particular, the observed band notably decreased in size, an observation that strongly suggests phosphorylation of multiple sites in p012.

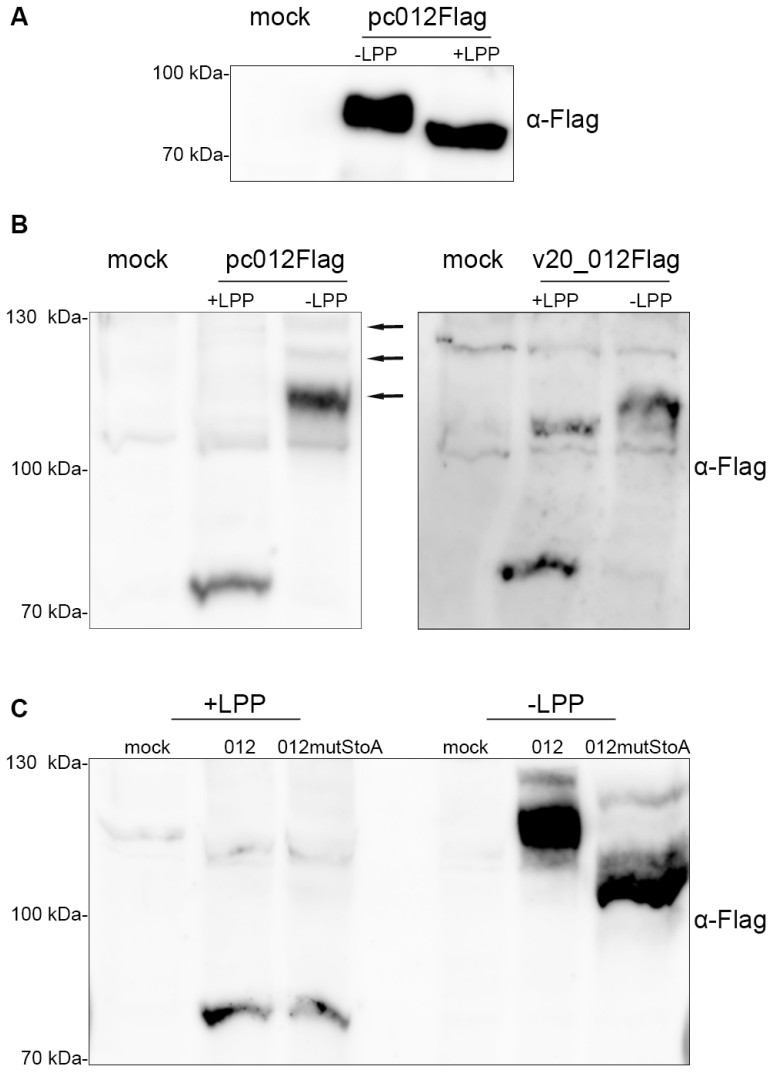

Figure 20: p012 is a phosphorylated protein. (A) Cells transfected with pc012Flag (or mock transfected) were lysed in Ripa buffer. Samples were subsequently treated LPP or mock treated for 30 min prior to SDS-Page and western blotting. Mock transfected cell lysates served as a control. (B) Lysates of transfected or infected cells, respectively, were treated as described in (A) and separated in SDS-Page containing 25 µM Phos-tag reagent and 1 mM $MnCl_2$. Note that Phos-tag decreases the mobility of phosphorylated proteins due to specific interaction (see Materials and Methods). Arrows indicate the position of differentially phosphorylated p012. (C) p012mutStoAFlag shows increased mobility compared to p012Flag in the presence of Phos-tag indicating decreased phosphorylation. Positions of weight marker bands are indicated on the left.

To further confirm the results, a phosphate-binding tag called Phos-tag™ was employed in combination with western blotting (see Materials and Methods). The reagent is capable of binding phosphorylated proteins in the presence of manganese ions thereby inducing slower migration in SDS-PAGE of phosphoproteins compared to their unaffected dephosphorylated counterparts[118,136]. However, it has to be noted that the addition of Phos-tag and $MnCl_2$ to acrylamide gels has bystander effects on migration of proteins within complex cellular lysates and effects like tailing or waving of bands have been described earlier[118]. As seen in Fig. 20B, a dramatic mobility shift of the phosphorylated form compared to LPP treated p012 was detected indicating phosphorylation at potentially multiple residues. In addition, several bands of phosphorylated p012 were identified (Fig. 20B, left panel, arrows), an effect that could reflect different phosphorylation states of the protein[136]. A comparable migration of p012 was detected in lysates of v20_012Flag infected CEC (Fig. 20B, right panel). As depicted in Fig. 12, p012 contains several potential targets for phosphorylation that were predicted with high probability. However, the phosphorylation of serines within the RS repeat described earlier is of particular interest since it could influence the function of the NLS and the protein, respectively[135]. Therefore an expression plasmid was generated in which the four serine residues of the RS repeat were substituted with alanines by site-directed mutagenesis (pc012mutStoA). When the migration of p012 to p012mutStoA was compared on Phos-tag western blots, a faster migration of the mutated form could indeed be detected (Fig. 20C). This result could point towards a less phosphorylated state of the modified protein due to the absence of four serine residues. When the localization of p012mutStoA was examined following transfection, a reduced number of cells with nuclear localization were noticed. However, the effect was less severe compared to 012mutRSrepeat (data not shown).

6.2.11 Transfection-based microarray analysis of DF-1 cells expressing MDV p012

Unfortunately, I was unable to propagate viral mutants to sufficient titers that would enable me to carry out high throughput experiments in an infection background. To shed some light on possible functions of p012, a preliminary transfection-based microarray experiment was performed in cooperation with Bertrand Pain, INSERM U846 Lyon, who carried out the actual analysis. Briefly, ORF012 (and ORF012Flag as a control, respectively) was cloned into the dual-expression vector pVitro2 containing GFP under one of two constitutive promotors. The construct was tested by transfection into DF-1 cells and subsequent immunofluorescence microscopy. Coexpression of GFP (green) as well as p012Flag (red) within the same cell could be verified (Fig. 21). In order to increase the amount of p012 positive cells prior to the microarray analysis, 1×10^6 GFP positive cells were sorted following transfection of pVitro-GFP-012 (or pVitro-GFP as a mock control). Total RNA was extracted and subsequently

used for a microarray analysis as described previously[120]. Table 5 shows a small selection of genes that were differently expressed in ORF012 positive cells compared to the control population. Most importantly, transcripts of interleukin 17B, a proinflammatory cytokine of the IL17 family[137,138] were downregulated in ORF012 transfected cells compared to the control (Log_2FC: -2,32). In addition, less transcripts that corresponded to an exocyst complex component could be detected in ORF012 expressing cells compared to the mock. The exocyst is a multiprotein complex that is involved in vesicle trafficking and exocytosis[139]. Furthermore, heat shock proteins were differently expressed (Table 5). However, the results only represent a first indication and have to be carefully analyzed since the quality of the RNA preparation and microarray experiment was suboptimal (Bertrand Pain, personal communication). Nevertheless, they give an interesting first insight into cellular functions potentially influenced by the protein.

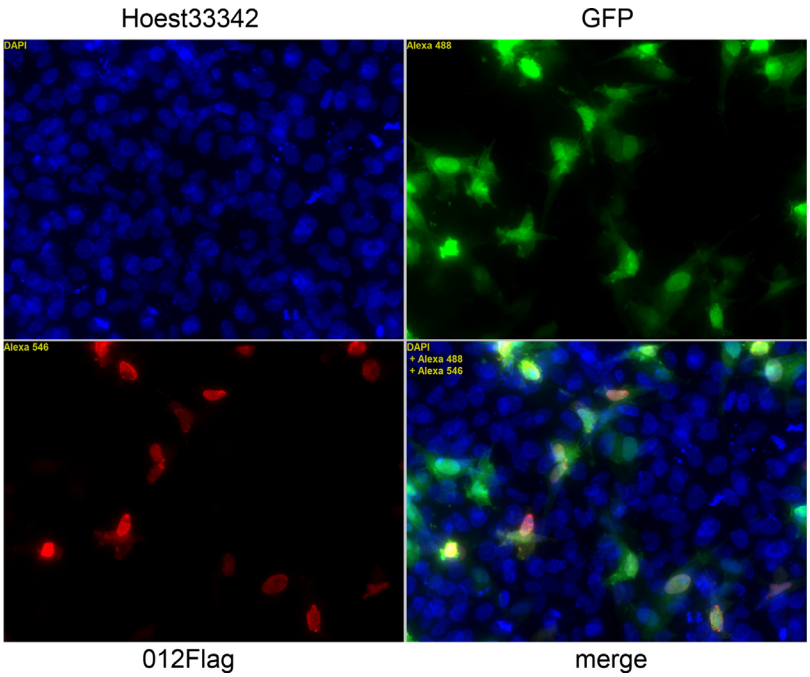

Figure 21: Evaluation of GFP-012 dual expression vectors for microarray analysis. DF-1 cells were transfected with pVITRO-GFP-012, which expresses GFP and MDV ORF012 under the control of two independent promotors. Coexpression of GFP (green) as well as p012Flag (red) within the same cell could be verified. 24 hpt cells were trypsinized, washed and GFP positive cells were cell-sorted using a BD FACSAria III cell sorter (kindly provided by the flow cytometry core facility of the MPI, Berlin). Sorted cells were pelleted and total RNA was extracted as described previously. The microarray experiment and its analysis (Table 5) were kindly performed by Dr. Bertrand Pain, INSERM Lyon.

Table 5. Differentially expressed genes in MDV ORF012 transfected DF-1 cells.

Name/Locus	Description	logFC	Avr.expr.	p values
HSP25	Heat shock protein 25	-5,117	12,494	0,0002
IL17B	interleukin 17B	-2,319	8,185	0,0002
HSPA2	heat shock 70kDa protein 2	-2,147	11,987	0,0060
LOC423478 (Sec6 family)	exocyst complex component 3-like, transcript variant X1	-2,310	9,401	0,0321
LOC423536 (KCNK4)	potassium channel subfamily K member 16 isoform X3 (predicted)	2,181	8,604	0,0444

Cutoff values of p ≤0.05 and a threshold of Log2 of the fold change (Log_2FC)>2 were used, Avr.expr.: average expression

6.2.12 Avian alphaherpesvirus proteins with similarity to MDV p012

As previously mentioned, genes that share similarity with ORF012 are encoded in different avian alphaherpesviruses including duck enteritis virus (DEV), HVT, GaHV-3, infectious laryngotracheitis virus (ILTV) as well as the recently sequenced falconid herpesvirus 1 (FaHV-1)[96]. Table 6 shows an identity percentage matrix based on protein sequence alignment. As expected, the p012 sequences of MDV and apathogenic GaHV-3 share the highest degree of similarity; however, both proteins deviate already by 50% in their composition. Given the fact that the sequence similarity of proteins of the two closely related viruses usually ranges from 50% to 80%[29], the value is on the lower end of the spectrum. Nevertheless, related proteins in other viruses deviate even more compared to MDV. ILTV UL0 and UL-1, which form a cluster due to a likely gene duplication event[140], showed the lowest overall identity to MDV p012. Table 7 summarizes mRNA splicing, occurrence of NLS sequences, as well as phosphorylation for the different candidate proteins, either based on experimental evidence or bioinformatic predictions. While all of the proteins share similar structural properties, functional relatedness remains to be established.

Table 6. Protein sequence identity matrix of proteins with similarity to MDV ORF012.

	% Identity to: [a]						
	HVT Lorf2	**GaHV-3 Lorf2**	**MDV ORF012**	**DEV Lorf3**	**FaHV Lorf3**	**ILTV UL0**	**ILTV UL-1**
HVT Lorf2	100	36	**41**	23	26	17	15
GaHV-3 Lorf2	36	100	**50**	26	27	17	16
MDV ORF012	41	50	**100**	28	26	17	16
DEV Lorf3	23	26	**28**	100	27	16	17
FaHV Lorf3	26	27	**26**	27	100	15	15
ILTV UL0	17	17	**17**	16	15	100	25
ILTV UL-1	15	16	**16**	17	15	25	100

[a] Percent identity based on amino acid alignment of candidate proteins using the Clustal Omega Server

Table 7. Properties of MDV p012 and similiar proteins.

Name	Splicing	NLS	Phosphorylation
MDV ORF012	experimental evidence	arginine-rich "highly basic" RS repeat	experimental evidence
GaHV3 Lorf2	predicted[R]	predicted "highly basic" RS repeat	predicted mainly serine
HVT Lorf2	predicted[R]	predicted arginine-rich RS repeat	predicted mainly serine
ILTV UL0	yes, experimental evidence[ref]	predicted arginine-rich	predicted mainly serine
ILTV UL-1	yes, experimental evidence[ref]	not predicted RS repeat	predicted mainly serine
FaHV Lorf3	predicted potential splice site upstream to gene[p.o]	predicted, "highly basic" arginine-rich	predicted mainly serine
DEV Lorf3	not predicted[p.o]	predicted arginine-rich	predicted mainly serine

R predicted according to RefSeq ref reference (149) p.o personal observation

7. Discussion

7.1 MDV pUL49.5 and its role in MHC class I downregulation

The original tenet that MDV could cause MHC class I downregulation was derived from the early observation that infection triggers the expansion of specific cytotoxic T cells; however, the CTL response appeared rather subdued compared to other infections[86]. Early on, this finding led to the hypothesis that MDV specifically modulates MHC class I on the surface of infected cells in order to evade destruction by the CTL response, an evasion mechanism that had already been established for other herpesviral species[83,87]. Nevertheless, the possibility to directly investigate the impact of immune evasion on tumorigenesis and disease progression in a natural virus-host model is what sets MDV apart from research on other herpesviruses[29].

First experimental evidence for MHC I immune evasion was obtained from studies in which infection of the chicken fibroblast cell line OU2 with MDV led to a pronounced downregulation of surface MHC class I molecules[87]. With these results at hand, the quest for the protein(s) responsible for this effect was on. Intriguingly, MDV lacks the usual suspects of immune evasion, the alphaherpesviral genes encoding the ICP47 and US6 proteins[98]. However, the MDV homologue of pUL49.5, which is a potent inhibitor of TAP in many varicelloviruses, has been a likely candidate[87].

A study by Tischer *et al.* claimed that MDV UL49.5 is essential for viral replication *in vitro*, a finding that appeared counter-intuitive given that the gene is dispensable in closely related viral species[88]. As mentioned earlier, the complete disruption of the small ORF by a selection marker could have interfered with unidentified regulatory elements (e.g. promoters, enhancers of other genes) within the gene. The development of seamless BAC mutagenesis techniques in which the marker cassette is removed from the final construct and integrity of the mutated region is largely restored, now allows the introduction of very small modifications that are sufficient to cause the desired gene knock-out while keeping the overall sequence changes and bystander effects low[111]. It was clearly demonstrated here that targeted disruption of the two potential start codons in MDV UL49.5 is sufficient to impede production of the protein (Fig. 7). Unexpectedly, the resulting virus was replication-competent. I therefore postulate that, in contrast to earlier findings, the UL49.5 gene and its product are dispensable for viral replication *in vitro*. The question as to whether the virus is viable during *in vivo* infections will have to be thoroughly investigated in the future.

A second study by Jarosinski *et al.* confirmed the possible involvement of pUL49.5 in MHC I downregulation by using *in vitro* infection as well as transient transfection assays[87]. In particular, a pU49.5 C-tail deletion mutant (v20_UL49.5ΔCt), which proved replication-

competent but less capable of MHC I modulation, indicated a central role for the cytoplasmic domain of the protein. This was in line with data published for BHV-1 in which the C-terminal domain of pUL49.5 is responsible for TAP degradation and thus MHC I modulation[82]. Surprisingly, when the novel UL49.5 knock-out virus was tested next to the published C-tail deletion mutant and the parental virus, no differences in surface MHC class I levels of infected CEC could be observed (Fig. 8). Unfortunately, I was not able to reproduce the original experiment with OU2 cells due to my inability to infect them despite multiple attempts. However, the data clearly show that UL49.5 is not responsible for MHC I downregulation in primary CEC. So far it is not clear if the contradictory results indicate a cell type dependency of pUL49.5's function that could be related to different MHC haplotypes. It is known that the TAP genes of chickens are at least as polymorphic as the MHC class I genes[141]. It is tempting to speculate that the dominant expression of certain alleles in any given cell line might influence pUL49.5's capability to bind to and interfere with individual TAPs but not others, thus explaining the contradictory results.

Given the apparent discrepancy, I set out to investigate whether pUL49.5 could modulate MHC I levels when produced from expression plasmids. Unfortunately, investigations of MDV pUL49.5's capacity to act on MHC I through TAP interference were obstructed by an obvious infection- and/or cell-dependent detectability of the protein in various assays (e.g., western blotting, immunofluorescence microscopy). Most importantly, the presence of pUL49.5 could not be detected following transfection of CEC with an expression plasmid (Fig. 6). Cellular degradation processes as a cause for posttranslational instability of pUL49.5 could virtually be excluded by inhibitor treatments (Fig. 9). In addition, the mutation of potential ubiquitination motifs and residues in the C-terminus could not increase protein levels in CEC. To exclude the possibility of transcript instability, pcUL49.5 was transfected into cell lines of different animal species. In all cases transcripts that derived from the expression plasmid were detectable by RT-PCR (Fig. 10). In contrast, only the chicken DF-1 cell line allowed stable detection of the protein on western blots (Fig. 10). This finding is very intriguing since the DF-1 cell line is derived from spontaneously immortalized chicken embryonic cells and thus should not differ extensively from primary CEC. Accordingly, there is currently no explanation why DF-1 support the production or detection of pUL49.5. Taken together I postulate a context-dependent expression (or detectability) of the protein that could be directly influenced by the presence or absence of interaction partners of viral or cellular origin. This option was explored by co-expressing pUL49.5's postulated interaction partner, gM, in CEC. In preliminary experiments, co-expression did not increase detectability (data not shown). Even more confusing, the protein was clearly detectable following cell-free *in vitro* transcription/translation reactions (Fig. 10). Finally, the addition of a C-terminal epitope tag seemed to stabilize pUL49.5 in the context of transfection. The mechanism behind

stabilization caused by addition of an artificial sequence remains elusive but could be induced by conformational changes.

Whether the observations regarding pUL49.5's stability result from epitope-masking by potential interaction partners remains an open question. In theory such interactions should be resolved by the reducing conditions during western blotting. However, if bound to a very large protein, UL49.5 could potentially end up in a heat-induced protein aggregate, which is difficult to separate by SDS-PAGE. However, neither the elimination of the heat denaturing step nor blotting of the stacking gel allowed detection of the protein in CEC (data not shown). It is not easy to integrate all of the obtained results into a model that delivers a satisfactory explanation for the detection issues. The fact that the target protein could always be identified in infected but not transiently transfected CEC could point towards a viral stabilization factor. However, the most likely candidate, gM, can apparently be excluded from these deliberations. The *in vitro* translation allowed detection of pUL49.5 when produced outside of a cellular context. This seems to be in direct contrast with the "viral interaction partner hypothesis" unless one would postulate a factor of cellular origin destabilizing the protein only in the absence of a second viral factor. In this scenario, the viral factor would shield UL49.5 from interaction with the destabilizing or epitope-masking cellular factor. Following my varying results with 4 transiently transfected cell lines, this cellular factor should be differently expressed (or maybe absent), thus explaining why pUL49.5 is detectable in the DF-1 cell line but not others. However, pinpointing such factors would demand comparative high-throughput methods such as proteomics, which were beyond the scope of this dissertation. In addition, fusion with an epitope tag was sufficient to stabilize pUL49.5. The possibility exists that tags induce structural modifications in pUL49.5 that subsequently might hamper the interaction with the postulated destabilizing factor thereby restoring detectability. Despite the fact that this model integrates all findings, it is still highly speculative at the moment and has to be verified in the future.

Nevertheless, a stably expressed Flag-tagged pUL49.5 construct led to a very mild downregulation of MHC class I surface levels in preliminary flow cytometry-based analysis of transfected DF-1 cells (Fig. 11). It has to be noted that the differences towards the negative control were not or only at the edge of significance in most of the experiments performed. Earlier studies demonstrated that transfection of UL49.5 into RP9 (a chicken B cell line) cells led to a more significant downregulation of MHC class I[87]. Again, haplotype differences as well as differences in the experimental setup could account for my divergent results. Interestingly, Verweij *et al.* were not able to reproduce MHC class I downregulation by MDV pUL49.5 in transfected chicken hepatoma cells (LMH) and a human melanoma cell line[84]. Taken together, the involvement of MDV pUL49.5 in MHC class I modulation is quite unlikely.

Accordingly, no significant differences in TAP expression levels could be observed in transfected or infected cells, making degradation-mediated TAP interference by pUL49.5 doubtful (Fig. 11). In theory, mechanism other than degradation, for example blockade of peptide transport, could be responsible for the inhibition of TAP, however those could not be tested due to time constraints. Therefore, future investigations should focus on TAP peptide transport assays as well as co-immunoprecipitation studies to identify potential interaction partners of pUL49.5.

In summary, three independent questions prevail. Firstly, is MHC class I evasion mediated by pUL49.5? Contrary to earlier publications, I found that MDV pUL49.5 is not essential for viral replication *in vitro* and does not contribute to MHC class I downregulation during infection of CEC *in vitro*. Detectability issues of the target protein raised many complicated and as yet unanswered questions. In general, *in vitro* studies offer the advantage of feasibility and simplicity. Yet, when such studies are concerned with immunoregulatory proteins, they always have to be interpreted with caution since a) the used cells are not necessarily a good model for the actual target cell *in vivo* and b) the modes of action (e.g., tropism and timing) might be influenced severely by the complexity of the immune system, which naturally is absent *in vitro*. A step closer towards a better *in vitro* model of MDV infection and at the same time another blow to the immunmodulation hypothesis, were results obtained by Prof. Bernd Kaspers, LMU München. His group first managed to infect isolated chicken B and T cells, the main targets of natural MDV infection, *in vitro*. Surprisingly, they were not able to demonstrate MHC class I downregulation in either of the two cell types (personal communication).

This notion leads to a somewhat provocative second question: Does MHC class I downregulation through MDV really happens *in vivo*? As intriguing this question might be, it is hard to study and therefore not many studies have addressed it. When Gimeno *et al.* infected chickens with MDV strains of different virulence, only a very virulent plus (vv+) strain caused MHC downregulation in the brain of infected animals as demonstrated by immunohistochemistry[142]. In addition, the authors stated that many different cell types lacked MHC class I on their surface but the minority of those cells was actually infected by the virus. In other words, infected and MHC class I-negative cells were not matched to each other making the involvement of intracellulary expressed immune evasins at least disputable.

A possible key experiment to determine *in vivo* immunmodulation would be the use of direct assays performed with cell populations isolated *ex vivo*. Infected animals would then serve as the source of MDV positive cells like macrophages, B and T cells, and epithelial cells of the skin or feather follicle at later time points during infection. What makes such studies rather challenging is the low numbers of infected cells at any given time during infection. Flow cytometry based studies are conceivable but would have to be carried out with copious

amounts of input material possibly obtained from many pooled individuals in order to reach statistically relevant cell numbers.

The third question deals with the impact of MHC class I downregulation on disease progression and tumorigenesis. The already described study by Jarosinski *et al.* made use of a replication competent UL49.5 C-tail deletion mutant to test *in vivo* effects in infected chickens[87]. Only in one out of three performed experiments could a statistically significant difference in disease incidence be observed between wildtype and mutant virus-infected animals. In addition, only mild effects could be observed in the MDV-resistant chicken line $B^{21}B^{21}$ but not in highly susceptible chickens of the $B^{19}B^{19}$ haplotype. It is not clear if the remaining N-terminal and transmembrane domains of pUL49.5 could have influenced the outcome of the experiments. This is important since both domains could play a role in MDV pUL49.5's function (see Fig. 5). Another interesting study regarding the impact of UL49.5 homologues on disease progression was published by Wei *et al.*[143]. The authors introduced modifications into the BHV-1 pUL49.5 that rendered the protein non-functional in terms of MHC I modulation. Upon infection of calves with the mutant virus, the authors could indeed show a more rapid induction of T cell responses which kicked in about a week earlier than those for wildtype infected animals. More importantly, calves of both groups showed comparable symptoms and clinical signs of disease indicating that the mutant virus retained significant pathogenicity[144].

A more general concept that might arise from those studies is that the deletion of immune evasins will not lead to a hypervirulent virus *per se*. Similarly, the presence of immune modulating proteins does not render the immune system incapable of responding to infection. It seems that immune evasins buy the virus time to replicate and spread before the immune response finally gets a hold on the intruder. This underlines the fine balance of pathogen-host interplay which possibly is a product of extensive co-evolution.

7.2 MDV p012 – a novel nuclear phosphoprotein and potential immune evasin

As the majority of MDV genes shares homology to their HSV or VZV counterparts, a number of MDV gene products have already been functionally analyzed in detail. However, unique and potentially unidentified genes exist in MDV, which could exert important functions in its complex replication cycle. In this work, I identified a novel MDV nuclear phosphoprotein which was translated from a spliced mRNA encoded by the ORF012 gene. The annotation of this region in MDV has been ambiguous with different names given to genes and ORFs, including ORF012. The majority of MDV genomes deposited in GenBank still define ORF011* and ORF012* as independent hypothetical genes. In contrast, other annotations omit ORF011* completely, placing just ORF012* in the region downstream of ORF010 (viral lipase, Lorf2) and upstream of ORF013 (glycoprotein L, UL1) and refer to it as Lorf3. Some of the newer annotations appreciate predicted splicing, but retain the gene 012 nomenclature. To add even more confusion, the 'Lorf terminology', starting with the first ORF that has its promoter in the UL region, is handled incoherently for different MDV strains. In particular, the inclusion or omission of Lorf1, a potential gene of unknown function, has led to different designations of all following genes in the U_L region. Therefore, depending on the MDV sequence under scrutiny, Lorf2 either stands for viral lipase[97] or the spliced gene that I describe here (GenBank NC_002229). Therefore, here I propose the term MDV ORF012 when referring to the gene identified in this report and hereafter. In general, the work underlines that bioinformatic predictions, in particular those used for genome-wide annotations, are an excellent tool for the determination of potential ORFs; however, they cannot replace experimental evidence to prove or refute their implications.

Splicing of messenger RNAs is a common principle of eukaryotic transcription. Despite its prevalence in eukaryotic cells, the mechanism was first identified in adenoviruses[145,146]. Apart from adenoviruses, splicing has also been found in herpesviruses and MDV is known to make extensive use of alternative splicing to generate diverse sets of transcripts from single genes, particularly in the repeat-long regions[147]. This mechanism serves to maximize the coding capacity of compact viral genomes with usually strict size limitations. Here, it was proven that MDV ORF012 is produced through mRNA splicing and this splicing occurs independent of other viral factors since the spliced transcript was also detected in cells transfected with an expression plasmid harbouring the target gene. The resulting splice product removed a small 82 bp intron within the 5' region of the immature message (Fig. 12). In order to ensure that ORF012 did not simply represent an alternative splice variant of an individually expressed ORF012*, epitope-tagging of (putative) viral proteins was employed to analyze the coding capacity of the entire region spanning MDV ORF011* to 012*. It was

clearly shown that the hypothetical p012* was not produced during infection. Regarding the expression of p012, the existence of a single band was confirmed in virus-infected cells that corresponded in size to the control protein expressed in DF-1 cells. Therefore, I concluded that only p012 is produced during viral infection.

One of the first questions that arise with newly identified gene products of viruses is whether the protein is dispensable for viral replication. Using an MDV ORF012- null mutant based on the vv strain RB-1B, it was evident that p012 is important for viral growth *in vitro* (Fig. 14). Although small plaques were produced upon reconstitution of infectious DNA in CEC, I was unable to expand the virus by passaging in multiple trials. A recent study published by Hildebrandt *et. al.* identified *de novo* mutations following extensive passaging of the Md5 strain *in vitro*. Among these mutations, two independent single nucleotide polymorphisms (SNPs) associated with ORF012, one in the putative promoter region and one within the 82 bp intron, led to reduced virulence in chickens[148]. However, in this report, the authors did not investigate whether and to what extent, either of the single point mutations may have affected p012 expression or function.

In order to approximate the role of p012 in MDV replication, epitope-tagged expression constructs, as well as expression of tagged protein versions from recombinant viruses were used to analyze the subcellular localization of p012. Interestingly, p012 showed predominant nuclear distribution in transfected cells and an even stronger nuclear accumulation in virus-infected cells (Fig. 16 & 17). The localization was reminiscent of the products of the duplicated U_L0 and U_L-1 genes of the distantly related ILTV, both of which were shown to be spliced. The U_L0 and U_L-1 proteins also accumulated in the nucleus of infected cells, but to date, no specific function or NLS has been assigned to the gene products[149]. In line with my results, it has also been reported that both proteins showed considerably higher molecular weights on western blots compared to calculated values deduced from their primary sequence. The actual size deviation of p012 from its calculated value on western blots, however, can only be partially explained by phosphorylation since LPP-treated p012 still migrated higher than expected. Other posttranslational modifications might therefore be responsible for this effect. This, however, will certainly warrant more extensive investigation in the future.

With the help of bioinformatic prediction tools, I was able to identify a NLS that mapped to a 23 amino acid stretch in the C-terminal region of p012. The first experimental evidence that the sequence can indeed control nuclear import was provided by infection experiments using a mutant virus carrying a deletion or substitution of the p012 C-terminal domain encompassing the NLS. Compared to parental virus, nuclear localization was completely abrogated in cells infected with the viral mutants (Fig. 17). In order to map the exact position of the NLS I utilized expression assays and quantified the effects of targeted alanine

substitutions within predicted NLS sequences. In accordance with the infection experiments, deletion of either the basic arginine core or the preceding serine-arginine rich repeat motif abolished nuclear import (Fig. 17). Furthermore, synthetic NLS-GFP fusion constructs were employed to directly test different portions of the NLS that were required for nuclear import. Only constructs encompassing the rather long sequence stretch ^{447}RSRSRSRSRERRRRRPRVRPGRR^{469} accumulated in the nucleus indicating that this motif can act as a transferable bona fide NLS (Fig. 18). However, fine mapping approaches like alanine scanning or single amino acid deletions will be necessary to identify the minimal core sequence in future experiments. Whereas consensus sequences for classical NLS motifs, either mono- or bipartite, are well established[100–102], it has become clear in recent years that many nuclear proteins contain non-classical signals that differ considerably in sequence[105,106]. Concerning the primary sequence of the p012 NLS, its categorization is not entirely obvious. The signal does not match the structure of a classical bipartite NLS[104] but rather presents a stretch of basic arginines being reminiscent of a monopartite SV40-type NLS[103]. Boulikas further subdivided classical monopartite NLS depending on their composition. In this regard, the core sequence would represent a 'highly basic NLS' which usually contains 5 or 6 (K/R) residues[150,151]. Nevertheless, I was able to verify that the basic motif (called short NLS here) is not sufficient for nuclear translocation. Only in combination with the preceding RS repeat cells with a clear nuclear accumulation of GFP could be detected. This demonstrates that the p012 NLS constitutes a rather large peptide.

A question that still remains open is whether the entire NLS of p012 represents a docking site for nuclear importins or whether both motifs fulfil different but complementary functions. In this regard, the phosphorylation state of p012 could play an important role in nuclear transport. It is known that phosphorylation of residues within or near the NLS can up- or down-regulate activity[135]. The mechanisms behind the modulations can be of varying nature, but are often related to increased (or decreased) affinity to the import factor. The classical SV40 NLS itself is embedded in a sequence of residues that can be phosphorylated by protein kinase CK2, a modification which massively enhances nuclear import[152]. The fact that substitution of the phosphorylation-accessible serines within the RS repeat of p012 decreased its phosphorylation state (Fig. 20) and partially inhibited nuclear import could point towards a functional involvement of phosphorylation. However, it is also conceivable that predominant localization to either the nucleus or the cytoplasm, respectively, influences the phosphorylation state of the protein. I will investigate a potential link between localization, NLS and phosphorylation state of p012 in future experiments.

Interestingly, despite the presence of a NLS, the distribution of p012 was not entirely nuclear. A rather constant percentage of cells displayed a predominantly cytoplasmic or mixed distribution in transfected or infected cells. This fraction could be increased significantly by

treatment with LMB, which inhibits leucine-rich export signals (Fig. 19). Although analysis of the protein sequence did not yield clear candidates for a NES, the high prevalence of leucine residues in p012, in addition to increased nuclear localization during LMB treatment, suggests these sequences may play a part in nuclear export. While in-depth functional characterization has not been performed yet, it is tempting to speculate about potential actions of p012. Several scenarios are conceivable.

Firstly, given the rapid accumulation inside the nucleus, p012 could represent a transcriptional activator or regulator of viral or cellular gene expression during infection. Several MDV proteins are known to fulfil similar functions. Among the most prominent examples range the homologue of HSV-1 ICP4[6], which regulates viral gene expression as well as the multifunctional transcriptional regulator Meq[93]. Unfortunately, I was unable to propagate viral mutants to sufficient titers that would enable me to perform high throughput experiments in an infection background. However, we were able to perform a preliminary transfection based microarray experiment in cooperation with Dr. Bertrand Pain, INSERM U846 Lyon, France. Interestingly, the results indicated the specific downregulation of chicken IL17B transcripts in DF-1 cells in the presence of ectopically expressed ORF012. The cytokine IL17B belongs to the recently described IL17 family[138]. The family contains six members (A to F) most of which are produced by activated T cells[137]. IL17 itself is a potent activator of cytokine production which attracts monocyte and neutrophils and in this regard it has proinflammatory function. Interestingly, IL17B is not only produced by T cells but rather by various tissues within the human body[137,138]. Despite the fact that our results still await confirmation by quantitative real-time PCR, the specific modulation of a proinflammatory cytokine by means of transcriptional repression would present an attractive viral strategy to escape immunosurveillance. The fact that IL17B might also be present in many tissues of the chicken, could pave the way for efficient systemic spread of the virus following its downregulation. It has to be noted that such a function would not necessarily explain the *in vitro* growth defects of vRb_012ΔMet. Future studies should also focus on whether DF-1 cells are capable of IL17B production and if the corresponding IL17B receptor is expressed on their surface. Alternatively, p012 could interfere with cellular signaling pathways which activate the transcription of cytokine genes thereby influencing the expression of IL17B by indirect means. Interestingly, it was shown that the ORF13 of herpesvirus samiri, a γ-herpesvirus that infects squirrel monkeys, shares 56% sequence identity with the IL17 cytokine of its host, making the protein a virokine that could modulate the IL17 cytokine network[153]. The fact that at least one other herpesvirus specifically tackles members of the IL17 family could make a similar role for p012 more likely.

Secondly, when I investigated replication of the ORF012 knock-out virus, only small plaques could be recovered following transfection. The inability to expand the virus upon passaging

may indicate a defect in virion formation. Virus particles might be produced early during the reconstitution in CEC but subsequently would be unable to spread efficiently to neighboring cells, thereby explaining the absence of cytopathic effects. Interestingly, Hildebrandt et al. showed that a mutation within the intron of ORF012 not only attenuated the virus *in vivo* but also caused the complete inability for horizontal spread[148]. Nevertheless, a link between the particular plaque phenotype *in vitro*, potentially incomplete maturation of virions and inability of horizontal spread from animal to animal is very speculative at the moment.

A third hypothesis focuses on the characteristic amino acid sequence of p012 and its potential role as a nuclear/cytoplasmic shuttling protein. In support of this; eukaryotic cells contain a class of proteins that have a characteristic arginine-serine rich motif in their C-terminus. These so-called 'SR proteins' are capable of nucleocytoplasmic shuttling, can be heavily phosphorylated, and fulfil various functions ranging from RNA transport to control of mRNA splicing[154]. Only recently, however, strict refinements of the properties defining a SR protein have been made[155]. The protein must contain one or two N-terminally located RNA binding domains (called RRM boxes) followed by an RS domain, which should contain at least 50 amino acids with an arginine-serine content of more than 40%. Only 12 proteins in the human genome actually match these requirements[155]. Given the lack of an obvious RNA binding domain as well as its short RS domain, p012 does not qualify as a SR protein *per se*. However, reports show that SR-like proteins that do not fully match all requirements exist and still carry out functions involving RNA. Herpesviruses encode proteins that are known to interact with cellular SR proteins[156]. Amongst the most intensively studied viral factors is the ICP27 of HSV-1. ICP27 is a multifunctional regulatory protein that mediates the export of viral RNAs and is capable of inhibiting splicing of viral as well as cellular mRNAs. In this regard the protein fulfils the function of a host shutoff protein[157]. Interestingly, ICP27 is able to interact with cellular SR proteins, modulating their distribution inside the nucleus as well as their phosphorylation. MDV also contains a homologue of ICP27 and the protein was shown to interact with SR proteins and inhibits splicing[158,159]. Therefore, the hypothetical role of p012 in splicing and/or mRNA export as well as interaction with ICP27 remains to be addressed.

8. Outlook

Immunomodulation and evasion in particular are very interesting fields of herpesvirus research. The immune system is instrumental in protecting the body from viral infections. Given its central role in host defense, it seems very intuitive that herpesviruses boast an impressive number of modulating proteins. Many viruses cause acute infections and follow a "hit and run" strategy[22]. They enter the host, replicate fast and leave the body in a matter of hours or few days, a time window that might be too short to launch effective counter measures of the adaptive immune response. Hence, evasins of the adaptive system might be less important in this context. In contrast, herpesviruses stay forever. Whereas latency itself represents a default way of evading immunosurveillance, the virus has to leave the host at one point and find new victims. It might be at this stage, the short moments of reactivation to lytic replication, in which immunomodulation is instrumental. Hence, there is no question that modulation of the immune system occurs during herpesvirus infection but the timing and location of this event is often vague. The matter here, at least partly, seems to be the quality of our *in vitro* models for many infections. *In vivo* models will always yield more relevant results, however, those models might simply not exist for many herpesviruses or not allow the necessary experimental investigations.

Regarding the potential MHC class I downregulation of MDV, future studies will benefit from a MDV UL49.5 knock-out virus generated here. Given the small effects of pUL49.5 in terms of MHC I downregulation, I concluded that cell type dependency of its expression and function, will be a major issue in future UL49.5 research. The theory that the target protein is also dependent on interaction partners to perform its putative role awaits confirmation. It has to be noted that I reassessed some of the earlier results in slightly different experimental setups and where not able to reproduce most of the described effects in my investigations. This might be a simple proof that MHC class I modulation in MDV infection is more complex than the current state of literature suggests. In summary, the proteins responsible for MHC class I downregulation in MDV infection remain to be identified.

The fact that p012 could be a novel modulator of a proinflammatory cytokine is very intriguing and illustrates that herpesviruses do not rely on a single strategy of immune evasion. It is conceivable that MDV uses fine-tuned expression of different proteins to modulate different immune responses during every step of its infectious cycle *in vivo*. Nevertheless, p012's structural resemblance with SR like proteins could also point towards other functions, potentially as an effector of RNA metabolism. In summary, I have identified a novel nuclear phosphoprotein in MDV that is important for replication and actively shuttles between the

nucleus and the cytoplasm. Further studies should be directed at addressing its role in shuttling and potential targets for its role in MDV replication.

9. Summary

In the process of co-evolution with their hosts, herpesviruses have developed advanced mechanisms to counteract and evade the innate and adaptive responses of their hosts. Herpesviruses boast an impressive number of immunomodulatory proteins, commonly referred to as immune evasins, and their functions range from decoy receptors and virokines to modulators of the cytotoxic T cell response.

Marek's disease virus (MDV), an alphaherpesvirus, is the causative agent of a lethal disease in chickens characterized by generalized nerve inflammation and rapid lymphoma development. During lytic replication, MDV induces a drastic reduction of major histocompatibility complex (MHC) class I expression on the surface of infected cells, which allows the virus to shield itself from destruction by the cytotoxic T cell response. Currently, it remains unclear a) which proteins are responsible for MDV MHC class I downregulation and b) to what extent this and other immune evasion strategies influence the severity of disease, in particular tumorigenesis.

The MDV homologue of the conserved herpesviral UL49.5 gene encodes a small endoplasmic reticulum (ER) transmembrane protein which has been postulated as a likely MHC class I modulator due to its supposed interference with the transporter associated with antigen processing (TAP), a function which has been demonstrated for members of the genus *Varicellovirus*. Through the generation of a mouse anti-UL49.5 antibody as well as a replication-competent UL49.5 knock-out virus in the course of my thesis project, novel tools for investigation of the pUL49.5 function are now available. However, the presented results within this thesis indicate that MDV pUL49.5 is not responsible for downregulation of MHC class I molecules on the surface of infected primary chicken embryo cells. Investigations with ectopically expressed UL49.5 confirmed those findings and additionally indicated that pUL49.5 does not lead to proteasome-mediated TAP degradation, a function which has been proposed in the past as its likely mode of action. Further investigations of pUL49.5 were obstructed by severe protein stability issues of unknown origin, which could not be solved by inhibiting cellular pathways of protein degradation. These enigmatic observations together with an obvious context- dependence of the protein's expression (e.g., cell type), make some of my results, as well as previous studies, regarding the function of MDV pUL49.5 difficult to interpret.

In a second part of my project, the previously unidentified MDV ORF012 gene was characterized in detail and first evidence for its involvement in immune evasion was obtained. The extensive colinearity of the MDV genome with related herpesviruses has

eased functional characterization of many MDV genes. However, MDV contains a number of unique open reading frames (ORFs) that have not yet been characterized regarding their full coding potential and the functions of their products. Among these unique ORFs are two putative ORFs, ORF011* and ORF012*, which are found at the extreme left end of the MDV unique-long region. Using reverse transcription PCR I showed that ORF011* and ORF012* are not individual genes, but encode a single gene through mRNA splicing of a small intron, giving rise to what I dubbed ORF012. An ORF012-null virus was generated using an infectious clone of MDV strain RB-1B. The deletion virus had a marked growth defect *in vitro* and could not be passaged in cultured cells suggesting an essential role for the gene product during virus replication. Further studies revealed that protein (p)012 localized to the nucleus in transfected and infected cells and I identified by site-directed mutagenesis and GFP reporter fusion assays a nuclear localization signal (NLS) that was mapped to a 23 amino acid sequence at the protein's C-terminus. Nuclear export was blocked using leptomycin B suggesting a potential role for p012 as a nuclear/cytoplasmic shuttling protein. Furthermore, p012 is phosphorylated at multiple residues, a modification that could possibly regulate the subcellular distribution of the protein. A preliminary microarray experiment also indicated that p012 decreases transcripts of chicken interleukin 17B, a proinflammatory cytokine, suggesting that the protein could be potential modulator of the host immune system.

10. Zusammenfassung

Im Zuge der Koevolution mit ihrem Wirt haben sich bei Herpesviren elegante Strategien zur Umgehung des angeborenen und des adaptiven Immunsystems entwickelt. Sie besitzen eine beeindruckende Anzahl von immunmodulatorischen Proteinen, sogenannten Immunevasine, die von viruskodierten Rezeptoren über virale Chemokine (Virokine) bis hin zu Modulatoren der zytotoxischen T-Zellantwort reichen.

Das Virus der Marekschen Krankheit (MDV) gehört zur Subfamilie der Alphaherpesviren und löst in Hühnern eine tödliche Erkrankung, die durch eine generalisierte Nervenentzündung und der Entstehung von Lymphomen geprägt ist, aus. Während der lytischen Infektion von Hühnerzellen mit dem MDV, kommt es zur einer drastischen Reduktion der Expression des sogenannten Haupthistokompatibilitätskomplexes der Klasse I (MHC-I) auf der Zelloberfläche. Dadurch kann das MDV der Zerstörung durch die zytotoxische T-Zellantwort des adaptiven Immunsystems entgehen. Momentan ist allerdings unklar, welche Proteine des MDV hierfür verantwortlich sind und in welchem Ausmaß diese und andere Immunevasionsstrategien die Schwere der Erkrankung, im Speziellen die Tumorentstehung, beeinflussen.

Das dem Herpes simplex virus UL49.5 homologe Gen in MDV, welches auch in anderen Herpesviren konserviert ist, kodiert für ein kleines Typ 1-Membranprotein mit Lokalisation im endoplasmatischen Retikulum (ER). Basierend auf früheren Studien mit Viren aus dem Genus *Varicellovirus* wurde postuliert, dass auch das MDV UL49.5-Protein (pUL49.5) die Reduktion von MHC Klasse I-Molekülen über die Blockade des Antigenpeptid-Transporters (TAP) steuern könnte. Diese Hypothese wurde in der vorliegenden Arbeit getestet.

Mit der Herstellung eines spezifischen pUL49.5-Antiserums in Mäusen sowie eines replikationsfähigen UL49.5-Deletionsviruses stehen nun zwei neue Werkzeuge zur Untersuchung des Proteins zur Verfügung. Die hier beschriebenen Ergebnisse implizieren, dass pUL49.5 nicht für die Reduktion von MHC Klasse I-Molekülen auf der Oberfläche von infizierten Hühnerembryozellen verantwortlich ist. Weitere Untersuchungen mit pUL49.5, welches nach Transfektion von entsprechenden Expressionsplasmiden gebildet wurde, bestätigten diese Ergebnisse und zeigten des Weiteren, dass pUL49.5 nicht zum Abbau von TAP durch das Proteasom führt. Dieser Abbau von TAP wurde bis dato als mögliche Funktionsweise des Proteins vorgeschlagen. Weitere Untersuchungen zum pUL49.5 wurden leider durch ungeklärte Probleme mit der Stabilität des Proteins, welche nicht durch die Inhibition von zellulären Abbaumechanismen gelöst werden konnten, gehemmt. Die Expression des Proteins schien durch weitere Faktoren, zum Beispiel den verwendeten

Zelltypen, beeinflusst zu sein. Zusammenfassend erschweren die aufgeführten Beobachtungen die Interpretation einiger der hier dargestellten Ergebnisse sowie derer früherer Veröffentlichungen deutlich.

In einem zweiten Projekt der Promotionsarbeit wurde das bislang unbekannte MDV-Gen ORF012 im Detail charakterisiert und erste Hinweise auf eine mögliche Funktion als immunmodulatorisches Gen erhalten. Die Koliniarität des MDV- Genoms mit dem verwandter Herpesviren hat in der Vergangenheit die Charakterisierung vieler MDV Gene vereinfacht. Dennoch enthält das MDV einige einzigartige Gene, die bisher noch nicht bezüglich ihrer Funktion untersucht worden. Unter diesen unbekannten offenen Leserastern (ORFs) befinden sich zwei vorhergesagte ORFs, die als ORF011* und ORF012* bezeichnet werden und sich am äußersten linken Ende der Unique-Long-Region des MDV-Genoms befinden. Im Zuge dieses Projektes wurde mit Hilfe von reverser Transkriptions-PCR gezeigt, dass es sich bei den Genen ORF011* und ORF012* eigentlich um ein einzelnes Gen (nun als ORF012 bezeichnet) handelt, welches durch das Spleißen eines kleinen Introns zur Herstellung einer einzelnen Boten-RNA (mRNA) führt. Basierend auf dem MDV-Stamm RB-1B wurde eine ORF012 Deletionsmutante hergestellt. Diese Virusmutante zeigte schwere Replikationsdefekte *in vitro* und die Infektion konnte nicht durch Passagierung infizierter Zellen ausgeweitet werden. Eine entscheidende Rolle des Proteins im Replikationszyklus des Virus ist daher wahrscheinlich. In weiteren Studien konnte die Lokalisierung des Proteins 012 (p012) im Zellkern von infizierten und transfizierten Zellen nachgewiesen werden. Mit Hilfe von spezifischer Mutagenese und GFP-basierten Reporterkonstrukten konnte im C-terminalen Ende des Proteins ein nukleäres Lokalisierungssignal identifiziert werden. Auch konnte der nukleäre Export des p012 durch den Inhibitor Leptomycin B unterbunden werden. Hieraus läßt sich schließen, dass es sich um ein, zwischen dem Zellkern und dem Zytoplasma pendelndes, Protein handeln könnte. Die starke Phosphorylierung von p012, welche die Verteilung des Proteins innerhalb der Zelle regulieren könnte, wurde ebenso nachgewiesen. Zum vorläufigen Abschluss des Projektes wurde ein Microarray-Experiment durchgeführt. Hierbei ergaben sich erste Hinweise, dass das Protein 012 die Menge der spezifischen mRNA des entzündungsfördernden Zytokins Interleukin 17B reduzierte. Dieses Ergebnis spricht für die Möglichkeit, dass es sich bei p012 um ein immunomodulatorisches Protein handelt.

11. References

1. Claverie, J.-M. & Ogata, H. Ten good reasons not to exclude giruses from the evolutionary picture. *Nat. Rev. Microbiol.* **7,** 615; author reply 615 (2009).

2. Moreira, D. & López-García, P. Ten reasons to exclude viruses from the tree of life. *Nat. Rev. Microbiol.* **7,** 306–11 (2009).

3. Sears, C. L. A dynamic partnership: celebrating our gut flora. *Anaerobe* **11,** 247–51 (2005).

4. Comeau, A. M. *et al.* Exploring the prokaryotic virosphere. *Res. Microbiol.* **159,** 306–13 (2008).

5. Davison, A. J. *et al.* The order Herpesvirales. *Arch. Virol.* **154,** 171–7 (2009).

6. Lamb, R., Krug, R. & Knipe, D. Fields virology. *Fields Virol.* **1445,** 1996 (2001).

7. Brown, J. C. & Newcomb, W. W. Herpesvirus capsid assembly: insights from structural analysis. *Curr. Opin. Virol.* **1,** 142–9 (2011).

8. Roizman, B. & Furlong, D. The Replication of Herpesviruses. 229–403 (1974). doi:10.1007/978-1-4684-2703-5_4

9. Taddeo, B. & Roizman, B. The virion host shutoff protein (UL41) of herpes simplex virus 1 is an endoribonuclease with a substrate specificity similar to that of RNase A. *J. Virol.* **80,** 9341–5 (2006).

10. Boehmer, P. E. & Lehman, I. R. Herpes simplex virus DNA replication. *Annu. Rev. Biochem.* **66,** 347–84 (1997).

11. Verschuren, E. W. The cell cycle and how it is steered by Kaposi's sarcoma-associated herpesvirus cyclin. *J. Gen. Virol.* **85,** 1347–1361 (2004).

12. Hertel, L., Chou, S. & Mocarski, E. S. Viral and cell cycle-regulated kinases in cytomegalovirus-induced pseudomitosis and replication. *PLoS Pathog.* **3,** e6 (2007).

13. Baltimore, D. Expression of animal virus genomes. *Bacteriol. Rev.* **35,** 235–41 (1971).

14. Pellett, P. E. Trunkloads of viruses. *J. Virol.* **88,** 13520–2 (2014).

15. English, T. J. & Hammer, D. A. Brownian adhesive dynamics (BRAD) for simulating the receptor-mediated binding of viruses. *Biophys. J.* **86,** 3359–72 (2004).

16. Spear, P. G. Herpes simplex virus: receptors and ligands for cell entry. *Cell. Microbiol.* **6,** 401–10 (2004).

17. Nicola, A. V & Straus, S. E. Cellular and viral requirements for rapid endocytic entry of herpes simplex virus. *J. Virol.* **78,** 7508–17 (2004).

18. Nicola, A. V, Hou, J., Major, E. O. & Straus, S. E. Herpes simplex virus type 1 enters human epidermal keratinocytes, but not neurons, via a pH-dependent endocytic pathway. *J. Virol.* **79,** 7609–16 (2005).

19. Sodeik, B., Ebersold, M. W. & Helenius, A. Microtubule-mediated transport of incoming herpes simplex virus 1 capsids to the nucleus. *J. Cell Biol.* **136,** 1007–21 (1997).

20. Hay, J. & Ruyechan, W. T. Alphaherpesvirus DNA replication. (2007). at <http://www.ncbi.nlm.nih.gov/books/NBK47379/>

21. Boehmer, P. E. & Nimonkar, A. V. Herpes virus replication. *IUBMB Life* **55,** 13–22 (2003).

22. Flint, S. J. *Principles of virology: Molecular biology, pathogenesis, and control of animal viruses.* (ASM Press, 2004).

23. Morissette, G. & Flamand, L. Herpesviruses and chromosomal integration. *J. Virol.* **84,** 12100–9 (2010).

24. Preston, C. M. & Efstathiou, S. Molecular basis of HSV latency and reactivation. (2007). at <http://www.ncbi.nlm.nih.gov/books/NBK47421/>

25. Homa, F. & Brown, J. Capsid assembly and DNA packaging in herpes simplex virus. *Rev. Med. Virol.* **7,** 107–122 (1997).

26. Nasseri, M. & Mocarski, E. S. The cleavage recognition signal is contained within sequences surrounding an a-a junction in herpes simplex virus DNA. *Virology* **167,** 25–30 (1988).

27. Mettenleiter, T. C., Klupp, B. G. & Granzow, H. Herpesvirus assembly: an update. *Virus Res.* **143,** 222–34 (2009).

28. Mettenleiter, T. C. Budding events in herpesvirus morphogenesis. *Virus Res.* **106,** 167–80 (2004).

29. Osterrieder, N., Kamil, J. P., Schumacher, D., Tischer, B. K. & Trapp, S. Marek's disease virus: from miasma to model. *Nat. Rev. Microbiol.* **4,** 283–94 (2006).

30. Jarosinski, K. W., Tischer, B. K., Trapp, S. & Osterrieder, N. Marek's disease virus: lytic replication, oncogenesis and control. *Expert Rev. Vaccines* **5,** 761–72 (2006).

31. Calnek, B. W. Pathogenesis of Marek's disease virus infection. *Curr. Top. Microbiol. Immunol.* **255,** 25–55 (2001).

32. Churchill, A. E. & Biggs, P. M. Agent of Marek's disease in tissue culture. *Nature* **215,** 528–30 (1967).

33. Biggs, P. M. & Payne, L. N. Studies on Marek's disease. I. Experimental transmission. *J. Natl. Cancer Inst.* **39,** 267–80 (1967).

34. Witter, R. L., Burgoyne, G. H. & Solomon, J. J. Preliminary studies on cell cultures infected with Marek's disease agent. *Avian Dis.* **12,** 169–85 (1968).

35. Davison, A. J. Evolution of the herpesviruses. *Vet. Microbiol.* **86,** 69–88 (2002).

36. Davison, A. J. Herpesvirus systematics. *Vet. Microbiol.* **143,** 52–69 (2010).

37. Baigent, S. J., Smith, L. P., Nair, V. K. & Currie, R. J. W. Vaccinal control of Marek's disease: current challenges, and future strategies to maximize protection. *Vet. Immunol. Immunopathol.* **112,** 78–86 (2006).

38. Murphy, K., Travers, P. & Walport, M. *Janeway's Immunobiology*. *Garland Science* **7,** 887 (2008).

39. Fritz, J. H. & Girardin, S. E. How Toll-like receptors and Nod-like receptors contribute to innate immunity in mammals. *J. Endotoxin Res.* **11,** 390–4 (2005).

40. Rietdijk, S. T., Burwell, T., Bertin, J. & Coyle, A. J. Sensing intracellular pathogens-NOD-like receptors. *Curr. Opin. Pharmacol.* **8,** 261–6 (2008).

41. Alcami, A. & Koszinowski, U. H. Viral mechanisms of immune evasion. *Immunol. Today* **21,** 447–455 (2000).

42. Ploegh, H. L. Viral Strategies of Immune Evasion. *Science (80-.).* **280,** 248–253 (1998).

43. Finlay, B. B. & McFadden, G. Anti-immunology: evasion of the host immune system by bacterial and viral pathogens. *Cell* **124,** 767–82 (2006).

44. Griffin, B. D., Verweij, M. C. & Wiertz, E. J. H. J. Herpesviruses and immunity: the art of evasion. *Vet. Microbiol.* **143,** 89–100 (2010).

45. Ressing, M. E., Luteijn, R. D., Horst, D. & Wiertz, E. J. Viral interference with antigen presentation: trapping TAP. *Mol. Immunol.* **55,** 139–42 (2013).

46. Loch, S. & Tampé, R. Viral evasion of the MHC class I antigen-processing machinery. *Pflugers Arch.* **451,** 409–17 (2005).

47. Kaufman, J. The simple chicken major histocompatibility complex: life and death in the face of pathogens and vaccines. *Philos. Trans. R. Soc. Lond. B. Biol. Sci.* **355,** 1077–84 (2000).

48. Kaufman, J. Co-evolving genes in MHC haplotypes: the "rule" for nonmammalian vertebrates? *Immunogenetics* **50,** 228–36 (1999).

49. Aki, M. *et al.* Interferon-gamma induces different subunit organizations and functional diversity of proteasomes. *J. Biochem.* **115,** 257–69 (1994).

50. Hudson, A. W. & Ploegh, H. L. The cell biology of antigen presentation. *Exp. Cell Res.* **272,** 1–7 (2002).

51. Hulpke, S. & Tampé, R. The MHC I loading complex: a multitasking machinery in adaptive immunity. *Trends Biochem. Sci.* **38,** 412–20 (2013).

52. Saunders, P. M. & van Endert, P. Running the gauntlet: from peptide generation to antigen presentation by MHC class I. *Tissue Antigens* **78,** 161–70 (2011).

53. Dolan, B. P. *et al.* Distinct pathways generate peptides from defective ribosomal products for CD8+ T cell immunosurveillance. *J. Immunol.* **186,** 2065–72 (2011).

54. Kim, Y., Yewdell, J. W., Sette, A. & Peters, B. Positional bias of MHC class I restricted T-cell epitopes in viral antigens is likely due to a bias in conservation. *PLoS Comput. Biol.* **9,** e1002884 (2013).

55. Yewdell, J. W. DRiPs solidify: progress in understanding endogenous MHC class I antigen processing. *Trends Immunol.* (2011). doi:10.1016/j.it.2011.08.001

56. Schubert, U. *et al.* Rapid degradation of a large fraction of newly synthesized proteins by proteasomes. *Nature* **404,** 770–4 (2000).

57. Smith, M. H., Ploegh, H. L. & Weissman, J. S. Road to ruin: targeting proteins for degradation in the endoplasmic reticulum. *Science (80-.).* **334,** 1086–1090 (2011).

58. Yewdell, J. W. & David, A. Nuclear translation for immunosurveillance. *Proc. Natl. Acad. Sci. U. S. A.* **110,** 17612–3 (2013).

59. David, A. *et al.* Nuclear translation visualized by ribosome-bound nascent chain puromycylation. *J. Cell Biol.* **197,** 45–57 (2012).

60. Levitskaya, J. *et al.* Inhibition of antigen processing by the internal repeat region of the Epstein-Barr virus nuclear antigen-1. *Nature* **375,** 685–8 (1995).

61. Wiertz, E. J. *et al.* The human cytomegalovirus US11 gene product dislocates MHC class I heavy chains from the endoplasmic reticulum to the cytosol. *Cell* **84,** 769–79 (1996).

62. Wiertz, E. J. *et al.* Sec61-mediated transfer of a membrane protein from the endoplasmic reticulum to the proteasome for destruction. *Nature* **384,** 432–8 (1996).

63. Jones, T. R. *et al.* Human cytomegalovirus US3 impairs transport and maturation of major histocompatibility complex class I heavy chains. *Proc. Natl. Acad. Sci. U. S. A.* **93,** 11327–33 (1996).

64. Eisfeld, A. J., Yee, M. B., Erazo, A., Abendroth, A. & Kinchington, P. R. Downregulation of class I major histocompatibility complex surface expression by varicella-zoster virus involves open reading frame 66 protein kinase-dependent and -independent mechanisms. *J. Virol.* **81,** 9034–49 (2007).

65. Coscoy, L. Immune evasion by Kaposi's sarcoma-associated herpesvirus. *Nat. Rev. Immunol.* **7,** 391–401 (2007).

66. Huang, T., Lehmann, M. J., Said, A., Ma, G. & Osterrieder, N. Major Histocompatibility Complex Class I Downregulation Induced by Equine Herpesvirus Type 1 pUL56 Is through Dynamin-Dependent Endocytosis. *J. Virol.* **88,** 12802–15 (2014).

67. Ma, G., Feineis, S., Osterrieder, N. & Van de Walle, G. R. Identification and characterization of equine herpesvirus type 1 pUL56 and its role in virus-induced downregulation of major histocompatibility complex class I. *J. Virol.* **86,** 3554–63 (2012).

68. Neefjes, J. J., Momburg, F. & Hämmerling, G. J. Selective and ATP-dependent translocation of peptides by the MHC-encoded transporter. *Science* **261,** 769–71 (1993).

69. Nijenhuis, M. & Hämmerling, G. J. Multiple regions of the transporter associated with antigen processing (TAP) contribute to its peptide binding site. *J. Immunol.* **157,** 5467–77 (1996).

70. Abele, R. & Tampé, R. Function of the transport complex TAP in cellular immune recognition. *Biochim. Biophys. Acta* **1461,** 405–19 (1999).

71. Koch, J., Guntrum, R., Heintke, S., Kyritsis, C. & Tampé, R. Functional dissection of the transmembrane domains of the transporter associated with antigen processing (TAP). *J. Biol. Chem.* **279,** 10142–7 (2004).

72. Koch, J., Guntrum, R. & Tampé, R. The first N-terminal transmembrane helix of each subunit of the antigenic peptide transporter TAP is essential for independent tapasin binding. *FEBS Lett.* **580,** 4091–6 (2006).

73. Chen, M., Abele, R. & Tampé, R. Peptides induce ATP hydrolysis at both subunits of the transporter associated with antigen processing. *J. Biol. Chem.* **278,** 29686–92 (2003).

74. Howarth, M., Williams, A., Tolstrup, A. B. & Elliott, T. Tapasin enhances MHC class I peptide presentation according to peptide half-life. *Proc. Natl. Acad. Sci. U. S. A.* **101,** 11737–42 (2004).

75. Koopmann, J. O., Post, M., Neefjes, J. J., Hämmerling, G. J. & Momburg, F. Translocation of long peptides by transporters associated with antigen processing (TAP). *Eur. J. Immunol.* **26,** 1720–8 (1996).

76. York, I. A. *et al.* The ER aminopeptidase ERAP1 enhances or limits antigen presentation by trimming epitopes to 8-9 residues. *Nat. Immunol.* **3,** 1177–84 (2002).

77. Früh, K. *et al.* A viral inhibitor of peptide transporters for antigen presentation. *Nature* **375,** 415–8 (1995).

78. Hill, A. *et al.* Herpes simplex virus turns off the TAP to evade host immunity. *Nature* **375,** 411–5 (1995).

79. Hewitt, E. W., Gupta, S. S. & Lehner, P. J. The human cytomegalovirus gene product US6 inhibits ATP binding by TAP. *EMBO J.* **20,** 387–96 (2001).

80. Tulman, E. R. *et al.* The Genome of a Very Virulent Marek's Disease Virus. *J. Virol.* **74,** 7980–7988 (2000).

81. Barnett, B. C., Dolan, A., Telford, E. A., Davison, A. J. & McGeoch, D. J. A novel herpes simplex virus gene (UL49A) encodes a putative membrane protein with counterparts in other herpesviruses. *J. Gen. Virol.* **73 (Pt 8),** 2167–71 (1992).

82. Koppers-Lalic, D. *et al.* Varicelloviruses avoid T cell recognition by UL49.5-mediated inactivation of the transporter associated with antigen processing. *Proc. Natl. Acad. Sci. U. S. A.* **102,** 5144–9 (2005).

83. Koppers-Lalic, D. *et al.* Varicellovirus UL 49.5 proteins differentially affect the function of the transporter associated with antigen processing, TAP. *PLoS Pathog.* **4,** e1000080 (2008).

84. Verweij, M. C. *et al.* The Capacity of UL49.5 Proteins To Inhibit TAP Is Widely Distributed among Members of the Genus Varicellovirus. *J. Virol.* **85,** 2351–63 (2011).

85. Verweij, M. C. *et al.* Structural and functional analysis of the TAP-inhibiting UL49.5 proteins of varicelloviruses. *Mol. Immunol.* **48,** 2038–2051 (2011).

86. Hunt, H. D. *et al.* Marek's disease virus down-regulates surface expression of MHC (B Complex) Class I (BF) glycoproteins during active but not latent infection of chicken cells. *Virology* **282,** 198–205 (2001).

87. Jarosinski, K. W., Hunt, H. D. & Osterrieder, N. Down-regulation of MHC class I by the Marek's disease virus (MDV) UL49.5 gene product mildly affects virulence in a haplotype-specific fashion. *Virology* **405,** 457–63 (2010).

88. Tischer, B. K., Schumacher, D., Messerle, M., Wagner, M. & Osterrieder, N. The products of the UL10 (gM) and the UL49.5 genes of Marek's disease virus serotype 1 are essential for virus growth in cultured cells. *J. Gen. Virol.* **83,** 997–1003 (2002).

89. Jones, D., Lee, L., Liu, J. L., Kung, H. J. & Tillotson, J. K. Marek disease virus encodes a basic-leucine zipper gene resembling the fos/jun oncogenes that is highly expressed in lymphoblastoid tumors. *Proc. Natl. Acad. Sci.* **89,** 4042–4046 (1992).

90. Parcells, M. S. *et al.* Marek's disease virus (MDV) encodes an interleukin-8 homolog (vIL-8): characterization of the vIL-8 protein and a vIL-8 deletion mutant MDV. *J. Virol.* **75,** 5159–73 (2001).

91. Cui, X., Lee, L. F., Reed, W. M., Kung, H.-J. & Reddy, S. M. Marek's disease virus-encoded vIL-8 gene is involved in early cytolytic infection but dispensable for establishment of latency. *J. Virol.* **78,** 4753–60 (2004).

92. Brown, A. C. *et al.* Interaction of MEQ protein and C-terminal-binding protein is critical for induction of lymphomas by Marek's disease virus. *Proc. Natl. Acad. Sci. U. S. A.* **103,** 1687–92 (2006).

93. Lupiani, B. *et al.* Marek's disease virus-encoded Meq gene is involved in transformation of lymphocytes but is dispensable for replication. *Proc. Natl. Acad. Sci. U. S. A.* **101,** 11815–20 (2004).

94. Engel, A. T., Selvaraj, R. K., Kamil, J. P., Osterrieder, N. & Kaufer, B. B. Marek's disease viral interleukin-8 promotes lymphoma formation through targeted recruitment of B cells and CD4+ CD25+ T cells. *J. Virol.* **86,** 8536–45 (2012).

95. Li, Y. *et al.* Molecular characterization of the genome of duck enteritis virus. *Virology* **391,** 151–61 (2009).

96. Spatz, S. J., Volkening, J. D. & Ross, T. A. Molecular Characterization of the Complete Genome of Falconid Herpesvirus strain S-18. *Virus Res.* (2014). doi:10.1016/j.virusres.2014.03.005

97. Kamil, J. P. *et al.* vLIP, a viral lipase homologue, is a virulence factor of Marek's disease virus. *J. Virol.* **79,** 6984–96 (2005).

98. Tulman, E. R. *et al.* The genome of a very virulent Marek's disease virus. *J. Virol.* **74,** 7980–8 (2000).

99. Lange, A. *et al.* Classical nuclear localization signals: definition, function, and interaction with importin alpha. *J. Biol. Chem.* **282,** 5101–5 (2007).

100. Görlich, D. & Kutay, U. Transport between the cell nucleus and the cytoplasm. *Annu. Rev. Cell Dev. Biol.* **15,** 607–60 (1999).

101. Chelsky, D., Ralph, R. & Jonak, G. Sequence requirements for synthetic peptide-mediated translocation to the nucleus. *Mol. Cell. Biol.* **9,** 2487–92 (1989).

102. LaCasse, E. C. & Lefebvre, Y. A. Nuclear localization signals overlap DNA- or RNA-binding domains in nucleic acid-binding proteins. *Nucleic Acids Res.* **23,** 1647–56 (1995).

103. Kalderon, D., Roberts, B. L., Richardson, W. D. & Smith, A. E. A short amino acid sequence able to specify nuclear location. *Cell* **39,** 499–509 (1984).

104. Robbins, J., Dilworth, S. M., Laskey, R. A. & Dingwall, C. Two interdependent basic domains in nucleoplasmin nuclear targeting sequence: identification of a class of bipartite nuclear targeting sequence. *Cell* **64,** 615–23 (1991).

105. Nigg, E. A. Nucleocytoplasmic transport: signals, mechanisms and regulation. *Nature* **386,** 779–87 (1997).

106. Lim, C. S. *et al.* Targeted delivery to the nucleus. *Adv. Drug Deliv. Rev.* **59,** 698–717 (2007).

107. Kataoka, N., Bachorik, J. L. & Dreyfuss, G. Transportin-SR, a nuclear import receptor for SR proteins. *J. Cell Biol.* **145,** 1145–52 (1999).

108. Hoelz, A., Debler, E. W. & Blobel, G. The structure of the nuclear pore complex. *Annu. Rev. Biochem.* **80,** 613–43 (2011).

109. Hutten, S. & Kehlenbach, R. H. CRM1-mediated nuclear export: to the pore and beyond. *Trends Cell Biol.* **17,** 193–201 (2007).

110. Jarosinski, K. W., Osterrieder, N., Nair, V. K. & Schat, K. A. Attenuation of Marek's disease virus by deletion of open reading frame RLORF4 but not RLORF5a. *J. Virol.* **79,** 11647–59 (2005).

111. Tischer, B. K., Smith, G. A. & Osterrieder, N. En passant mutagenesis: a two step markerless red recombination system. *Methods Mol. Biol.* **634,** 421–30 (2010).

112. Petherbridge, L. *et al.* Oncogenicity of virulent Marek's disease virus cloned as bacterial artificial chromosomes. *J. Virol.* **78,** 13376–80 (2004).

113. Spatz, S. J. Accumulation of attenuating mutations in varying proportions within a high passage very virulent plus strain of Gallid herpesvirus type 2. *Virus Res.* **149,** 135–42 (2010).

114. Spatz, S. J., Rue, C., Schumacher, D. & Osterrieder, N. Clustering of mutations within the inverted repeat regions of a serially passaged attenuated gallid herpesvirus type 2 strain. *Virus Genes* **37,** 69–80 (2008).

115. Schat, K. A. *A Laboratory Manual for the Isolation and Identification of Avian Pathogens*. pp. 223–234 (Am Assoc Avian Pathol, 1998).

116. Sambrook, J. & W Russell, D. Molecular Cloning: A Laboratory Manual. *Cold Spring Harb. Lab. Press. Cold Spring Harb. NY* 999 (2001).

117. Huston, J. S. *et al.* Protein engineering of antibody binding sites: recovery of specific activity in an anti-digoxin single-chain Fv analogue produced in Escherichia coli. *Proc. Natl. Acad. Sci. U. S. A.* **85,** 5879–83 (1988).

118. Kinoshita, E., Kinoshita-Kikuta, E., Takiyama, K. & Koike, T. Phosphate-binding tag, a new tool to visualize phosphorylated proteins. *Mol. Cell. Proteomics* **5,** 749–57 (2006).

119. Brock, I., Krüger, M., Mertens, T. & von Einem, J. Nuclear targeting of human cytomegalovirus large tegument protein pUL48 is essential for viral growth. *J. Virol.* **87,** 6005–19 (2013).

120. Jean, C. *et al.* Transcriptome analysis of chicken ES, blastodermal and germ cells reveals that chick ES cells are equivalent to mouse ES cells rather than EpiSC. *Stem Cell Res.* (2014). doi:10.1016/j.scr.2014.11.005

121. Lee, D. H. & Goldberg, A. L. Proteasome inhibitors: valuable new tools for cell biologists. *Trends Cell Biol.* **8,** 397–403 (1998).

122. Hart, P. D. & Young, M. R. Ammonium chloride, an inhibitor of phagosome-lysosome fusion in macrophages, concurrently induces phagosome-endosome fusion, and opens a novel pathway: studies of a pathogenic mycobacterium and a nonpathogenic yeast. *J. Exp. Med.* **174,** 881–9 (1991).

123. Bowman, E. J., Siebers, A. & Altendorf, K. Bafilomycins: a class of inhibitors of membrane ATPases from microorganisms, animal cells, and plant cells. *Proc. Natl. Acad. Sci. U. S. A.* **85,** 7972–6 (1988).

124. Steinman, R. M., Mellman, I. S., Muller, W. A. & Cohn, Z. A. Endocytosis and the recycling of plasma membrane. *J. Cell Biol.* **96,** 1–27 (1983).

125. Rudolph, J., Seyboldt, C., Granzow, H. & Osterrieder, N. The Gene 10 (UL49 . 5) Product of Equine Herpesvirus 1 Is Necessary and Sufficient for Functional Processing of Glycoprotein M. *Society* **76,** 2952–2963 (2002).

126. Lipińska, A. D. *et al.* Bovine herpesvirus 1 UL49.5 protein inhibits the transporter associated with antigen processing despite complex formation with glycoprotein M. *J. Virol.* **80,** 5822–5832 (2006).

127. Liu, X. *et al.* Unique sequence characteristics of genes in the leftmost region of unique long region in duck enteritis virus. *Intervirology* **52,** 291–300 (2009).

128. Brunak, S., Engelbrecht, J. & Knudsen, S. Prediction of human mRNA donor and acceptor sites from the DNA sequence. *J. Mol. Biol.* **220,** 49–65 (1991).

129. Shi, Y. *et al.* Abnormal SDS-PAGE migration of cytosolic proteins can identify domains and mechanisms that control surfactant binding. *Protein Sci.* **21,** 1197–209 (2012).

130. Brameier, M., Krings, A. & MacCallum, R. M. NucPred--predicting nuclear localization of proteins. *Bioinformatics* **23,** 1159–60 (2007).

131. Nguyen Ba, A. N., Pogoutse, A., Provart, N. & Moses, A. M. NLStradamus: a simple Hidden Markov Model for nuclear localization signal prediction. *BMC Bioinformatics* **10,** 202 (2009).

132. Seibel, N. M., Eljouni, J., Nalaskowski, M. M. & Hampe, W. Nuclear localization of enhanced green fluorescent protein homomultimers. *Anal. Biochem.* **368,** 95–9 (2007).

133. Wolff, B., Sanglier, J. J. & Wang, Y. Leptomycin B is an inhibitor of nuclear export: inhibition of nucleo-cytoplasmic translocation of the human immunodeficiency virus type 1 (HIV-1) Rev protein and Rev-dependent mRNA. *Chem. Biol.* **4,** 139–47 (1997).

134. Kudo, N. *et al.* Leptomycin B inactivates CRM1/exportin 1 by covalent modification at a cysteine residue in the central conserved region. *Proc. Natl. Acad. Sci. U. S. A.* **96,** 9112–7 (1999).

135. Nardozzi, J. D., Lott, K. & Cingolani, G. Phosphorylation meets nuclear import: a review. *Cell Commun. Signal.* **8,** 32 (2010).

136. Kinoshita, E., Kinoshita-Kikuta, E. & Koike, T. Separation and detection of large phosphoproteins using Phos-tag SDS-PAGE. *Nat. Protoc.* **4,** 1513–21 (2009).

137. Onishi, R. M. & Gaffen, S. L. Interleukin-17 and its target genes: mechanisms of interleukin-17 function in disease. *Immunology* **129,** 311–21 (2010).

138. Shi, Y. *et al.* A novel cytokine receptor-ligand pair. Identification, molecular characterization, and in vivo immunomodulatory activity. *J. Biol. Chem.* **275,** 19167–76 (2000).

139. Heider, M. R. & Munson, M. Exorcising the exocyst complex. *Traffic* **13,** 898–907 (2012).

140. Ziemann, K., Mettenleiter, T. C. & Fuchs, W. Infectious laryngotracheitis herpesvirus expresses a related pair of unique nuclear proteins which are encoded by split genes located at the right end of the UL genome region. *J. Virol.* **72,** 6867–74 (1998).

141. Walker, B. A., van Hateren, A., Milne, S., Beck, S. & Kaufman, J. Chicken TAP genes differ from their human orthologues in locus organisation, size, sequence features and polymorphism. *Immunogenetics* **57,** 232–47 (2005).

142. Gimeno, I. M. *et al.* Marek's Disease Virus Infection in the Brain: Virus Replication, Cellular Infiltration, and Major Histocompatibility Complex Antigen Expression. *Vet. Pathol.* **38,** 491–503 (2001).

143. Wei, H., He, J., Paulsen, D. B. & Chowdhury, S. I. Bovine herpesvirus type 1 (BHV-1) mutant lacking U(L)49.5 luminal domain residues 30-32 and cytoplasmic tail residues 80-96 induces more rapid onset of virus neutralizing antibody and cellular immune

responses in calves than the wild-type strain Cooper. *Vet. Immunol. Immunopathol.* **147,** 223–9 (2012).

144. Wei, H., He, J., Paulsen, D. B. & Chowdhury, S. I. Bovine herpesvirus type 1 (BHV-1) mutant lacking U(L)49.5 luminal domain residues 30-32 and cytoplasmic tail residues 80-96 induces more rapid onset of virus neutralizing antibody and cellular immune responses in calves than the wild-type strain Cooper. *Vet. Immunol. Immunopathol.* (2012). doi:10.1016/j.vetimm.2012.04.015

145. Berget, S. M., Moore, C. & Sharp, P. A. Spliced segments at the 5' terminus of adenovirus 2 late mRNA. *Proc. Natl. Acad. Sci.* **74,** 3171–3175 (1977).

146. Chow, L. T., Gelinas, R. E., Broker, T. R. & Roberts, R. J. An amazing sequence arrangement at the 5′ ends of adenovirus 2 messenger RNA. *Cell* **12,** 1–8 (1977).

147. Jarosinski, K. W. & Schat, K. A. Multiple alternative splicing to exons II and III of viral interleukin-8 (vIL-8) in the Marek's disease virus genome: the importance of vIL-8 exon I. *Virus Genes* **34,** 9–22 (2007).

148. Hildebrandt, E., Dunn, J. R., Perumbakkam, S., Niikura, M. & Cheng, H. H. Characterizing the molecular basis of attenuation of Marek's disease virus via in vitro serial passage identifies de novo mutations in the helicase-primase subunit gene UL5 and other candidates associated with reduced virulence. *J. Virol.* **88,** 6232–42 (2014).

149. Ziemann, K., Mettenleiter, T. C. & Fuchs, W. Infectious Laryngotracheitis Herpesvirus Expresses a Related Pair of Unique Nuclear Proteins Which Are Encoded by Split Genes Located at the Right End of the UL Genome Region. *J. Virol.* **72,** 6867–6874 (1998).

150. Boulikas, T. Putative nuclear localization signals (NLS) in protein transcription factors. *J. Cell. Biochem.* **55,** 32–58 (1994).

151. Boulikas, T. A compilation and classification of DNA binding sites for protein transcription factors from vertebrates. *Crit. Rev. Eukaryot. Gene Expr.* **4,** 117–321 (1994).

152. Xiao, C. Y., Hübner, S. & Jans, D. A. SV40 large tumor antigen nuclear import is regulated by the double-stranded DNA-dependent protein kinase site (serine 120) flanking the nuclear localization sequence. *J. Biol. Chem.* **272,** 22191–8 (1997).

153. Yao, Z. *et al.* Herpesvirus Saimiri encodes a new cytokine, IL-17, which binds to a novel cytokine receptor. *Immunity* **3,** 811–21 (1995).

154. Boucher, L., Ouzounis, C. A., Enright, A. J. & Blencowe, B. J. A genome-wide survey of RS domain proteins. *RNA* **7,** 1693–1701 (2001).

155. Manley, J. L. & Krainer, A. R. A rational nomenclature for serine/arginine-rich protein splicing factors (SR proteins). *Genes Dev.* **24,** 1073–4 (2010).

156. Ote, I. *et al.* Varicella-zoster virus IE4 protein interacts with SR proteins and exports mRNAs through the TAP/NXF1 pathway. *PLoS One* **4,** e7882 (2009).

157. Sandri-Goldin, R. M. The many roles of the regulatory protein ICP27 during herpes simplex virus infection. *Front. Biosci.* **13,** 5241–56 (2008).

158. Ren, D., Lee, L. F. & Coussens, P. M. Identification and characterization of Marek's disease virus genes homologous to ICP27 and glycoprotein K of herpes simplex virus-1. *Virology* **204,** 242–50 (1994).

159. Amor, S. *et al.* ICP27 protein of Marek's disease virus interacts with SR proteins and inhibits the splicing of cellular telomerase chTERT and viral vIL8 transcripts. *J. Gen. Virol.* **92,** 1273–8 (2011).

12. Publications

The ORF012 gene of Marek's disease virus (MDV) produces a spliced transcript and encodes a novel nuclear phosphoprotein essential for virus growth. Schippers T, Jarosinski K, Osterrieder N. J Virol. 2014 Nov 12. pii: JVI.02687-14. [Epub ahead of print]

13. Acknowledgements

First and foremost, I would like to thank Prof. Klaus Osterrieder for giving me the opportunity to work on an interesting topic and for guiding me through my thesis. I would also like to thank Prof. Rupert Mutzel, FU Berlin, for his willingness to supervise and evaluate my thesis and Dr. Karsten Tischer, Prof. Benedikt Kaufer and Dr. Armando Damiani for helpful discussions and support. Without the funding from the Dahlem Research School, FU Berlin, as well as the IMPRS ZIBI Graduate School, Berlin, this work would have not been possible. In particular I would like to thank the coordinators Angela Daberkow from the DRS and Susann, Martina, Christoph, Juliane, Susanne and Andreas for organizing the ZIBI Graduate School.

I would also like to thank all past and present members of the Institut für Virologie, FU Berlin, who have supported and helped me during the last years. In particular, I would like to thank Veljko, Dušan, Annachiara, Nina, Inês, Annemarie, Matthias, Nora, Tobi, Imme, Aiste, Bart, Dimitris, Maren, Jakob, Kathrin, Kia, Walid, Pratik and everyone who was not named here. My special thanks for help in all those years goes to Ann, Annett and Michaela. Many thanks to my friend and colleague Stefan for helping me with cell sorting.

Without the support of my family I would not be where I am today. For their friendly donation of genes, I would like to thank my parents Karin and Hans. I would also like to thank my sister Kristin.

Sina, I thank you for all your support, your patience, your love and for reminding me that every journey begins with a single step.

14. Curriculum vitae

For reasons of data protection,
the curriculum vitae is not included in the online version

For reasons of data protection,
the curriculum vitae is not included in the online version

For reasons of data protection,
the curriculum vitae is not included in the online version

For reasons of data protection,
the curriculum vitae is not included in the online version